SEDIMENTARY GEOLOGY OF THE CAMBRO-ORDOVICIAN SIGNAL MOUNTAIN FORMATION AS EXPOSED IN THE WICHITA MOUNTAINS OF SOUTHWESTERN OKLAHOMA

By

CURTIS LEON DITZELL

Bachelor of Science in Geoscience
University of Tulsa
Tulsa, Oklahoma
1982

Bachelor of Science in Criminal Justice Studies
University of Tulsa
Tulsa, Oklahoma
1975

Submitted to the Faculty of the Graduate College
of the Oklahoma State University
in partial fulfillment of the requirements
for the degree of
Master of Science
December, 1984

SEDIMENTARY GEOLOGY OF THE CAMBRO-ORDOVICIAN
SIGNAL MOUNTAIN FORMATION AS EXPOSED
IN THE WICHITA MOUNTAINS OF
SOUTHWESTERN OKLAHOMA

Thesis Approved:

Norvell Donovan
Thesis Adviser

Gary J. Stewart

Roger N. Randolph

Norman N. Durham
Dean of the Graduate College

PREFACE

This thesis is dedicated to my parents Leon S. and Jean E. Ditzell, Jr.; for without their steadfast encouragement and support, the Degree of Master of Science may not have been attainable.

I appreciate the assistance from my thesis adviser, Dr. R. Nowell Donovan, with the petrography of the Formation and with the editing of this thesis. My other committee members, Dr. Gary Stewart and Mr. Roger Planalp, provided valuable assistance and recommendations on the final manuscript.

A special friendship was established with Mr. Charlie-Bob Oliver, manager of the Kimbal Ranch, and his wife Dixie, during my stay in the Wichita Mountains. Sincere thanks is offered to Mr. David Kimball, as well as the Olivers, for allowing me and many other students to camp and have unrestricted access to the outcrops on the Kimball Ranch. Many other ranchers and farmers also graciously allowed access to outcrops on their lands.

A final note of appreciation is given to the Oklahoma Geological Survey for a grant to cover field expenses.

TABLE OF CONTENTS

Chapter

Page

LIST OF FIGURES

PLATE

CHAPTER I

INTRODUCTION

Purpose

The purpose of this thesis is to describe the sedimentology, stratigraphy, and sedimentary petrography of the Cambro-Ordovician Signal Mountain Formation at exposures in the Slick Hills, northeast of the Wichita Mountain uplift, southwestern Oklahoma. To date, a detailed sedimentological study of the Signal Mountain has not been published, although many authors have measured sections and described the stratigraphy in both the Wichita and Arbuckle Mountains of Oklahoma (Ulrich, 1932; Decker, 1939; Frederickson et al., 1956; Harlton, 1963; Brookby, 1969; Stitt, 1968, 1969).

Location of Study Area

The study area is located in easternmost Kiowa and northernmost Comanche Counties, Oklahoma (Figure 1), in the frontal fault zone between the Wichita Mountain uplift to the southwest and the Anadarko Basin to the northeast (Figure 2). The frontal fault zone is complex (Beauchamp, 1983; McConnell, 1983; Stubbs, 1984), the principal tectonic elements are a series of northwest-trending faults and folds. The study area is located on the Blue Creek horst, in particular on the northeast limb of the Blue Creek Canyon anticline. The Blue Creek horst is

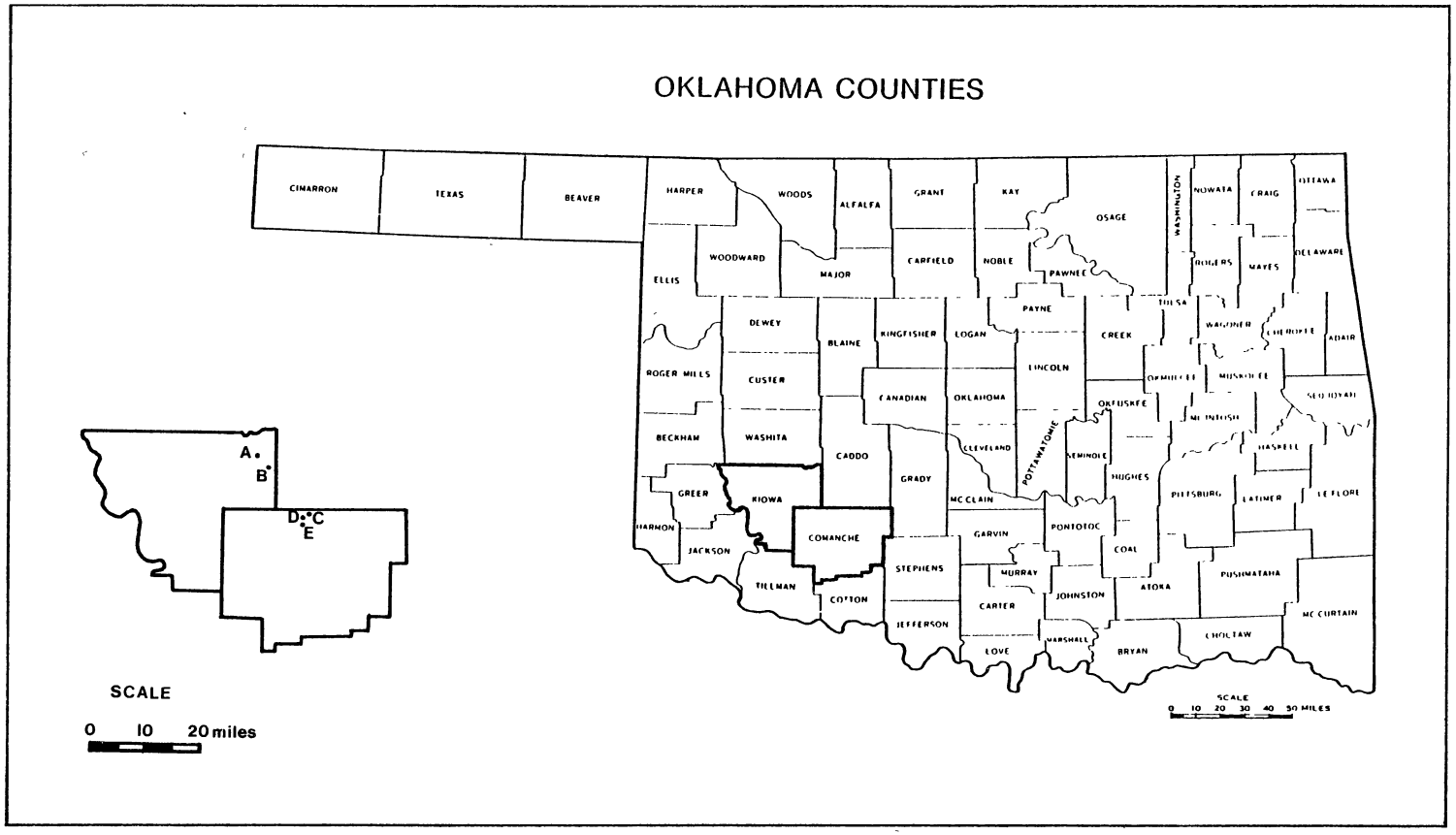

Figure 1. Oklahoma Counties map showing the location of the study areas. (A) Zodletone Mountain measured section, NW/4, 16-T6N-R14W; (B) Bally Mountain measured section, SE/4, 26-T6N-R14W; (C) Ring Top Mountain measured section, E/2, 1-T4N-R13W and W/2, 7-T4N-R13W; (D) Redhill reference location, SW/4, 2-T4N-R13W; and (E) Kimball Ranch reference location, E/2, 14-T4N-R13W.

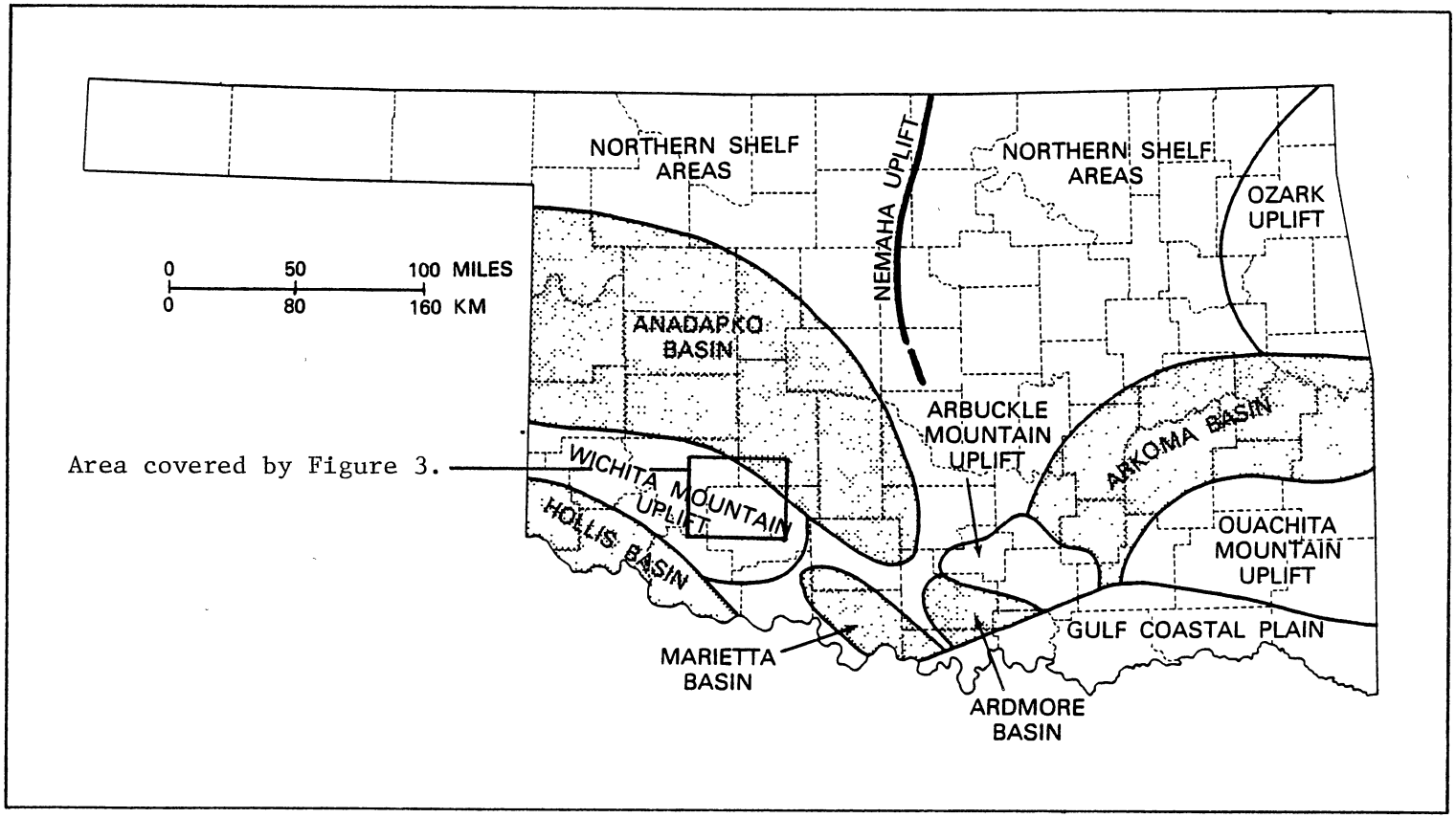

Figure 2. Major Geologic Provinces of Oklahoma (Johnson, et al., 1979).

bounded by the Blue Creek Canyon fault to the southwest and the Mountain View fault to the northeast (Figure 3).

Local Stratigraphy

Lower Paleozoic sedimentary rocks rest unconformably on the Carlton Rhyolite Group. The Carlton Rhyolite Group generally is usually composed of rhyolite porphyry lavas 525 + 25 million years old, according to a "Lithostratigraphic Classification of Basement Rocks of Wichita Province, Oklahoma" compiled by Gilbert (1982). The Carlton Rhyolite unconformity is seen as an uneven paleo-landscape characterized by smooth hills with topographic relief up to 300 feet. In the W/2, section 26-T6N-R14W, east of Bally Mountain, the Cambrian Reagan Sandstone and Honey Creek Limestone of the Timbered Hills Group, onlap a Carlton Rhyolite paleo-topographic high. This same stratigraphic relationship is observed in Blue Creek Canyon, Comanche County, Oklahoma. An observation made by Rafalowski (1984) at Stumbling Bear Pass along Highway 58 (NW/4, section 24-T4N-R13W, approximately 2 miles north of Lake Lawtonka Comanche County, Oklahoma), suggests that the Fort Sill Formation onlaps a Carlton Rhyolite hill at that location. This observation is evidence for an even greater paleo-topographic relief than previously recorded.

Cambrian-Ordovician sediments of the Arbuckle Group disconformably overlie the Timbered Hills Group. In ascending order, the Fort Sill (locally including the Royer Dolomite), Signal Mountain, McKenzie Hill, Cool Creek, Kindblade, and West Spring Creek Formations make up the Arbuckle Group (Figure 4). The top of the West Spring Creek Formation is the top of the Arbuckle Group and it is unconformably overlain by the Middle Ordovician Simpson Group. In the Wichita Mountains, Permian

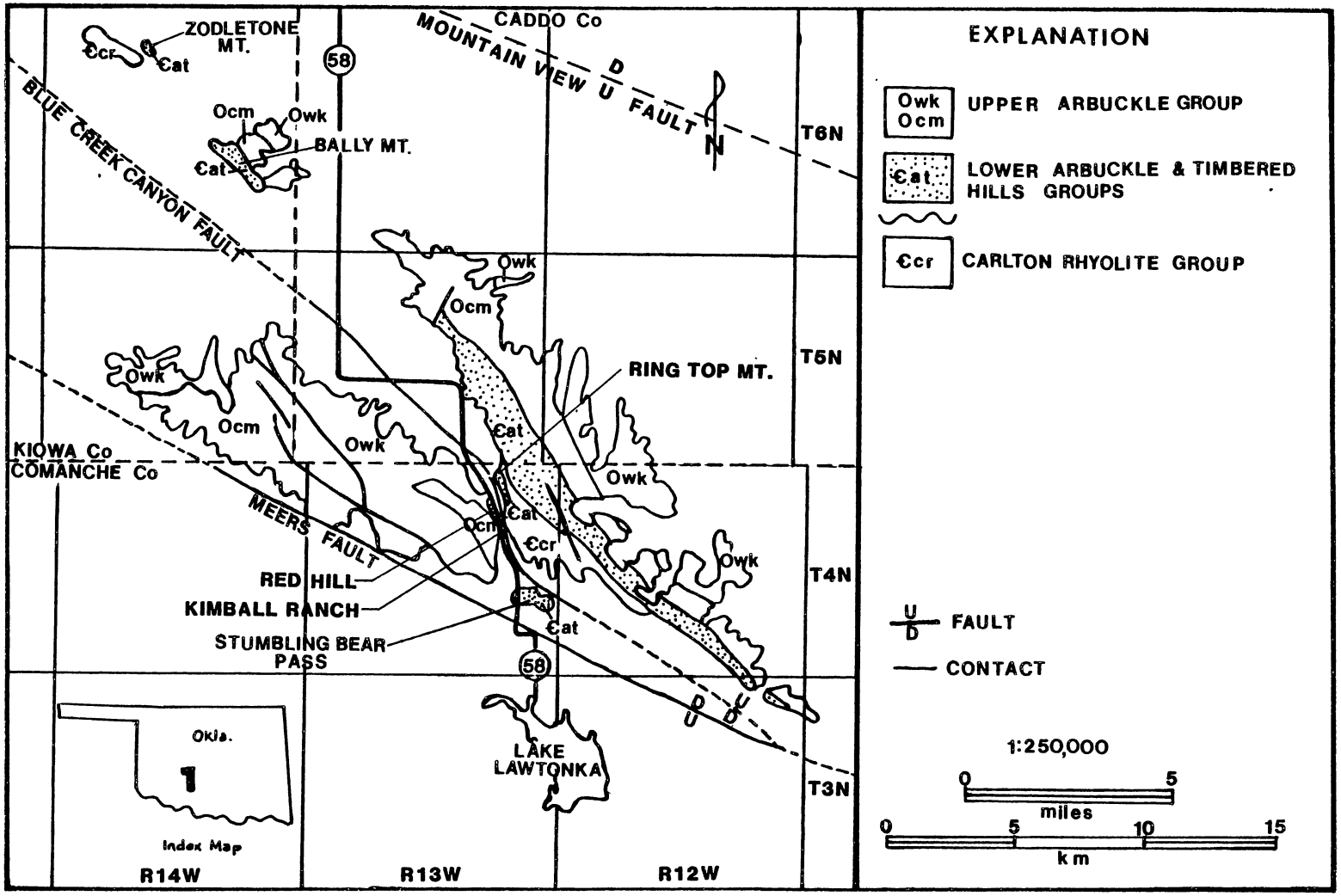

Figure 3. Principal tectonic elements of the study area. (Haves, 1977; Donovan, 1983) (Drafted by M. Rafalowski, 1984).

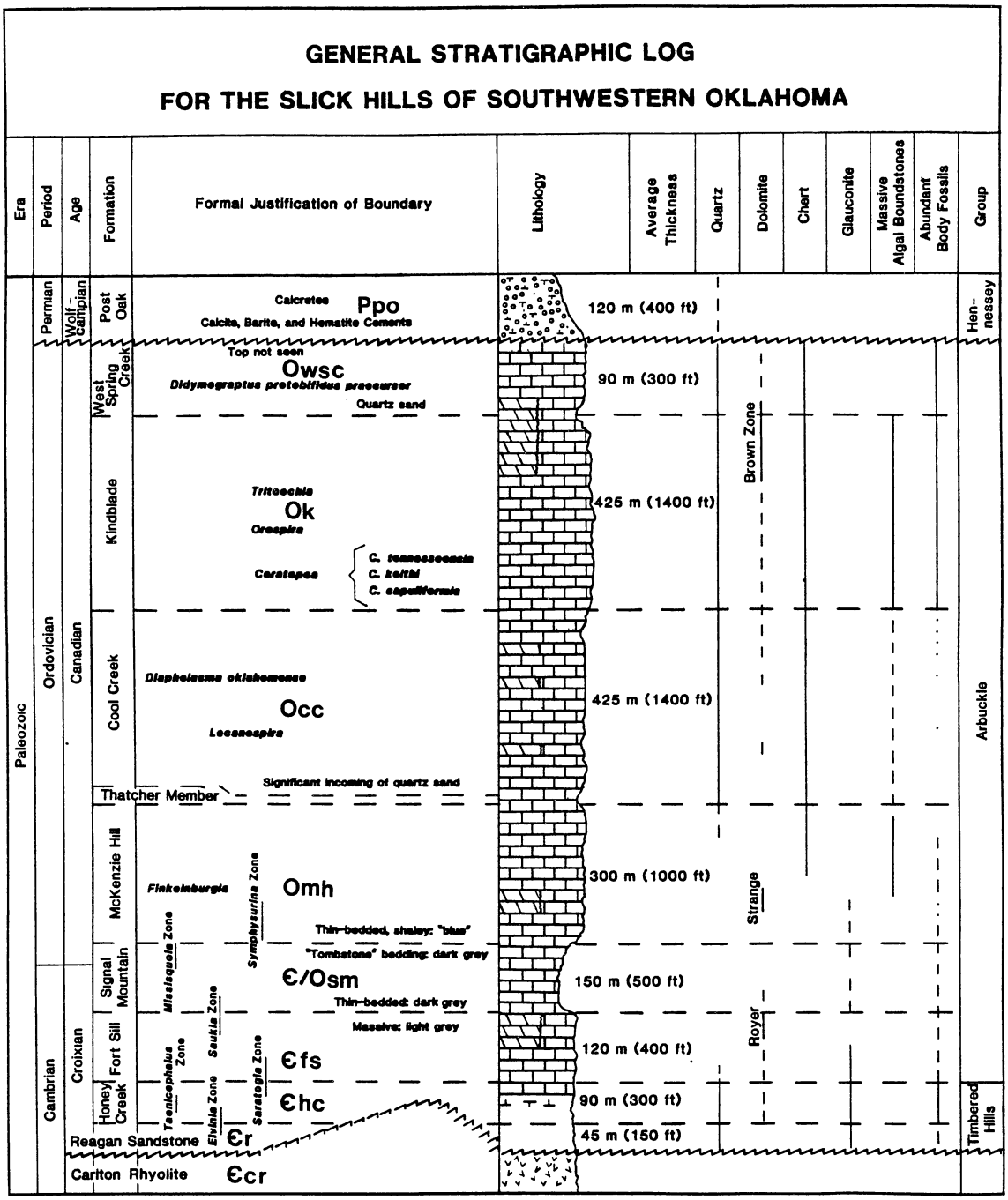

Figure 4. General stratigraphic log for the Slick Hills of southwestern Oklahoma (Donovan and Ragland, 1983).

sedimentary rocks of the Hennessey Group, principally the Post Oak Conglomerate, overlie Cambrian-Ordovician rocks in angular unconformity and conceal the Arbuckle-Simpson contact.

The Signal Mountain Formation disconformably overlies the Fort Sill Formation. This contact is clearly defined by a pronounced lithological change from boundstones into very thinly bedded grainstones, packstones, wackestones, and mudstones.

The Signal Mountain Formation conformably underlies the McKenzie Hill Formation. This contact is difficult to position because grainstones, packstones, wackestones, and mudstones, typical of both Formations at the contact, interfinger for approximately 100 feet. The contact is positioned at the base of the first continuous blocky to massive partings, common to the McKenzie Hill Formation, which contrast with the flaggy to slabby parting of the Signal Mountain Formation.

The Cambrian-Ordovician boundary is in the Signal Mountain Formation; it is recognized on the basis of trilobite assemblages. Stitt (1971), from work in the Arbuckle Mountains, Murray County, Oklahoma, discovered that in Cambrian, Saukia Zone, and Ordovician, Missisquoia Zone, trilobites do not occur together. He found the earliest Ordovician trilobites 4 feet above the latest Cambrian trilobites within the Signal Mountain Formation. The Cambrian-Ordovician boundary was specifically located between the Corbina apopis (Upper Cambrian) and the Plethopeltis arbucklensis (Lower Ordovician) trilobite subzones. Stitt also located the Cambrian-Ordovician boundary for Brookby (1969) at two locations in the Wichita Mountains; one in the SE/4, section 26-T6N-R14W, Kindblade Ranch measured section, Kiowa County and the

other in the SE/4, section 17-T4N-R12W, Chandler Creek measured section, Comanche County.

Previous Investigations

Ulrich (1932) designated the type section for the Signal Mountain Formation as a sequence of limestones outcropping on the western slope of McKenzie Hill in section 8-T2N-R12W, Comanche County, approximately 4 miles northwest of Lawton, Oklahoma.

He named the Signal Mountain Formation for a prominent hill of Precambrian igneous rock at the southeastern end of the Wichita Mountain Range, approximately one mile north of the type section. Ulrich assigned a 185 foot thickness to the type section and measured greater thicknesses on the northeast side of the Wichita Mountains.

Decker (1939) remeasured the type section, using a greater dip, and obtained a thickness of 290 feet. Many other partial to complete sections were measured by Decker, including a 350-foot-thick complete section east of Bally Mountain in section 26-T6N-R14W, Kiowa County. Frederickson (1956) and Harlton (1963) also measured sections at the section 26-T6N-R14W location and each obtained 400 feet of Signal Mountain.

The Cambrian-Ordovician boundary was determined by Bridges (1936), Decker (1939), and Frederickson (1956), using trilobite zones, to be at the top of the Signal Mountain Formation in the Wichita MOuntains and at the top of the Butterly Dolomite in the Arbuckle Mountains. In the Arbuckle Mountains, the Signal Mountain Formation is overlain by the Butterly Dolomite and underlain by the Royer Dolomite. As noted previously, Stitt (1968, 1971) discovered that the Cambrian-Ordovician

boundary actually within the Signal Mountain Formation. His boundary determination was based on additional trilobite subzones unknown to the previous authors.

After Stitt located the Cambrian-Ordovician boundary, Brookby (1969) measured several sections of only the Ordovician portion of the Signal Mountain Formation, near Bally Mountain (NW/4, SE/4, section 26-T6N-R14W, Kiowa County), near Tahoe Creek (SW/4, NW/4, section 23-T5N-R14W, Caddo County), and near Chandler Creek (NE/4, SE/4, section 17-T4N-R12W, Comanche County). The respective thicknesses were 328 feet, 411 feet, and 440 feet.

Since 1975, Donovan (the author's thesis supervisor) has conducted research in the Slick Hills (Wichita Mountains) of southwestern Oklahoma. This work has provided a source for many master's theses on the sedimentology, stratigraphy, and structural geology of the area. The structure of the western half of the Slick Hills (west of Highway 58 in Blue Creek Canyon), Caddo and Comanche Counties, was discussed in the theses of Beauchamp (1983) and McConnell (1983). Sedimentological theses discussing the Reagan and Cool Creek Formations were completed by Tsegay (1983) and Ragland (1983).

Research is presently under completion by Kelly Cloyd, Steve Bridges, Cathy Bridges, Mary Rafalowski, and Milton Stubbs. These master's students are respectively addressing the dolomitization in the Arbuckle Group, stratigraphy and structural geology of Permian and Quaternary sediments, sedimentology and stratigraphy of the Honey Creek and Fort Sill Formations, and structural geology of the eastern half of the Slick Hills, (east of Highway 58 in Blue Creek Canyon).

CHAPTER II

METHODS OF INVESTIGATION

Two complete sections of the Signal Mountain Formation were measured; one east of Bally Mountain in the SE/4, section 26-T6N-R14W, Kiowa County and the other east of Ring Top Mountain in the E/2, section 1-T4N-R13W and the W/2, section 6-T4N-R12W, Comanche County. A reference section was measured northeast of Zodletone Mountain in the NW/4, section 16-T6N-R14W, Kiowa County (where only the lower 236 feet of Signal Mountain is exposed). The sections were measured using a 5-foot Jacob's staff equipped with a dip correctable hand level. In addition, two Comanche County reference locations were examined for sedimentological features and the nature of the basal contact with the Fort Sill Formation; one north of Red Hill, in the SW/4, section 2-T4N-R13W and the other south of the Kimball Ranch headquarters, in the E/2, section 14-T4N-R13W (Figure 1).

The principal section studied was that at Bally Mountain. From that section the author collected 193 hand-sample specimens of limestone and dolomite for laboratory examination. At the Zodletone Mountain section 69 hand-samples were collected. Additional hand-samples were collected at the two reference locations and at the Ring Top Mountain section. All hand-samples were oriented and marked with the footage above or below the base of the Signal Mountain. Footage numbers were prefixed by "BM", "ZM", "RM", "RH," or "KR" to indicate whether the

specimen was collected at Bally Mountain, Zodletone Mountain, Ring Top Mountain, Red Hill, or the Kimbell Ranch headquarters respectively.

Hand-samples from the Bally Mountain and Zodletone Mountain sections were slabbed, polished, etched with 15%+ hydrochloric acid, and described using a 10X to 30X zoom stereoscopic microscope.

Eighty-five thin sections were made; 75 from throughout the Bally Mountain section and 10 from the lowermost 40 feet of the Zodletone Mountain section. Each thin section was assigned the number corresponding to its parent sample. A solution of Alizarin Red S and potassium ferricyanide, prepared according to Evamy (1963), was used to stain each thin section. This staining technique distinguished between calcite, dolomite, and ferroan carbonate cements. Petrographic examination of the thin sections more accurately identified allochems, replacement fabrics, and non-carbonate constituents. Several thin sections were analyzed by X-ray diffraction to identify accurately the ferroan dolomite cement.

CHAPTER III

STRATIGRAPHY OF THE SIGNAL MOUNTAIN FORMATION

Boundaries of the Formation

Lower Contact

As previously mentioned, the Signal Mountain Formation rests disconformably on the Fort Sill Formation. The upper 50 to 60 feet of Fort Sill, at all locations examined, consists of white to pale light gray, massive hummocky, fenestrate algal mound boundstones together with very thinly interbedded algal-mat boundstones and algal intraclast sand grainstones (Figures 5 and 6).

At the Bally Mountain and Zodletone Mountain measured sections, the base of the Signal Mountain consists of 3 to 4 feet of thinly interlaminated light gray to light brown microsparitic mudstones and light orange-weathering crystalline dolostones. This interval has weathered to a soil covered bench profile, but where exposed (or uncovered) it has distinctive shaley partings (Figures 7 and 8). Above the basal thinly interlaminated unit is a 6 foot interval of medium orange and medium gray mottled, slabby to blocky weathering dolomitic mudstone which has partly recrystallized to microspar (Figures 9 and 10). Oxidation of ferroan dolomite (ankerite), which has selectively replaced burrow filling micrite and bioturbated micrite zones, has produced the distinctive and characteristic orange color.

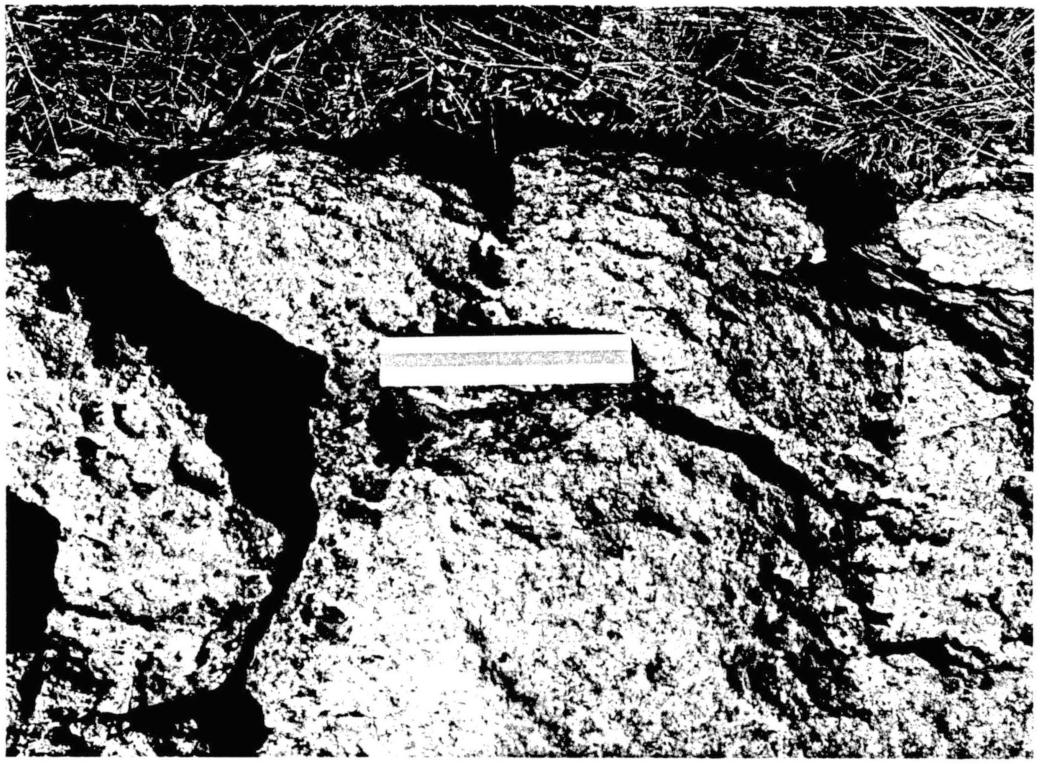

Figure 5. Upper Fort Sill Formation, Bally Mountain measured section. The photograph shows the characteristic color and hammocky appearance. The top of this interval is 12 feet below the Signal Mountain-Fort Sill Formational contact. The scale is 6 inches (15 cm) long.

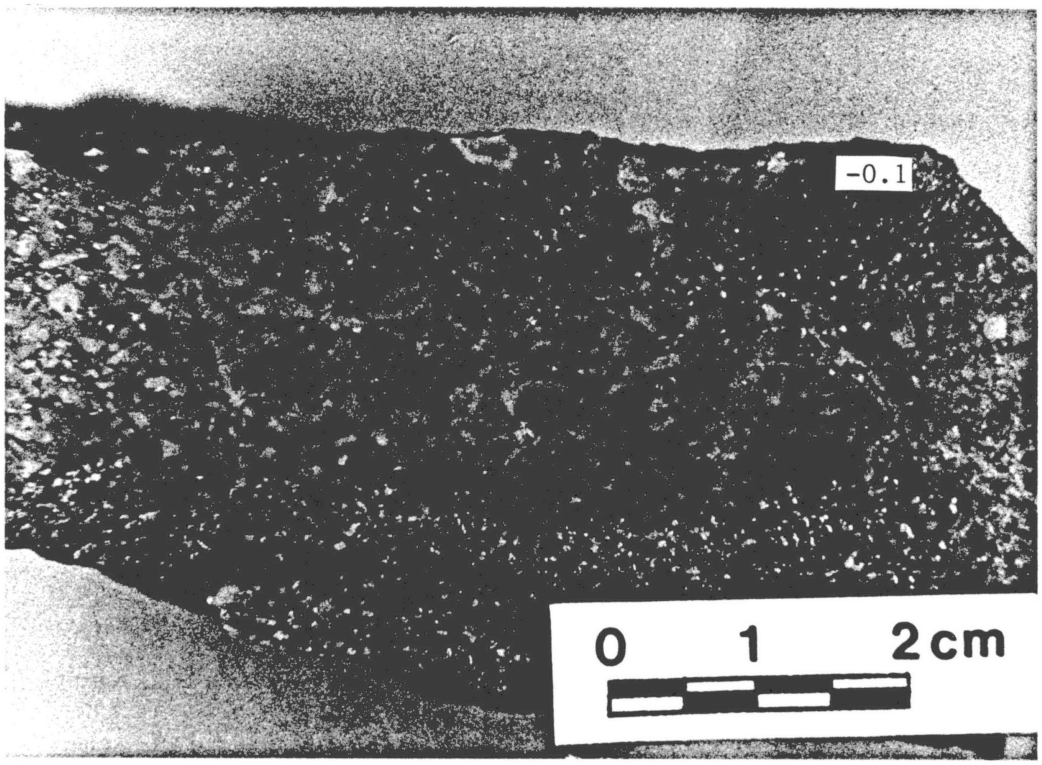

Figure 6. A dolomitic algal intraclast sand grainstone. The dolomite, ferroan ankerite, appears light to medium orange, due to the oxidation of iron from the ankerite lattice to form limonite-hematite. Intraclasts are rip-up clasts of algal boundstone. BM -0.1 indicates that this sample was collected from the Bally Mountain measured section 0.1 feet below the Signal Mountain-Fort Sill Formational contact.

Figure 7. Basal interval of Signal Mountain Formation, Zodletone Mountain measured section. The red flag is 5 feet above the Signal Mountain-Fort Sill contact. Jacob's staff is divided into tenths of a foot.

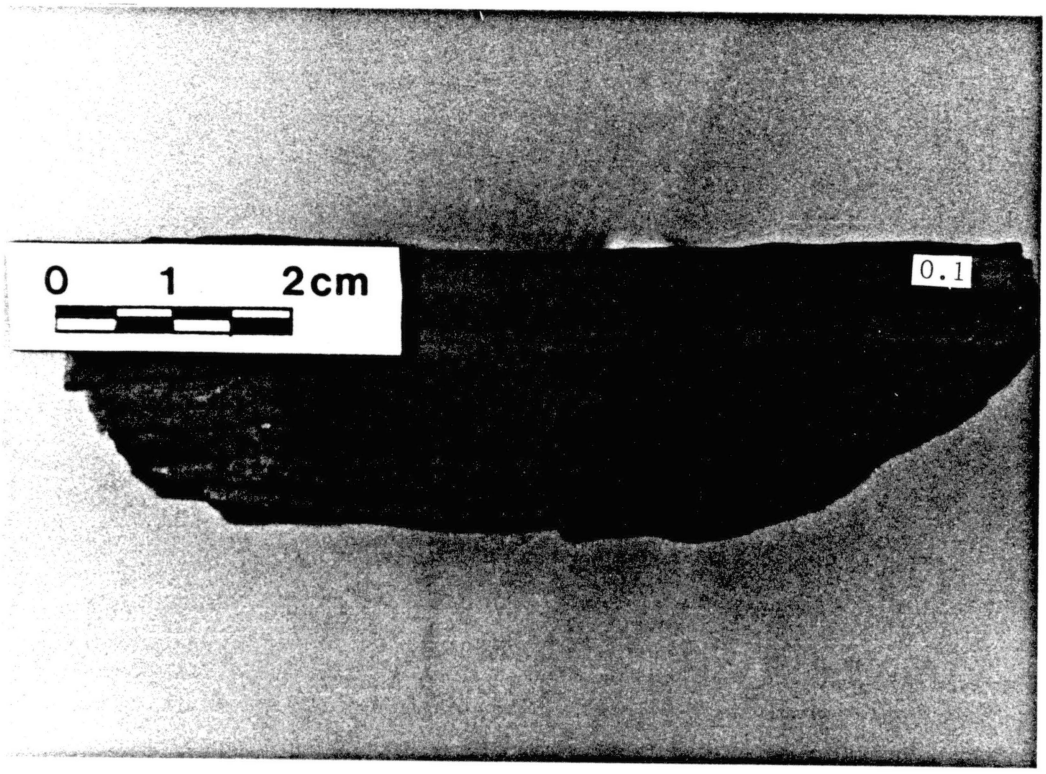

Figure 8. Thinly interlaminated microsparitic mudstone and crystalline dolostone, basal interval of Signal Mountain Formation. Microsparitic mudstone laminae are light gray to light brown and crystalline dolostone laminae are light orange. This sample is characteristic of the basal Signal Mountain Formation of the Bally Mountain and Zodletone Mountain measured section.

Figure 9. Exposure characteristic of the orange-mottled dolomitic mudstone interval. The photograph was taken at 8 feet above the Signal Mountain-Fort Sill contact at the Bally Mountain measured section.

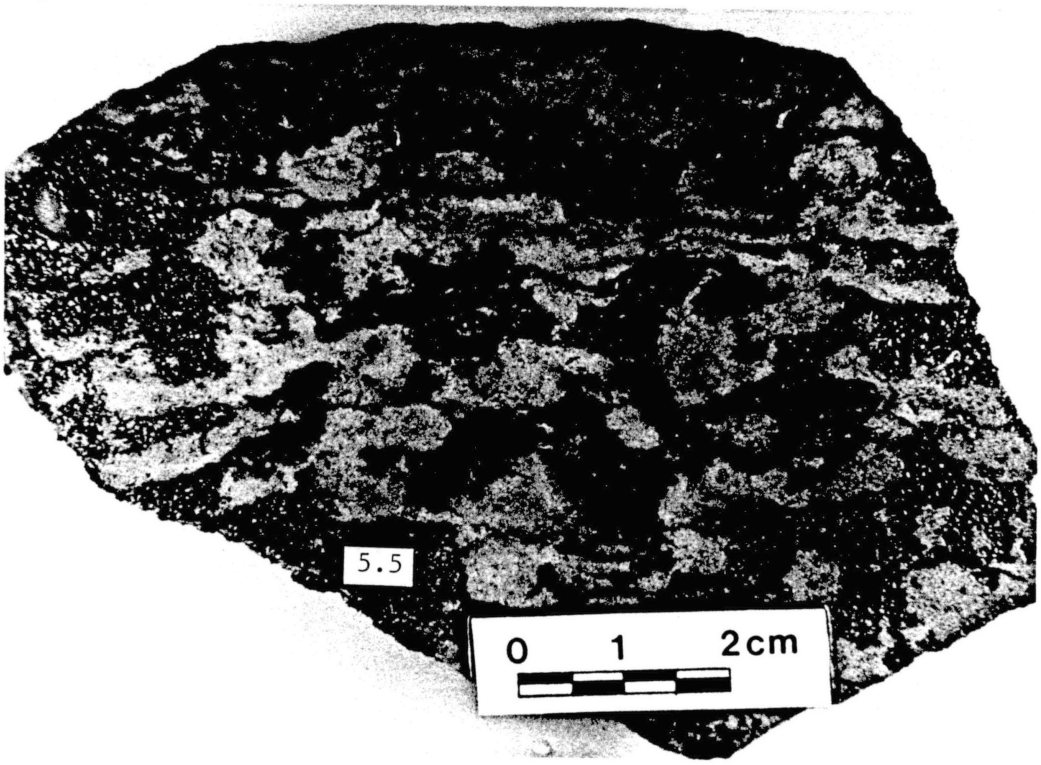

Figure 10. Mottled medium orange and medium gray dolomitic mudstone. This sample is from the interval shown in Figure 9. Ferroan dolomite, ankerite, has selectively replaced burrows and bioturbated zones. Black wavy horizontal lines are incipient low amplitude interconnected stylolites.

At the Ring Top measured section, Red Hill, and Kimbell Ranch reference locations the thinly interlaminated mudstone and crystalline dolostone interval are not present. In these areas, as well as throughout the remainder of Blue Creek Canyon, the orange mottled, very dolomitic mudstone interval is in contact with the Fort Sill boundstones and algal grainstones (Figure 11).

A distinctive facies interfingered between characteristic Signal Mountain and Fort Sill lithologies is in the lower 12 feet of the Signal Mountain Formation. On top of the orange-mottled, dolomitic mudstone interval lie approximately 3 feet of thinly interbedded white to pale light gray algal-mat boundstones and algal intraclast sand grainstones similar to those in the upper Fort Sill Formation (Figure 12). This algal unit is good evidence that the formational contact is likely to be diachronous on a regional scale. The upper boundstone is at both Bally Mountain and Ring Top Mountain, but is not conspicuous at Zodletone Mountain.

Upper Contact

Also noted previously, the Signal Mountain-McKenzie Hill Formational contact is conformable and difficult to position due to the interfingering of similar lithologies over approximately a hundred feet. The upper Signal Mountain Formation, at the Bally Mountain measured section, consists predominantly of medium gray to brownish medium gray, laminated to thinly laminated mudstones and mudstones very thinly interbedded with wackestones (Figures 13 and 14), packstones or grainstones. Allochems are principally combinations of intraclasts and fossils.

Figure 11. Signal Mountain-Fort Sill contact, Ring Top Mountain measured section. The base of the Jacob's staff is on the contact. Fort Sill white to light gray boundstone is on the left and the Signal Mountain orange-mottled dolomitic mudstone interval is on the right. The Signal Mountain thinly laminated light gray microsparitic mudstone and orange weathered, crystalline dolostone interval is not present. Jacob's staff is divided into tenths of a foot.

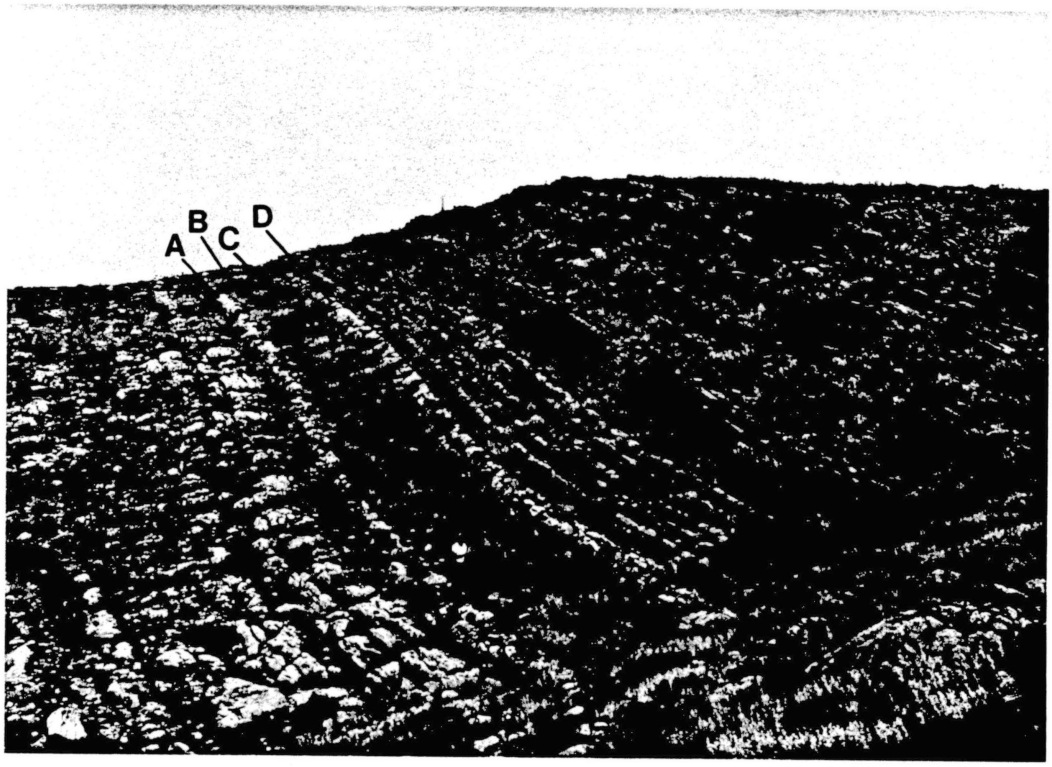

Figure 12. Signal Mountain-Fort Sill contact, Bally Mountain measured section. The geologist is standing on the contact. View is northwest along strike. Beds are dipping to the northeast. (A) white to light gray algal mat boundstones thinly interbedded with algal intraclast sand grainstones, (B) light gray, microsparitic mudstones interlaminated with light orange, crystalline dolostones, (C) orange mottled dolomitic mudstone, and (D) white to light gray algal maty boundstones thinly interbedded with algal intraclast sand grainstones comparable to the upper Fort Sill Formation.

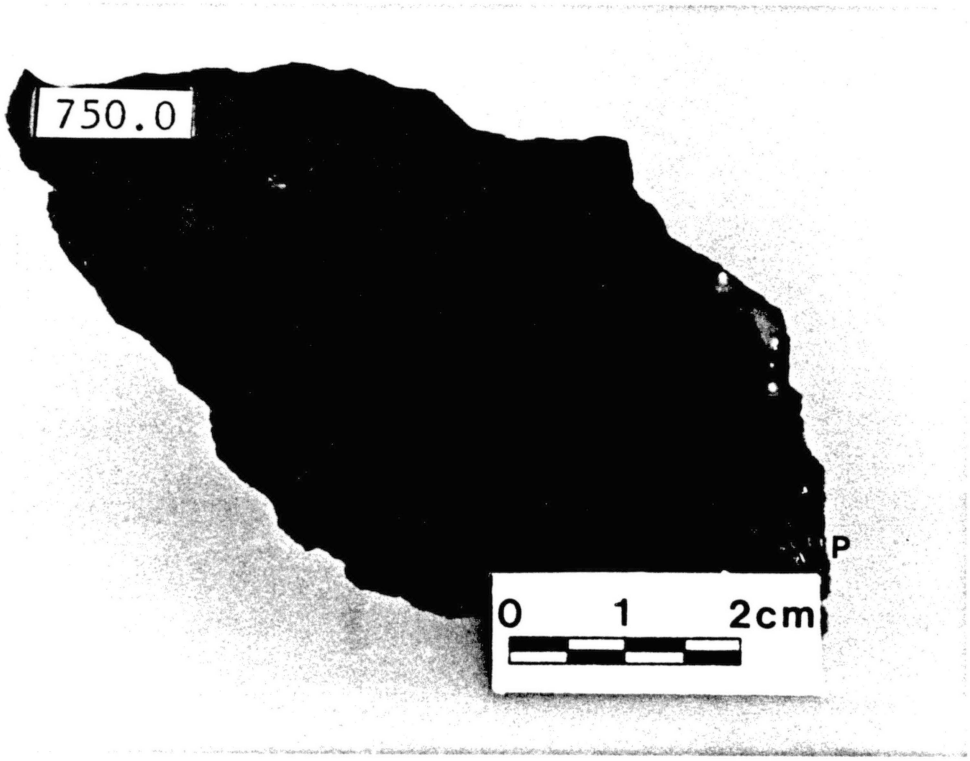

Figure 13. A slightly fenestrate mudstone. This mudstone is very thinly bedded, moderately bioturbated, and intensely stylolitic (bedded). An intraclast sand packstone (P) (not easily recognizable in photograph) is located near the base of the sample. This sample is from the Signal Mountain Formation, 4 feet below the Signal Mountain-McKenzie Hill contact.

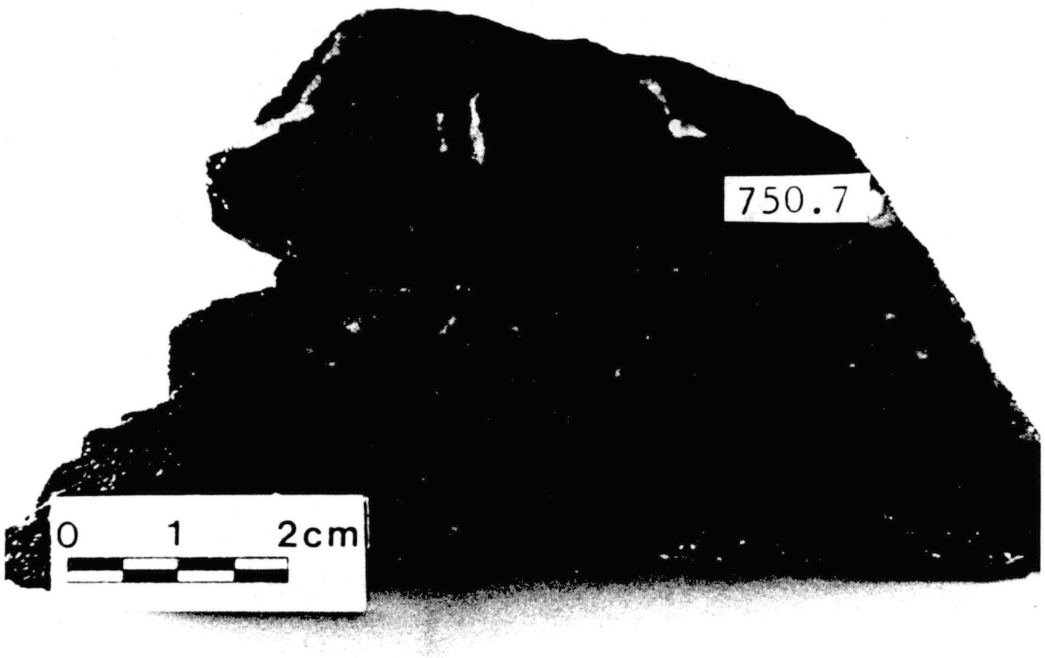

Figure 14. A pelmatozoan sand wackestone. Allochems are abundant pelmatozoan, common trilobite, and rare gastropod fragments and common intraclasts. Fossils are very fine to fine sand size, as large as coarse sand size, rounded to well rounded, and well to moderately sorted. Intraclasts are very coarse sand size, subrounded, commonly contain finely disseminated hematite, and composed of mudstone and fossil sand wackestone. This wackestone is thinly bedded, very bioturbated, slightly fenestrate, and slightly stylolitic. At least two hardgrounds (HG) are present. Sample is 3.3 feet below the Signal Mountain-McKenzie contact.

Fossils consist of trilobite carapaces, pelmatOzoan parts, brachiopod valves, and gastropod shells.

Basal McKenzie Hill lithology, at the Bally Moutain measured section, consists of medium gray, indistinctly bedded, intraclast packstones that commonly contain trilobites, pelmatozoans or gastropods and very thin beds of mudstone (Figure 15). Above the basal packstones are very thinly interbedded grainstones, mudstones, and wackestones (Figure 16). Allochems are similar to those found in the Signal Mountain Formation with the addition of abundant peloids, common ooliths, and a greater abundance of gastropod shells.

The similarity and facies interfingering of the two formations would make locating the contact nearly impossible if they did not exhibit distinctly different parting features. The upper Signal Mountain has weathered to flaggy to slabby partings, often producing a tombstone topography. In contrast, the McKenzie Hill exhibits blocky to massive partings. These different parting characteristics enable the field geologist to place the contact at the base of the first relatively thick sequence of massive-parting limestone of the McKenzie Hill Formation (Figure 17). In the upper 100 feet of the Signal Mountain Formation, there are several massive limestones beds whose lithology appears consistent with that of the McKenzie Hill Formation. These units represent the interfingering of the two formations. Unlike the lower contact, where the lithology and color of the Fort Sill are distinctly different from those of the Signal Mountain Formation, the similarity of lithologies at this contact does not allow precise stratigraphic placement of the contact in incomplete sequences found in the more tectonically disturbed areas of the Slick Hills.

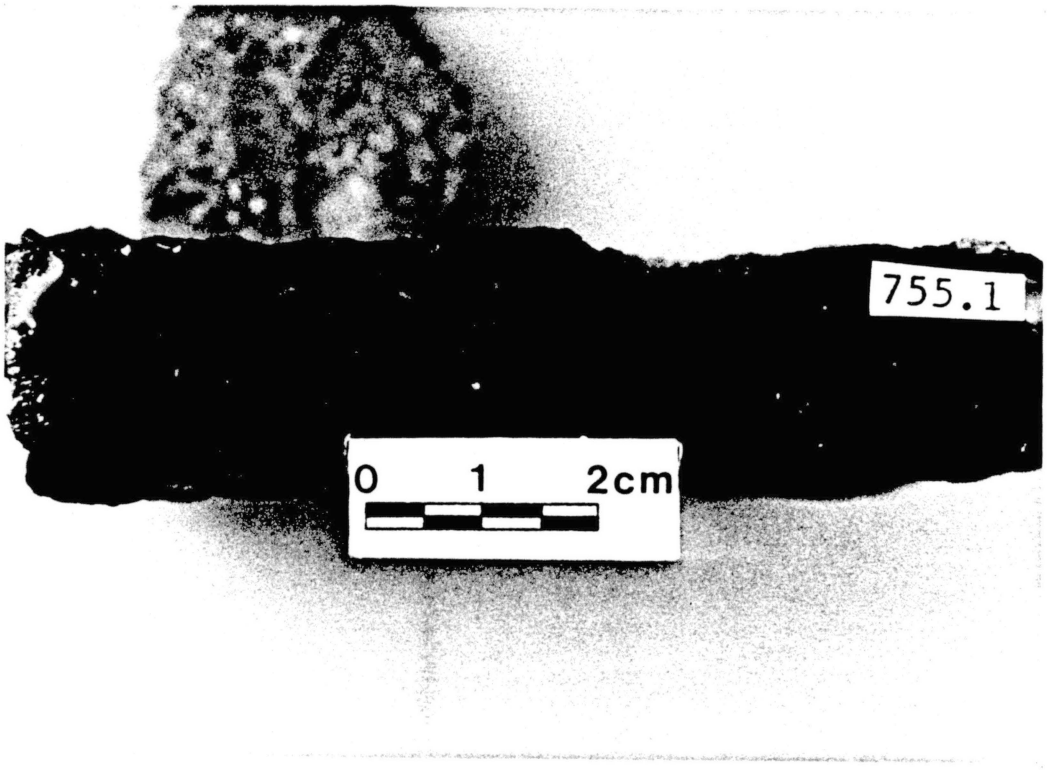

Figure 15. A pebble intraformational conglomerate (IFC) limestone. The matrix is composed of sand intraclasts and fossil fragments (trilogite, pelmatozoan, and gastropod) cemented by micrite. IFC'c and sand intraclasts are flat to irregularly spheroidal-shaped, commonly hematite-rimmed, and composed of mudstone. Fossils are fine to coarse sand size, angular to subrounded, and poorly sorted This IFC limestone is indistinctly bedded, very stylolitic (pseudobrecciated), and contains 1% ferroan dolomite (medium orange specks). Sample is 1.1 feet above the Signal Mountain-McKenzie Hill contact.

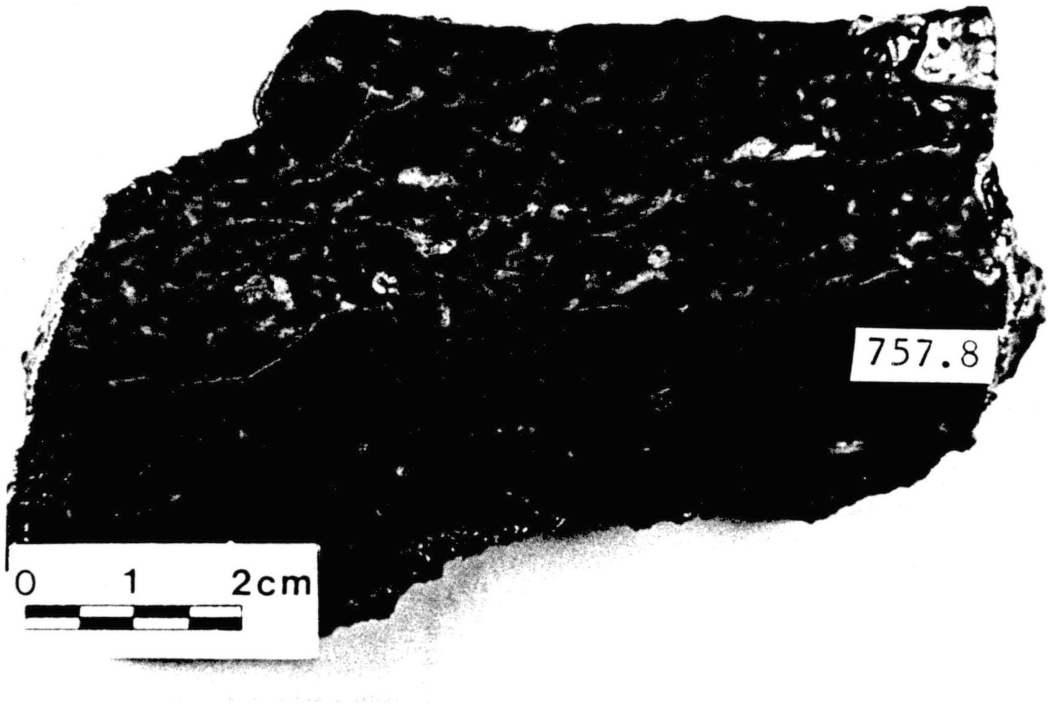

Figure 16. A calcite spar-cemented IFC limestone (top) and a mudstone (bottom) grading upward into a micrite-cemented IFC limestone. IFCs are fine to very fine pebble size, irregular spheroidal to flat, poorly sorted, commonly hematite rimmed, and composed of mudstone. The matrix is composed of intraclast sand cemented by micrite in the lower half of the sample and by calcite spar in the upper half. The mudstone commonly contains trilobite shells and intraclasts. These carbonates are thinly interbedded, scoured, highly bioturbated, and slightly stylolitic. Sample is from 3.8 feet above the Signal Mountain-McKenzie Hill Formational contact.

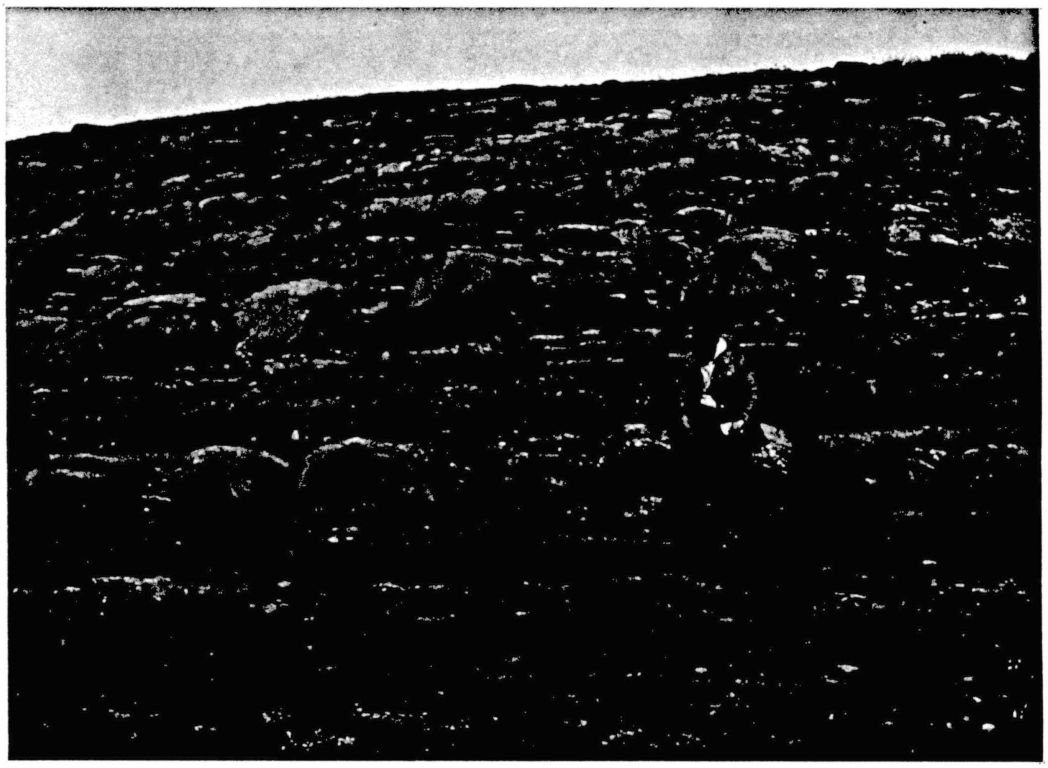

Figure 17. Signal Mountain-McKenzie Hill contact, Bally Mountain measured section. Contact is at the base of the massive-parting limestone upon which sites the geologist. Note the difference between the massive parting McKenzie Hill Formation (above) and the flaggy- to slabby-parting Signal Mountain Formation (below).

The criterion of parting differences as a contact indicator, fails in areas of poor exposure. Therefore, in such areas the recognition of a laterally-persistent marker bed is a prerequisite to the accurate placement of the upper boundary. At the Bally Mountain measured section, the top of a 0.6 foot thick zone of dark gray mudstone and mudstones thinly interbedded with peloidal wackestones, was chosen as the approximate Signal Mountain-McKenzie Hill contact (Figures 18 and 19). This dark gray zone is located between a flaggy-parting "Signal Mountain" lithology and a massive-parting "McKenzie Hill" lithology.

At the Ring Top Mountain section, the top of a 0.6 foot thick zone, of orange- to reddish brown-mottled, thinly interbedded, hematitic, dolomitic, mudstones and trilobite intraclast sand wackestones, was chosen as the approximate Signal Mountain-McKenzie Hill contact (Figure 20). The dark gray zone associated with the upper contact at the Bally Mountain section is either missing or concealed. Except for a greater dolomite content, the limestones across the contact appear similar to those examined at the Bally Mountain section. Placement of the contact was made more difficult and uncertain by the poor outcrops (Figure 21).

Stitt (1983) placed the Signal Mountain-McKenzie Hill contact within the Symphysurina trilobite zone at his Chandler Creek measured section, sections 17 and 18-T4N-R12W, Comanche County, in the Wichita Mountains. More specifically the contact is located between the Symphysurina brevispicata (Signal Mountain) and Symphysurina bulbose (McKenzie Hill) subzones. Without advanced paleontological skills and extensive manual labor to recover whole trilobite tests, the biostratigraphic boundary is impractical to the field for mapping. Therefore, the most

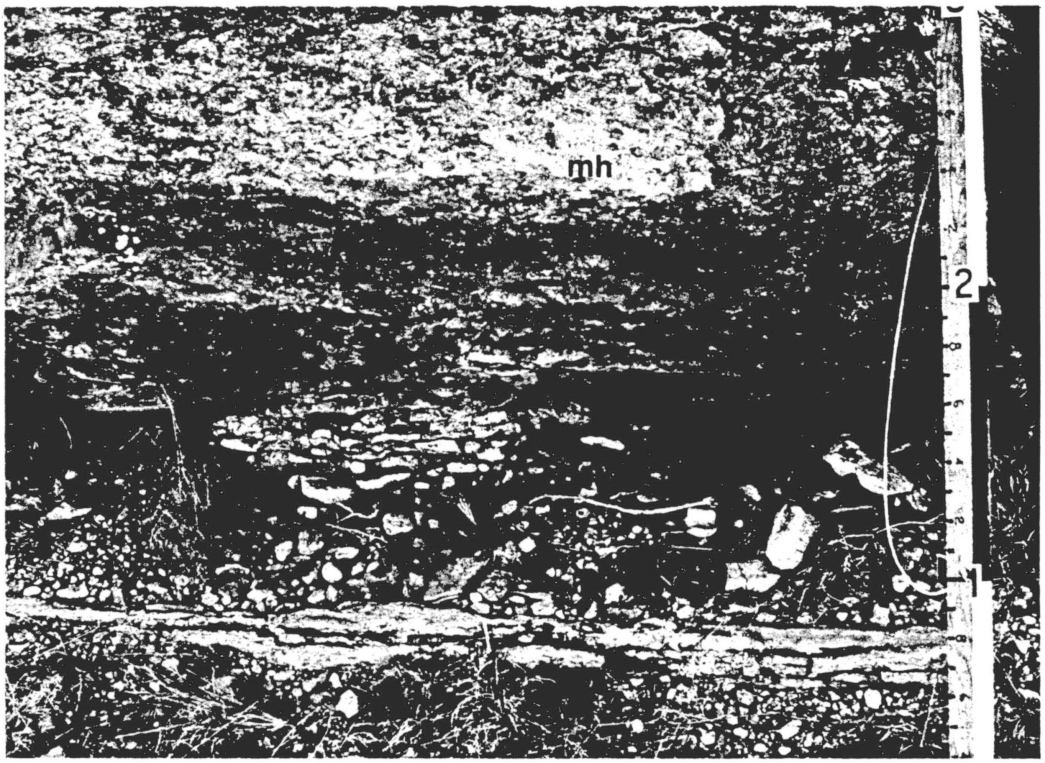

Figure 18. Dark gray mudstone of the Signal Mountain-McKenzie Hill contact, Bally Mountain measured section. The contact is placed at the top of the dark gray zone; the McKenzie Hill Formation (mh) is above and the Signal Mountain Formation (sm) is below.

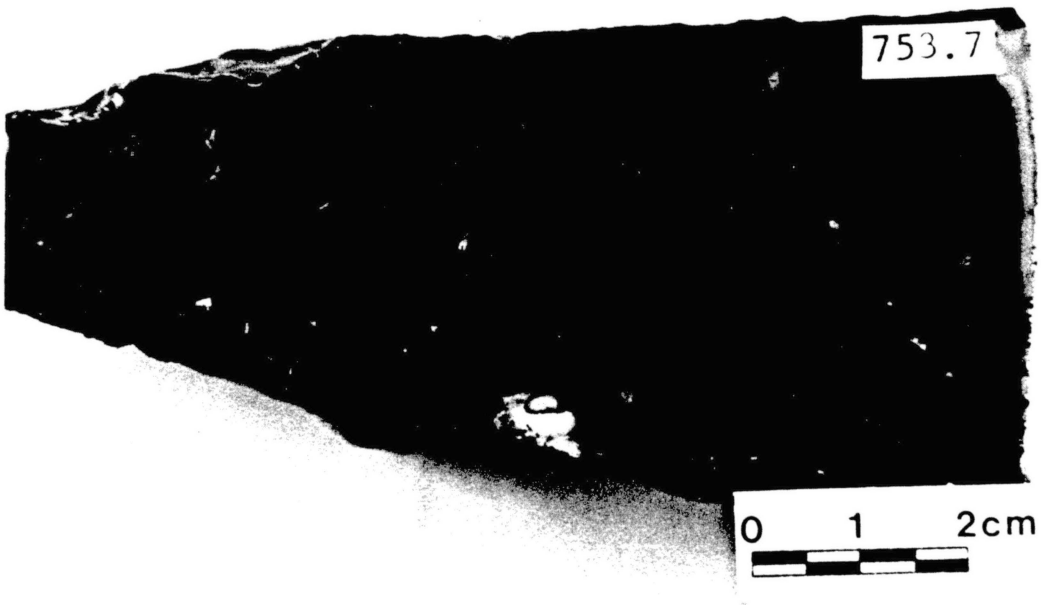

Figure 19. A medium to dark gray mudstone. The mudstone is indistinctly bedded, slightly burrowed, moderately stylolitic, slightly jointed (vertical to inclined), slightly fenestrate, and contains 1% ferroan dolomite (orange specks). Drusy calcite fills a gastropod shell at the bottom of the sample. Sample is from the center of the dark gray zone shown in Figure 18.

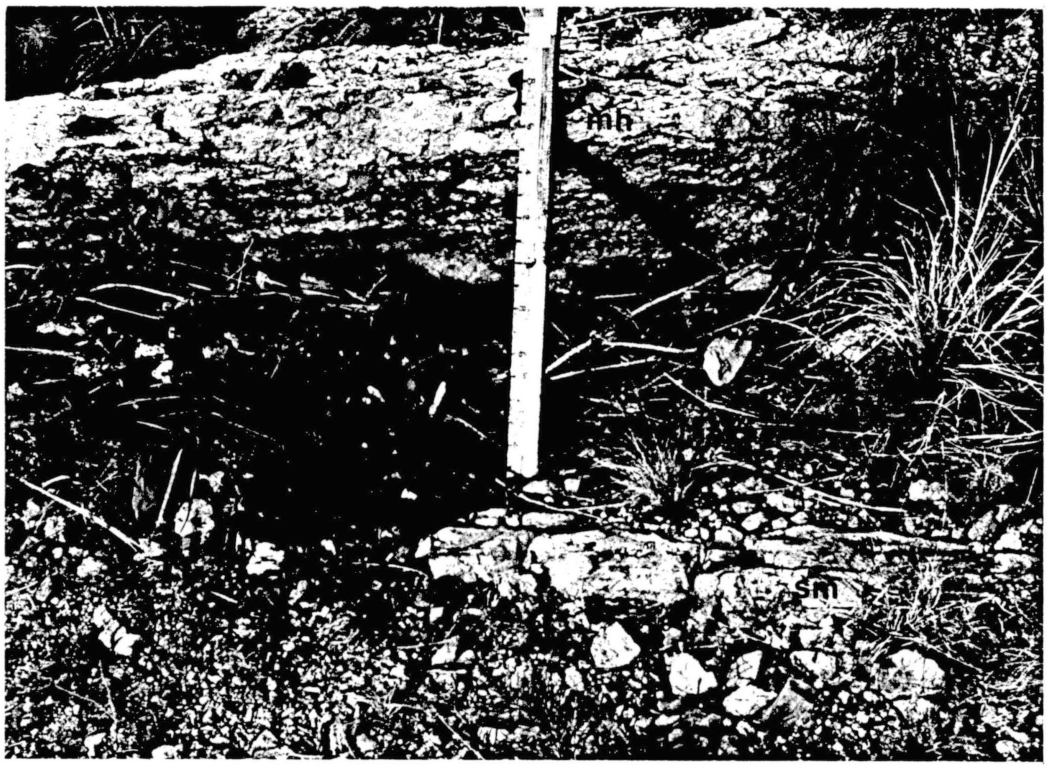

Figure 20. Orange-mottled mudstones and wackestones at the Signal Mountain-McKenzie Hill contact, Ring Top Mountain measured section. The Jacob's staff is on the top of the orange-mottled interval. The McKenzie Hill Formation (mh) is above and the Signal Mountain Formation (sm) is below.

Figure 21. Signal Mountain-McKenzie Hill contact, Ring Top measured section. The base of the Jacob's staff is on the contact; McKenzie Hill Formation (mh) is above and the Signal Mountain Formation (sm) is below. Note how poorer outcrop makes contact placement much more difficult (refer to Figure 17).

obvious lithostratigraphic break is usually chosen as the approximate contact.

Basic Log of the Formation

Research concentrated on a detailed examination of the Bally Mountain measured section (Figure 22). Best exposed at this location, the Signal Mountain Formation is part of a nearly continuous outcrop of homoclinal beds striking northwestward and dipping northeastward. The average dip across the upper Fort Sill Formation is 36° to the 046° azimuth. Up the section dips increase gradually to an average of 41° to the 051° azimuth across the lower 300 feet of Signal Mountain Formation and 41° to the 053° azimuth across the remainder of the Signal Mountain Formation and into the lower McKenzie Hill Formation.

The Signal Mountain Formation is 754.0 feet thick. Brookby (1969) marked the Cambrian-Ordovician boundary, the base of his measured section, with red paint at a location in the SE/4, section 26, approximately 1,850 feet W.E.L. and 1,550 feet N.S.L. Measuring to Brookby's Cambrian-Ordovician marker, the author determined the Cambrian portion of the Signal Mountain to be 339 feet thick and consequently the Ordovician portion is 415.0 feet thick. Previous investigators (refer to Chapter I, previous investigations) measured 350 to 400 feet of Signal Mountain at this location, at least 50 feet of which this author assigns to the upper Fort Sill Formation. The actual thickness of Signal Mountain Formation measured by these previous investigators would have been approximately 300 to 350 feet. The author has been unable to account for the difference in measured thicknesses, but surmises that a

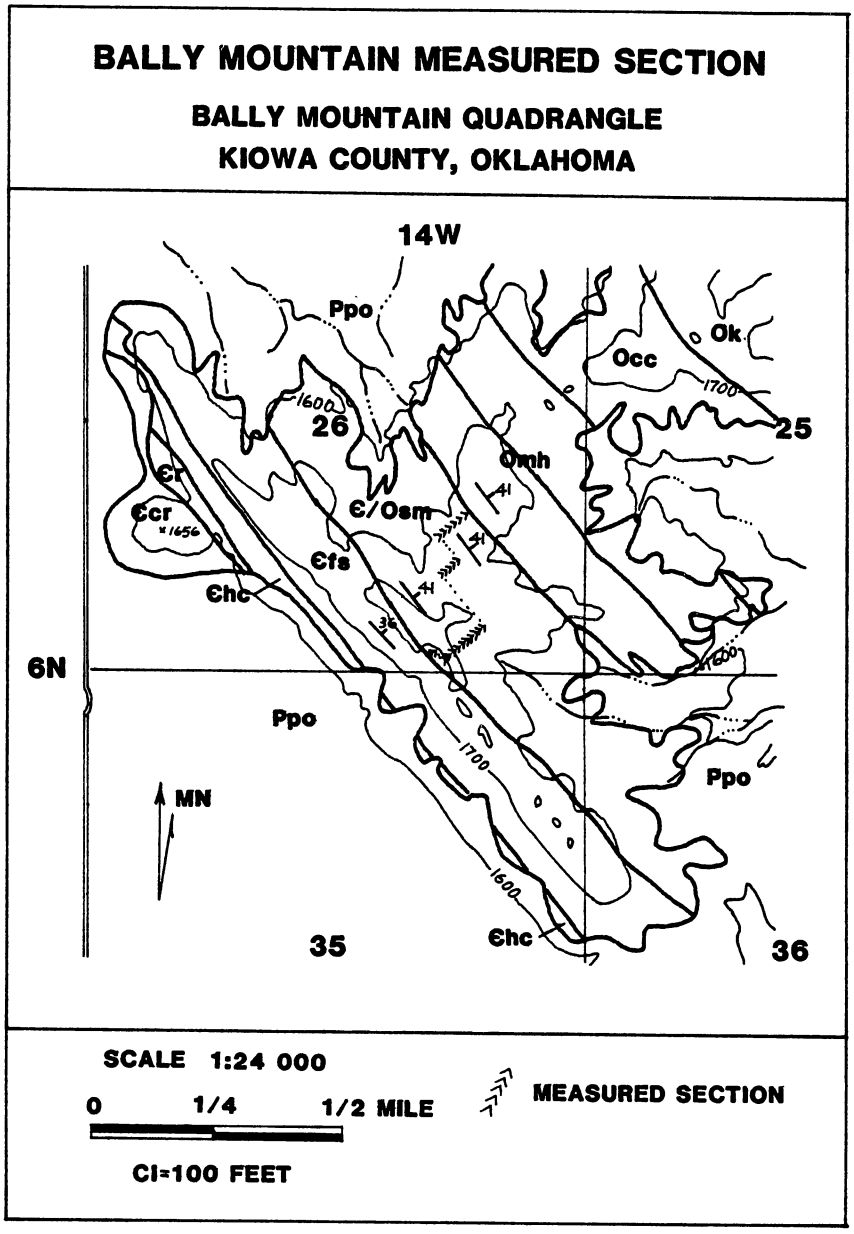

Figure 22. Bally Mountain measured section location map. (Compiled from maps of Donovan and Cloyd, 1983; Tsegay, 1983). Lithologic symbols are identified in Figure 4.

lesser dip, of approximately 20°, or a less accurate method of measurement was used.

Plate I is a detailed lithostratigraphic log of the Bally Mountain measured section. The log was primarily based on field observations and descriptions of prepared representative samples collected on an average of 4 foot spacings. Textures observed in thin section were used as a supplementary source of information.

The log's scale is 1 inch = 8 feet. Vertical columns record the footage, outcrop profile, lithology, fossils, sedimentary structures, particle/crystal size, occurrence of stylolites, and special comments. Symbols and abbreviations (Swanson, 1981; Ragland, 1983) were used to simplify and condense detailed hand-sample descriptions. Dots, alongside the outcrop profile, indicate from where hand-samples were collected.

In general, the Signal Mountain Formation consists of abundant intraformational (IFC) limestones, grainstones, packstones, and wackestones, with allochems of intraclasts and fossils in two zones (a) from 0 to 277 feet above the base and (b) from 480 to 754 feet above the base. The zone from 277 to 480 feet above the base contains abundant mudstones, although the other lithotypes are still common. Some key marker beds are as follows:

Feet above the base	Comments
729.0-728.0	Ferroan dolomitized cone-shaped gastropod shells
706.5	Silicified brachiopod shells
693.9	Silicified brachiopod shells
649.7-648.7	Imbricate packed, flat, very coarse pebble IFC limestone

Feet above the base	Comments
639.0-638.0	Small scale trough cross-bedding in flat pebble IFC limestone with thinly laminated mudstones
635.0-634.0	Small scale through cross-bedding in very thinly interbedded intraclast sand grainstones, fossil-peloid wackestones, and mudstones
629.0-626.0	Ferroan dolomitized cone-shaped gastropod shells
612.0-604.0	Ferroan dolomitized cone-shaped gastropod shells
591-586	Ooiliths
577-570	Chert nodules, ooliths
565.2	Silicified burrows
560-559	Chert nodules
548-547	Chert nodules, ferroan dolomitized-silicified gastropod shells
533-531	Ooliths
531-528	Ferroan dolomitized gastropod shells
513-510	Ooliths
490-489	Small scale trough cross-bedding
465-464	Silicified brachiopod shells, chert nodules
457-456	Silicified brachiopod shells
438-436	Silicified brachiopod shells
428-425	Ooliths
400-394	Chert nodules
383-380	Ooliths
358-354	Ooliths

Feet above the base	Comments
326.5	Irregular spheroidal IFC limestone wackestone similar to RM 321.0 & RM 402.6
267-266	Ooliths
251-235	Ooliths
214.5	Silicified ornamented brachiopod shells
190.5	Silicified ornamented gastropod shells
176-173	Ooliths
147.0	Silicified brachiopod shells
138-133	Ooliths, chert nodules
119.2	Silicified brachiopods
111-110	Chert nodules
101.6	Silicified ornamented brachiopod shells
96-93	Chert nodules, silicified brachiopod shells, silicified burrows
28-22	Ooliths
11.8-9.0	Fort Sill Formation boundstone facies interfinger
9.0-2.8	Orange-mottled dolomitic mudstone
2.8-0.0	Thinly interlaminated light gray to light brown microsparitic mudstone and light orange crystalline dolostone.
below base	Fort Sill Formation algal mound boundstones and algal intraclast sand grainstones

Ring Top Mountain Measured Section

The Ring Top Mountain section (Figure 23) was measured to establish the Signal Mountain thickness in Blue Creek Canyon and to look for any

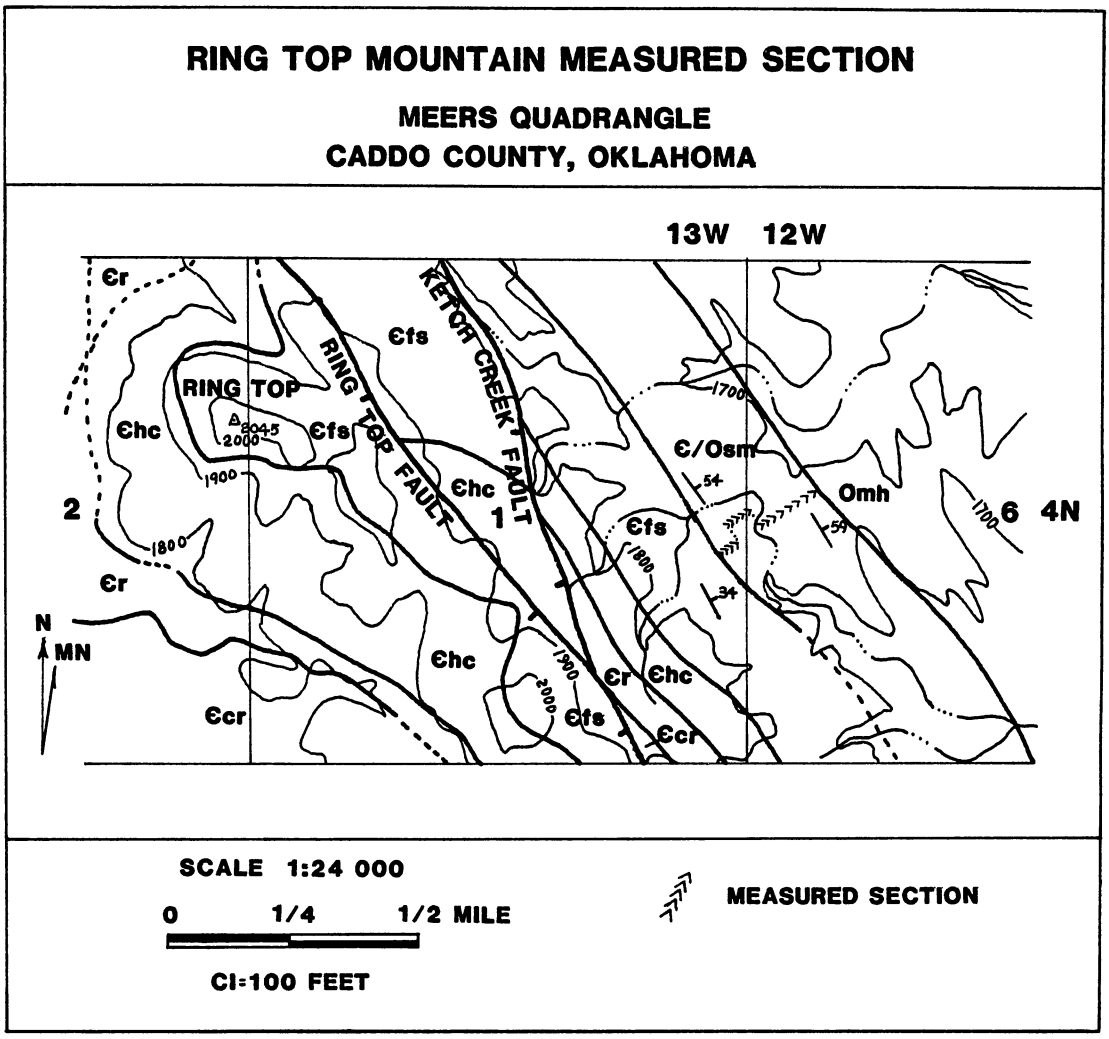

Figure 23. Ring Top Mountain measured section location map. (Geology adapted from Stubbs, 1983). Lithologic symbols are identified in Figure 4.

major lithologic or sedimentologic changes. This section is also composed of relatively homoclinal beds striking northwestward and dipping northeastward. Abundant joints, fractures, and small normal faults (as much as 5 feet of throw) break and offset the section. The lower section is especially broken up. These structural features are related to the tectonics that formed the northwest to southeast trending Ring Top and Ketch Creek Faults located approximately a half mile to the southwest. Fortunately the structural elements do not destroy the general continuity of beds. Outcrop exposure is good to poor.

The upper Fort Sill Formation dips 34° to the 061.5° azimuth. Dip and dip direction of Signal Mountain beds are as follows:

Feet above the base	Dip-dip direction (azimuth)
829 to 600	41° - 059°
600 to 500	44° - 064°
500 to 415	42° - 059°
415 to 265	40° - 059°
265 to 185	37° - 059°
120 to 185	35° - 054°
120 to 0	32° - 058°

The Ring Top Mountain section of Signal Mountain Formation is 829.0 feet thick. Thicknesses of the Cambrian and Ordovician portions of the Signal Mountain were not measured, because the Cambrian-Ordovician boundary has not been located there. Brookby (1969) reported 440 feet of Ordovician Signal Mountain at a Chandler Creek section in the NE/4, SE/4, section 17-T4N-R12W, approximately 2.5 miles to the southeast. Brookby did not measure the Cambrian Signal Mountain, but, assuming the Signal Mountain has a constant thickness, the Cambrian-Ordovician

boundary is estimated to be 389 feet above the Fort Sill-Signal Mountain Formational contact.

The following is a summary of observations made while measuring the Ring Top section:

Feet above the base	Comments
829.0	Top of the Signal Mountain Formation
781.6	Abundant silicified gastropod shells
709.0	Ferroan dolomitized burrows and gastropod shells
704.0	Ferroan dolomitized burrows
620.0	Vertical stylolites with chert nodules
547.0	Silicified brachiopod, gastropod, and pelmatazoan fragments
540.5	Ferroan dolomitized burrows, highly bioturbated
530.0	Silicified brachiopod shells
408.6	Medium scale trough cross-bedded, yellow, intraclast sand grainstone
402.6	Irregular spheroidal pebble IFC limestone similar to BM 326.5
371.5	Ferroan dolomitized burrows
338.0	Ferroan dolomitized-silicified fossil hash
321.0	Irregular spheroidal pebble IFC limestone similar to BM 326.5
284.0	Silicified brachiopod shells
238.3	Silicified fossil hash, brachiopod and pelmatazoan fragments
227.0	Silicified pelmatazoan hash
216.2	Ferroan dolomitized burrows, highly bioturbated
208.7	Silicified pelmatazoan hash

Feet above the base	Comments
199.8	Silicified pelmatazoan hash
197.4	Silicified gastropod and brachiopod fragments
193.2	Silicified pelmatazoan hash, small wormy chert nodules, silicified burrows
185.5	Ferroan dolomitized pelmatazoan and gastropod shell fragments
178.4	Silicified pelmatazoan and gastropod shell fragments
168.5	Silicified pelmatazoan fragments and small chert nodules
153.0	Nodular chert, ferroan dolomitized-silicified burrows, silicified fossil hash
147.7	Silicified fossil hash
112.5	Silicified-ferroan dolomitized cone-shaped gastropod shells
87.7	Silicified brachiopod shells and silicified-ferroan dolomitized cone-shaped gastropod shells
11.4	Top of Fort Sill Formation boundstone facies interfinger
4.0	Top of the orange-mottled, dolomitic mudstone interval
0.0	Signal Mountain-Fort Sill Formational contact
below base	Upper Fort Sill white to pale light gray, massive, hammocky, fenestrate algal mound boundstones and algal intraclast sand grainstones

Principal Lithotypes

The principal lithotypes of the Signal Mountain Formation are clastic limestones and mudstones. Clastic limestones include grainstones,

packstones, wackestones, and IFC limestones. Allochems present are abundant intraclasts, rare ooliths, common peloids, and abundant fossils. Fossils consist of abundant trilobite carapaces, abundant pelmatazoan parts, common gastropod shells, and common brachiopod valves. Grainstones, packstones, and wackestones may be composed of one principal allochem type or any combination thereof.

CHAPTER IV

PETROGRAPHIC CONSTITUENTS OF THE SIGNAL MOUNTAIN FORMATION

Introduction

The Signal Mountain Formation is composed of predominantly limestone with moderate amounts of dolomite. Siliciclastic rocks are minor and usually recognized only in thin section.

The following are the chief constituents of the Signal Mountain Formation:

1. Intraclasts
2. Ooids
3. Peloids
4. Skeletal Fragments
5. Siliciclastics
6. Diagenetic Constituents
7. Miscellaneous Diagenetic Features.

A petrographic log of the thin sections from the Bally Mountain measured section is provided in Appendix A.

Intraclasts

Intraclasts are a principal component and characteristic texture of the Signal Mountain Formation. Intraclasts occur rarely as small

cobbles (64 to 128 mm), commonly as pebbles (2 to 64 mm) and sand (0.062 to 2 mm). Pebble and cobble intraclasts are primarily disc- and blade-shaped and may be thick or thin (Figures 24 and 25 respectively). Occasionally they are irregular spheroidal-shaped (Figures 26 and 27). Sand intraclasts are mostly angular to rounded grains similar to siliciclastic sands (Figure 28). Coarser sand size intraclasts may also be disc- and blade-shaped.

Most intraclasts are mudstone, but wackestones and packstones are also common. Few grainstones have contributed to the intraclast population. Some intraclasts are themselves fragments of intraformational conglomerates (IFC). All of the clasts are composed of lithologies found within the Formation, indeed in many places clasts clearly were derived from beds lying immediately beneath the conglomerate horizon.

Ferroan dolomite and hematite commonly selectively replaced the micrite of intraclasts. Dolomite formed sparry rhombs within the micrite. Hematite commonly rims clasts, is finely dispersed, and exceptionally it may have replaced the entire clast. A few intraclasts have been replaced by glauconite.

Ooids

Ooids are not common. They consistently range in size from 0.23 to 0.38 mm, are spherical to oblate, and composed of radial fibrous calcite (Figure 29). The nuclei are mostly pelmatazoan fragments, but commonly trilobite shell fragments and less commonly pellets, intraclasts, or gastropod shell fragments serve as nuclei. Many ooids are superficial. Ooids of this type are commonly oblate, have nuclei of trilobite shell

Figure 24. Thick disc- and blade-shaped pebble and cobble IFCs. Hand-sample BM 638.7 is a flat cobble IFC limestone. The matrix is composed of pelmatozoan and intraclast sand cemented by sparry calcite. IFCs are thinly laminated mudstone and peloidal wackestone. Note the erosional surface from which these IFCs were derived.

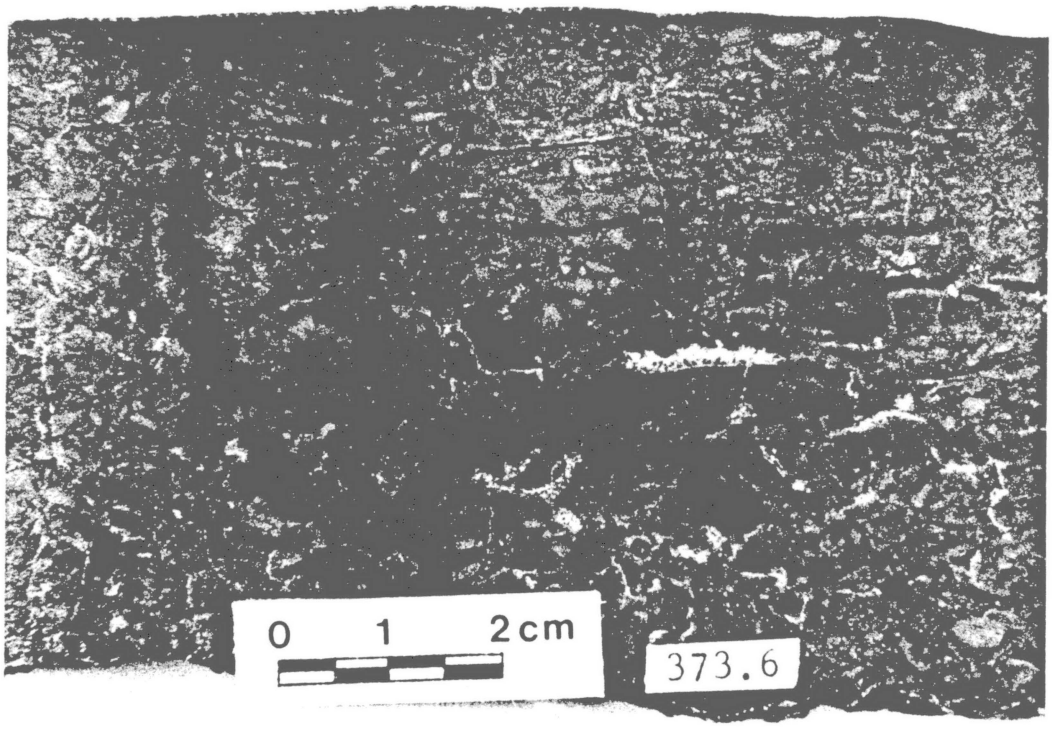

Figure 25. Thin disc- and blade-shaped pebble IFCs. Hand-sample BM 373.6 is a flat pebble IFC limestone. The matrix is micrite and locally drusy calcite. This sample shows bimodal imbricate stacking of the IFCs. IFCs are mudstone.

Figure 26. Irregularly spheroidal-shaped pebble IFCs. A sandy spheroidal pebble IFC (A) is very thinly interbedded with mudstones and pebbly intraclast sand packstone-wackestones. Note the erosional scale is in inches on the left and centimeters on the right. This interval is 326.5 feet above the base of the Bally Mountain measured section.

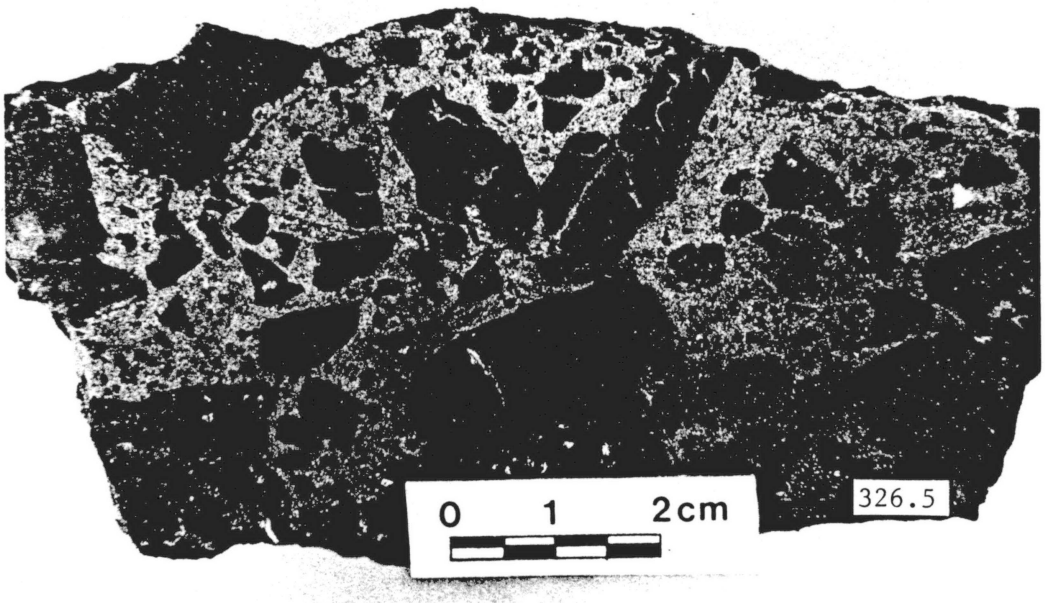

Figure 27. Irregularly spheroidal-shaped pebble IFC limestone, BM 326.5. This hand-sample was collected from the interval shown in Figure 26. The matrix is a trilobite-pelmatozoan, intraclast sand cemented by micrite.

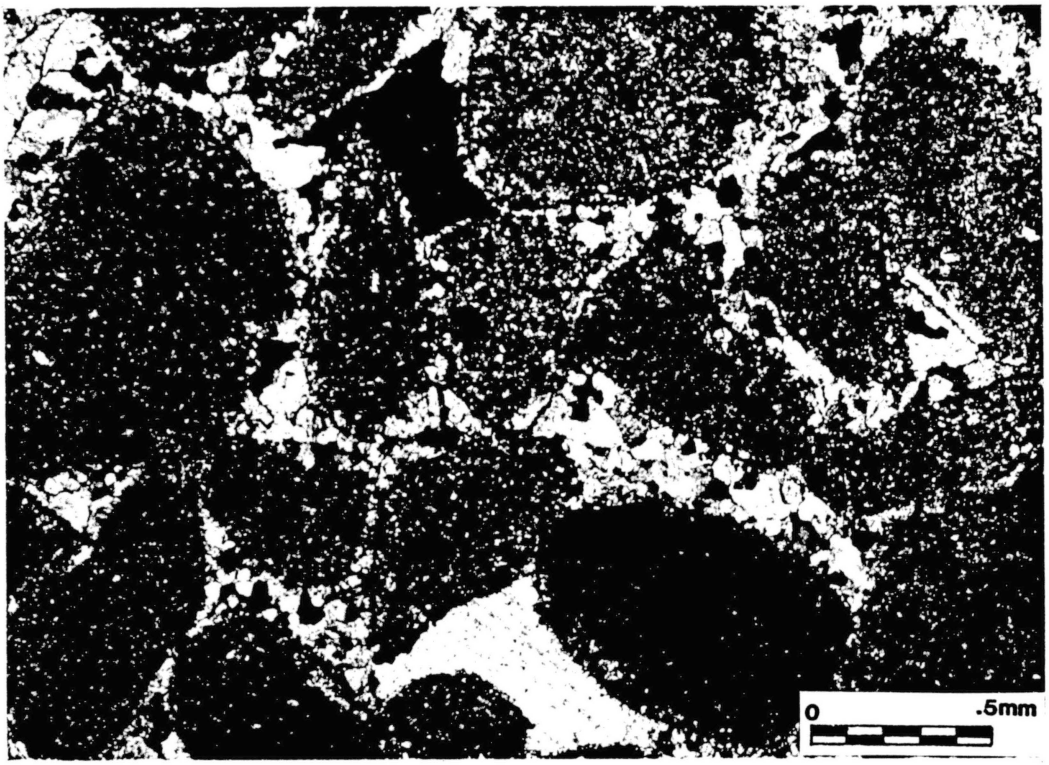

Figure 28. Coarse sand intraclasts. The photomicrograph of BM 251.6, crossed nicols (XN), illustrates an intraclast sand grainstone. Intraclasts are subrounded to well rounded clasts of mudstone. Cement is a single generation of drusy ssparite.

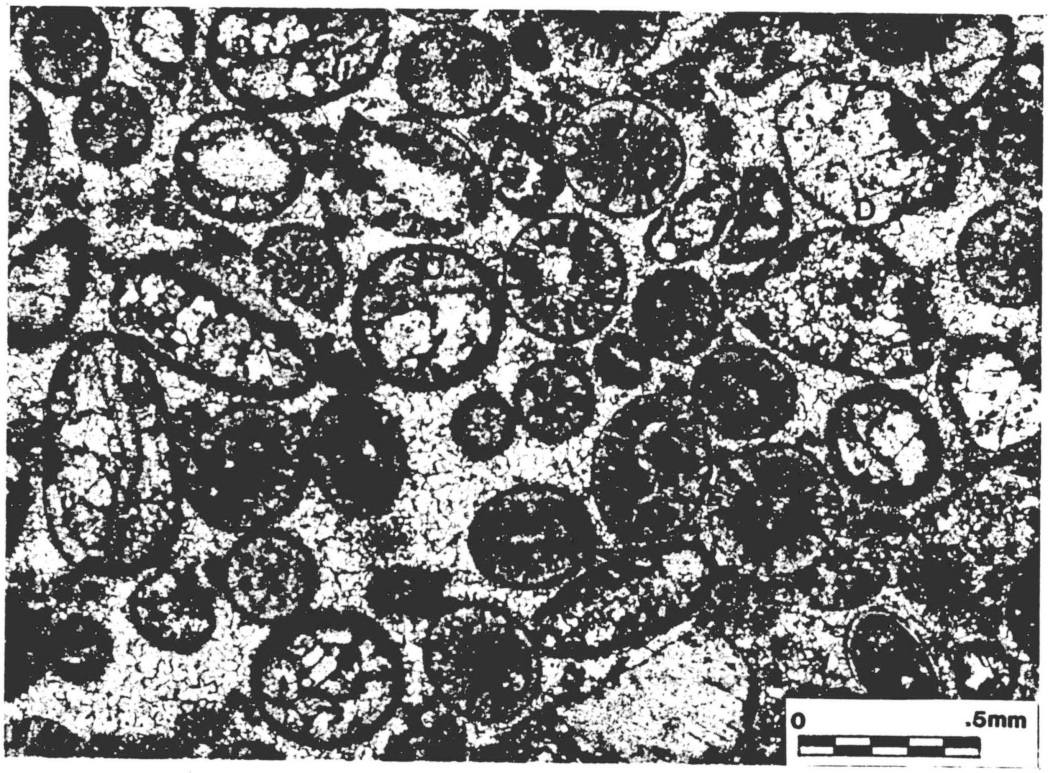

Figure 29. Ooids. The photomicrograph of BM 532.8, plane polarized light (PPL) illustrates an oolitic grainstone. Ooids display a radial fibrous calcite fabric with nuclei of pelmatozoan and trilobite shell fragments. Ferroan dolomite (D) (baroque ankerite), stained blue, selectively replaced pelmatozoan and micrite nuclei. Note that there are several superficial ooids (SO). Cement is a single generation of drusy calcite.

or elongate palmatozoan fragments, and range in length from 0.30 to 0.70 mm (somewhat larger than normal ooids).

Ferroan dolomite, usually baroque ankerite, commonly has replaced the pelmatazoan and micrite nuclei of ooids. Some ooids appear to have been replaced by hematite.

Peloids

Peloids are a common constituent of many lithologies. They form discrete laminae, but more commonly are disseminated in a lime mud or sparry matrix with other allochems. Most peloids are consistently 0.04 to 0.07 mm in diameter, have a rounded regular shape, and appear rich in organic matter (Figure 30). These parameters, coupled with the common gastropod shells and abundant bioturbation throughout the Formation, suggest that the peloids are faecal pellets.

Less common are peloids of 0.07 to 0.20 mm in diameter. Some peloids of this size may also be faecal, but the author believes the majority are very fine to fine sand-sized intraclasts.

Skeletal Fragments

Trilobites

Trilobites are abundant throughout the Formation. As a rule trilobites occur as broken fragments. Whole trilobite shells seem to be rare; they are seldom found whole during the extraction of hand-samples from the outcrop. Fragments and whole shells range from 0.05 to 10 mm long, but are most commonly 0.50 to 3 mm long. Two types of trilobites have been defined in thin section: (i) thin shell, 0.02 to 0.05 mm

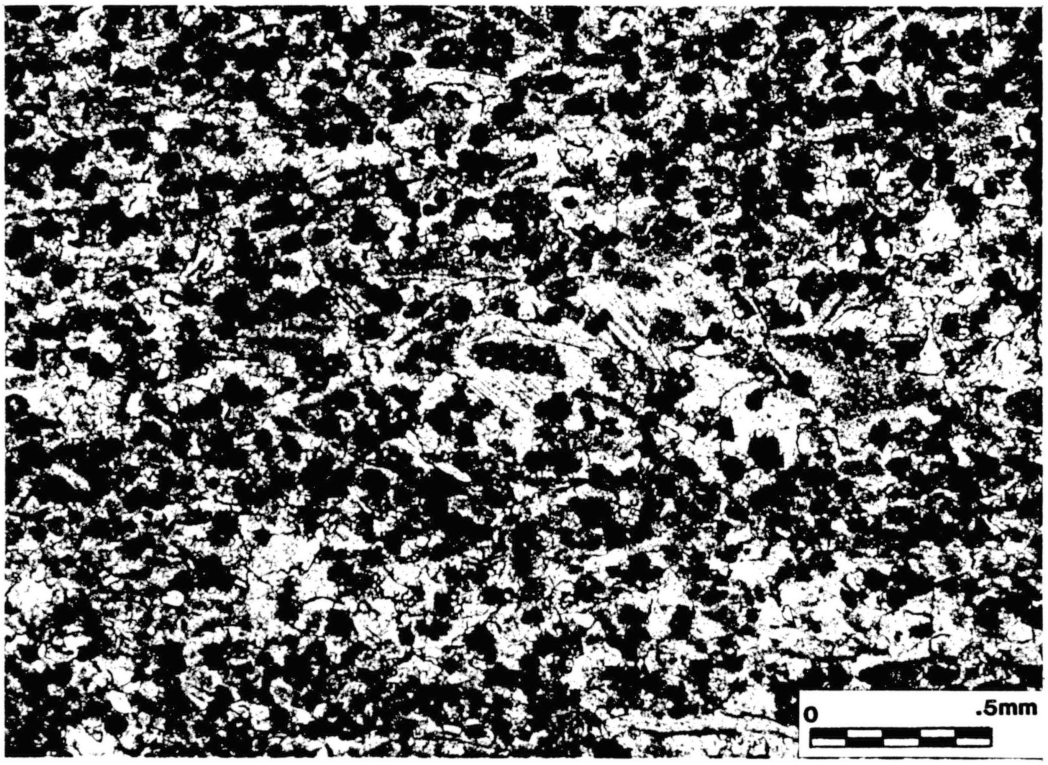

Figure 30. Peloids interpreted to be fecal pellets. The photomicrograph of BM 57.0A (PPL) illustrates a slightly dolomitic pelleted pelmatozoan sand grainstone. Note the consistency of size, shape, and composition of the pellets. This grainstone is primarily cemented by syntaxial calcite overgrowths on pelmatozoan parts.

thick and (ii) thick shell, 0.12 to 0.25 mm thick (Figures 31 and 32). Shell thickness may be of paleocological significance. Trilobites of the Signal Mountain Formation were identified in Chapters I and III.

Pelmatozoans

Pelmatozonas are difficult to see in hand-sample, but are readily recognizable in thin section. Plates and columnals are the recognizable skeletal parts (Figure 33). The skeletal parts vary in size from 0.1 to 2.5 mm in diameter, but most commonly fall within the 0.30 to 0.55 mm range. Although the fossils are now low magnesium calcite, petrographic evidence confirms that the pelmatozoans were once high magnesium calcite (Figure 34). Modern pelmatozoans have a high Mg content and it is believed that ancient pelmatozoans did as well (Tucker, 1981). Some pelmatozoan skeletal parts are partly to completely replaced by ferroan dolomite and silica.

Brachiopods

Although brachiopod shells are relatively common, they are generally concentrated in a series of discrete zones throughout the Formation. They are commonly exposed on weathered bedding-plane surfaces at outcrop (Figure 35). Whole shells range in size from 1.5 to 8 mm across and shell fragments are commonly 0.30 to 0.80 mm across. Most shells can be referred to the Orthis genus; Ordovician brachiopods of the Signal Mountain Formation have been identified as the Apheoorthis species (Brookby, 1969). In addition, the author found phosphatic inarticulate

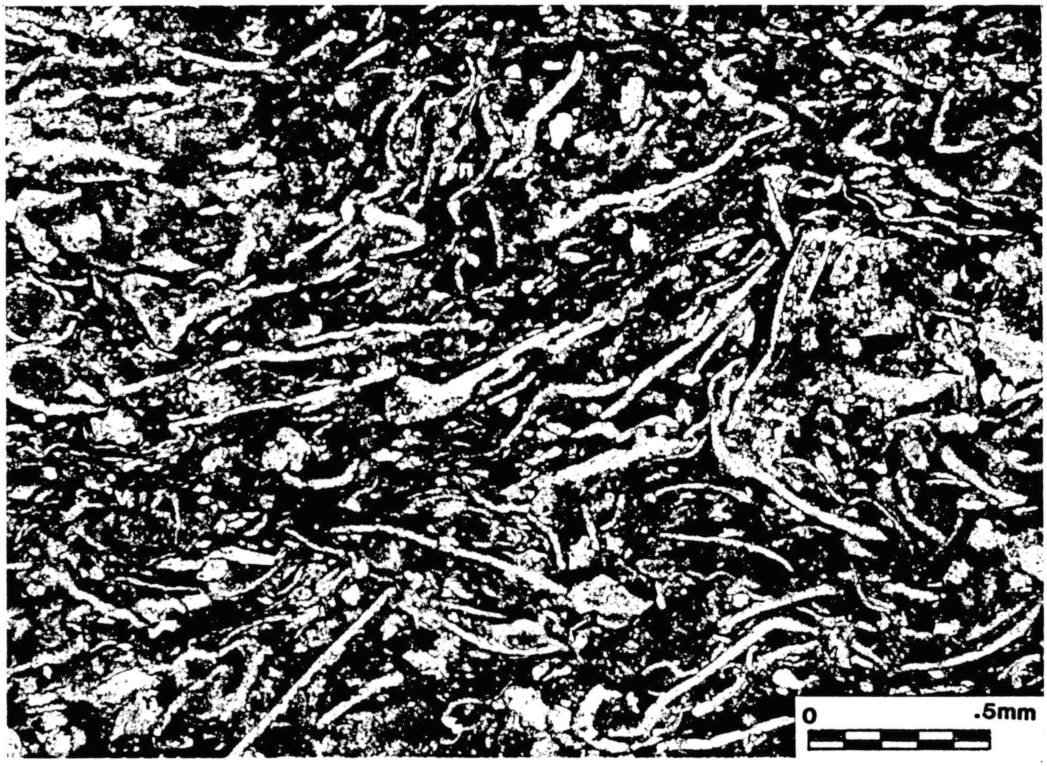

Figure 31. Thin-shelled trilobites. The photomicrograph of BM 537.0 (PPL) illustrates a trilobite hash packstone. Trilobite shells are 0.02 to 0.03 mm thick. Note how the trilobite carapaces are imbricately packed.

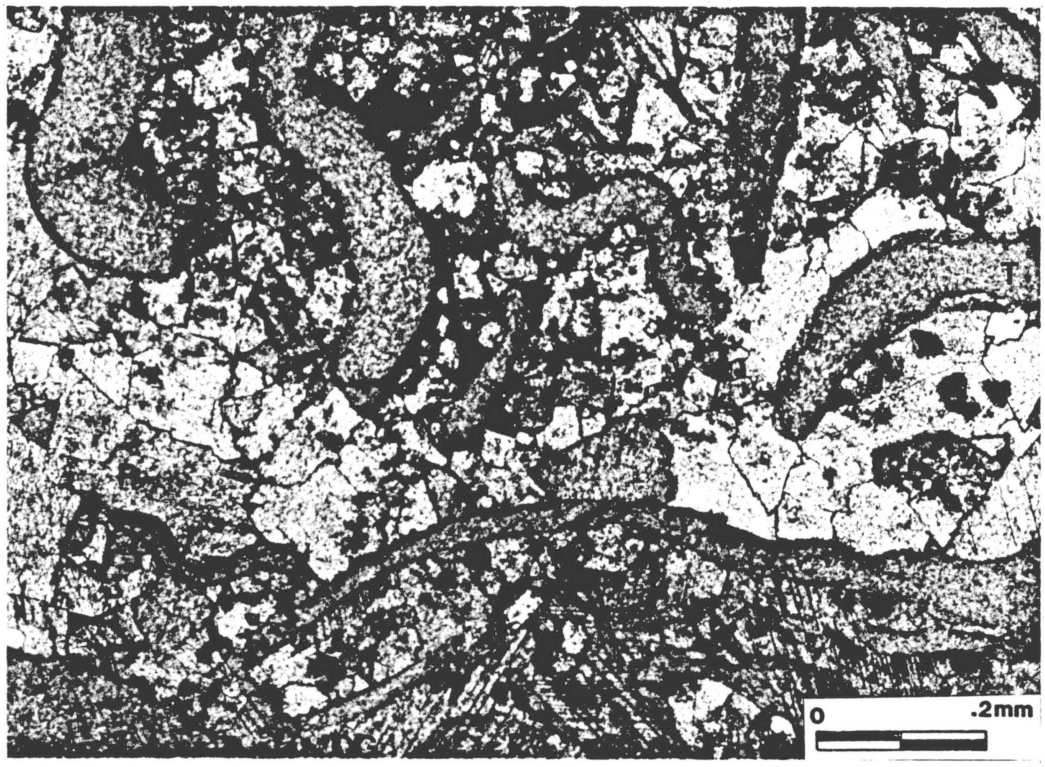

Figure 32. Thick shelled trilobites. The photomicrograph of BM 370.2 (PPL) illustrates thick shell trilobites (T) in a dolomitic pelmatozoan (P)-trilobite hash grainstone. The principal cement in the photograph is baroque ankerite and the secondary cement is syntaxial calcite overgrowths (OG) on pelmatozoan fragments. Close inspection of the dolomite crystals identifies ghost structures of pelmatozoan fragments, now seen as dusty crystal centers. The ankerite has completely replaced many pelmatozoan parts and their overgrowths.

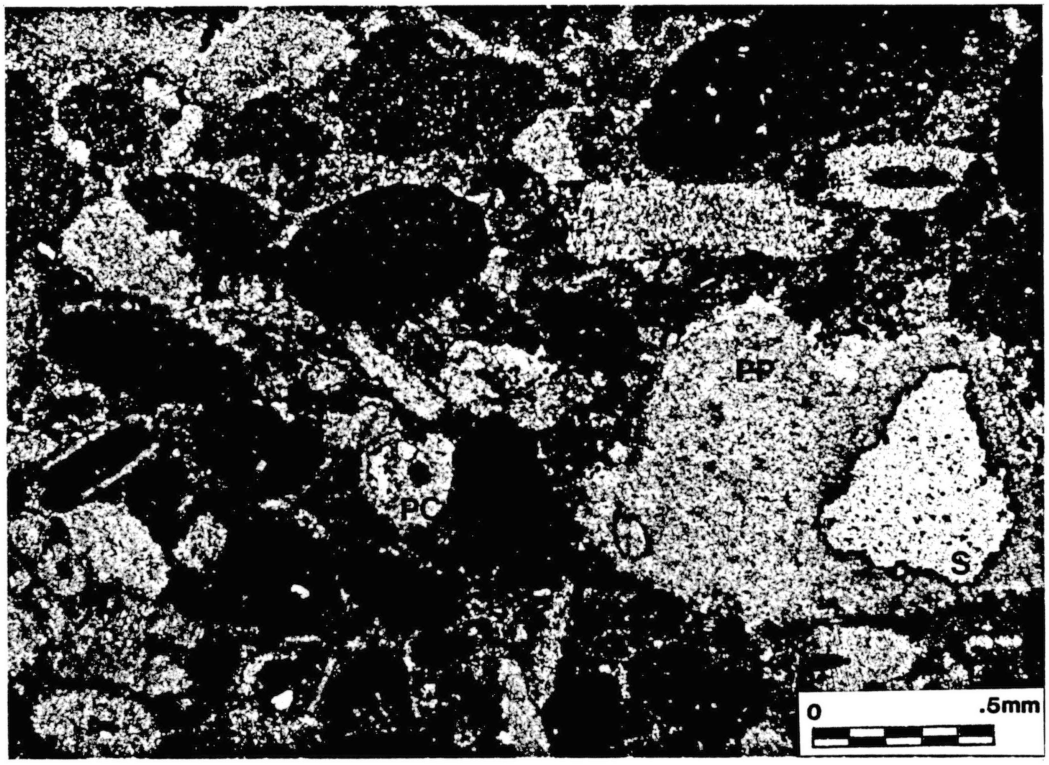

Figure 33. Pelmatozoan plates and columnals. The photomicrograph of BM 556.0 (PPL) illustrates pelmatozoan columnals (PC) and plates (PP) in an intraclast pelmatozoan sand packstone. Some pelmatozoan parts are replaced by silica (S).

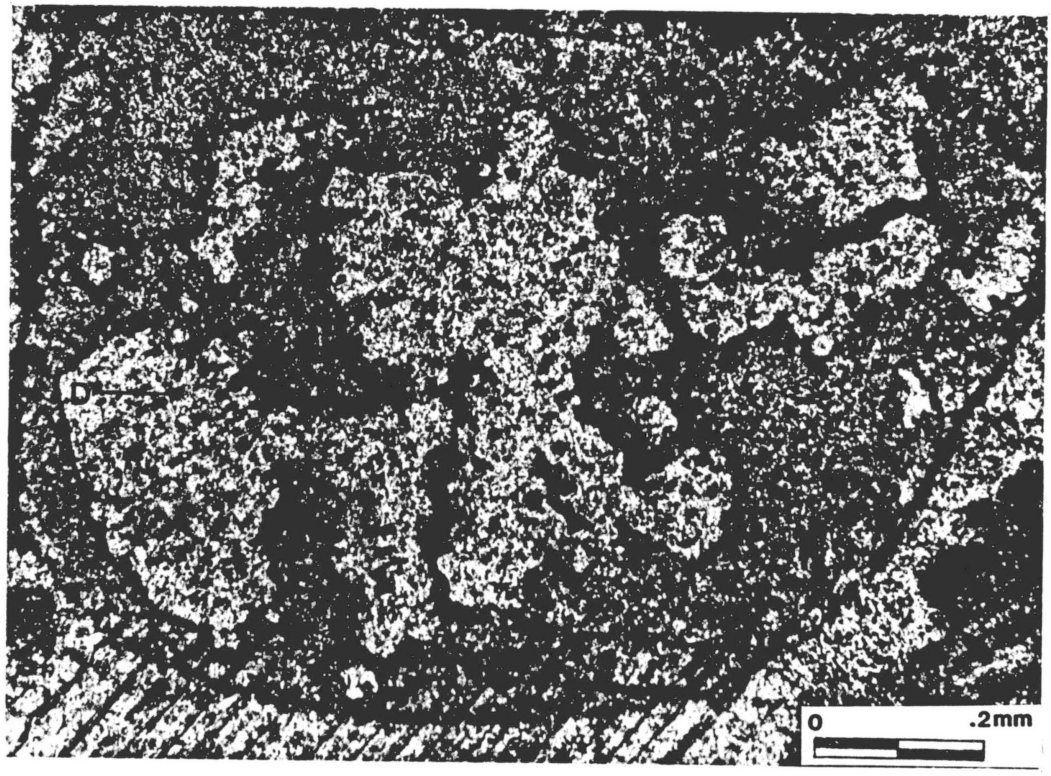

Figure 34. Microdolomite inclusions in a partly silicified pelmatozoan plate. The photomicrograph is from BM 24.5 B (PPL) and illustrates a partially silicified (S) pelmatozoan plate (PP) with numerous microdolomite (D) inclusions. These inclusions formed before silicification at the time the pelmatozoan plate converted from high magnesium to low magnesium calcite (Leutloff and Meyers, 1984). Microdolomite inclusions are clearly seen where the pelmatozoan plate is silicified. They are present in the non-silicified portion of the plate, but not easily recognizable in the photograph.

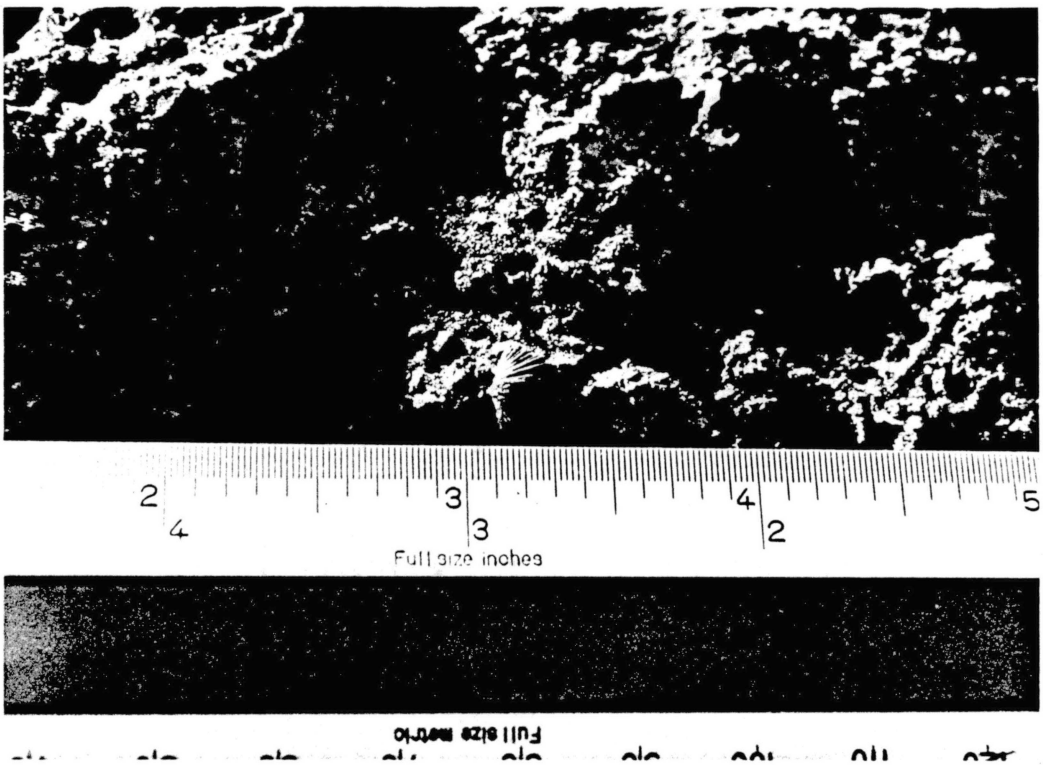

Figure 35. Silicified Oorthis brachiopod shell exposed on a bedding plane surface. The photograph was taken 119.2 feet above the base of the Bally Mountain measured section.

Lingulella brachiopods in trace amounts in several thin sections. Brachiopod shells tend to be partially to completely silicified (Figure 36).

Gastropods

At outcrop gastropods are commonly exposed on weathered bedding plane surfaces. (Figure 37). Gastropods are more generally found as whole shells rather than broken fragments. Whole shells range in size from 2 to 10 mm across and broken fragments are 0.25 to 1 mm across. Shell walls are typically drusy sparite (Figure 38) with no internal structure preserved. These shell textures are characteristic evidence that the crystallization of calcite occurred in a void produced by the dissolution of an originally aragonitic shell. Ferroan dolomite (Figure 39) and silica also commonly fill shell voids.

Siliciclastics

Minor amounts (trace to 3%) of siliciclastics are commonly dispersed throughout the Signal Mountain Formation. Grain sizes range from 0.02 to 0.2 mm (medium silt to fine sand). The vast majority of siliciclastic grains are 0.02 to 0.05 mm in size (medium to coarse silt). Their size makes the grains difficult to see in hand samples, but they are readily identifiable in thin section (Figure 40). In thin section, many limestones contain as much as 30% siliciclastics whereas others surprisingly contained siltstone laminae, the existence of which was not apparent in hand specimen (Figure 41).

The siliciclastics are almost wholly quartz. Plagioclase, orthoclase, microcline, and muscovite are present in trace amounts.

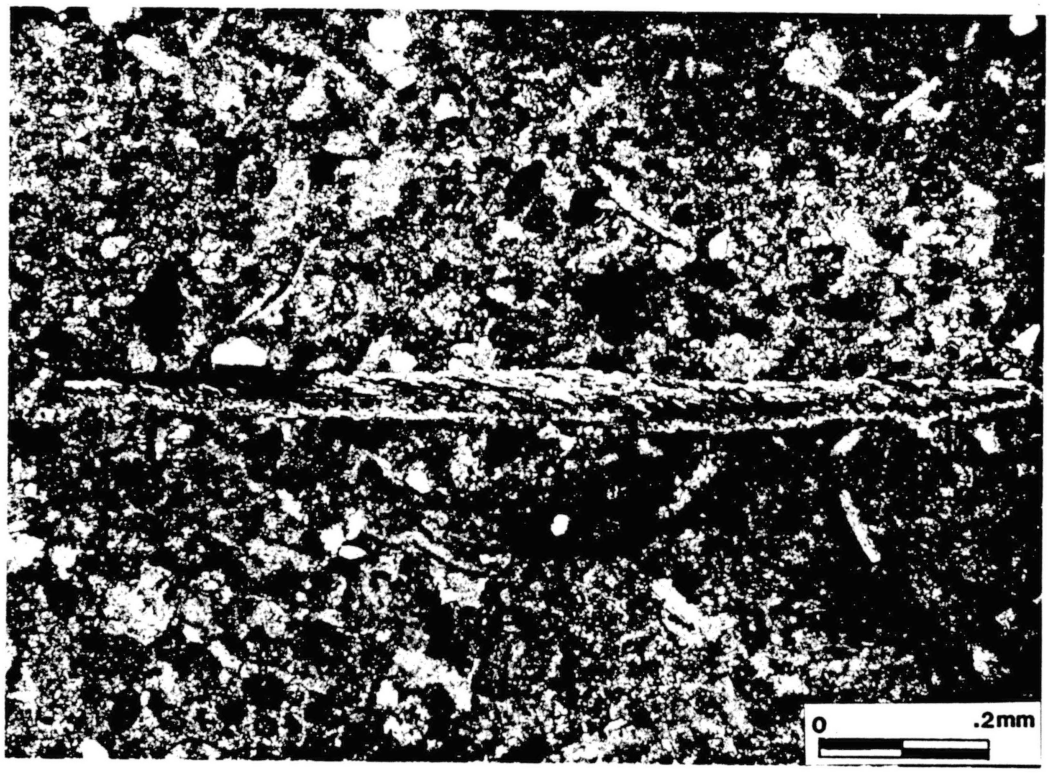

Figure 36. Partially silicified brachiopod shell. The photomicrograph of BM 146.5 (XN) illustrates a partially silicified brachiopod shell in a peloidal pelmatozoan sand wackestone. Internal structure of the shell is preserved and accentuated by the silicification.

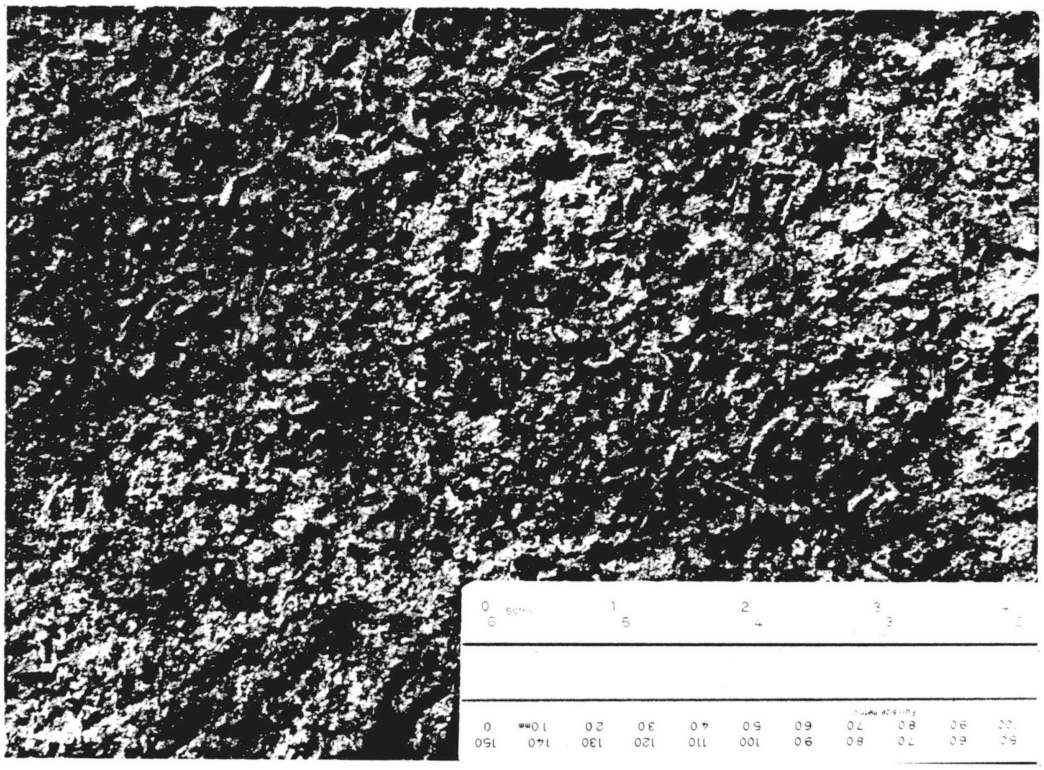

Figure 37. Ferroan dolomite gastropod shells exposed on a bedding plane surface. The photograph was taken 729.0 feet above the base of the Bally Mountain measured section. This zone is a distinctive marker bed.

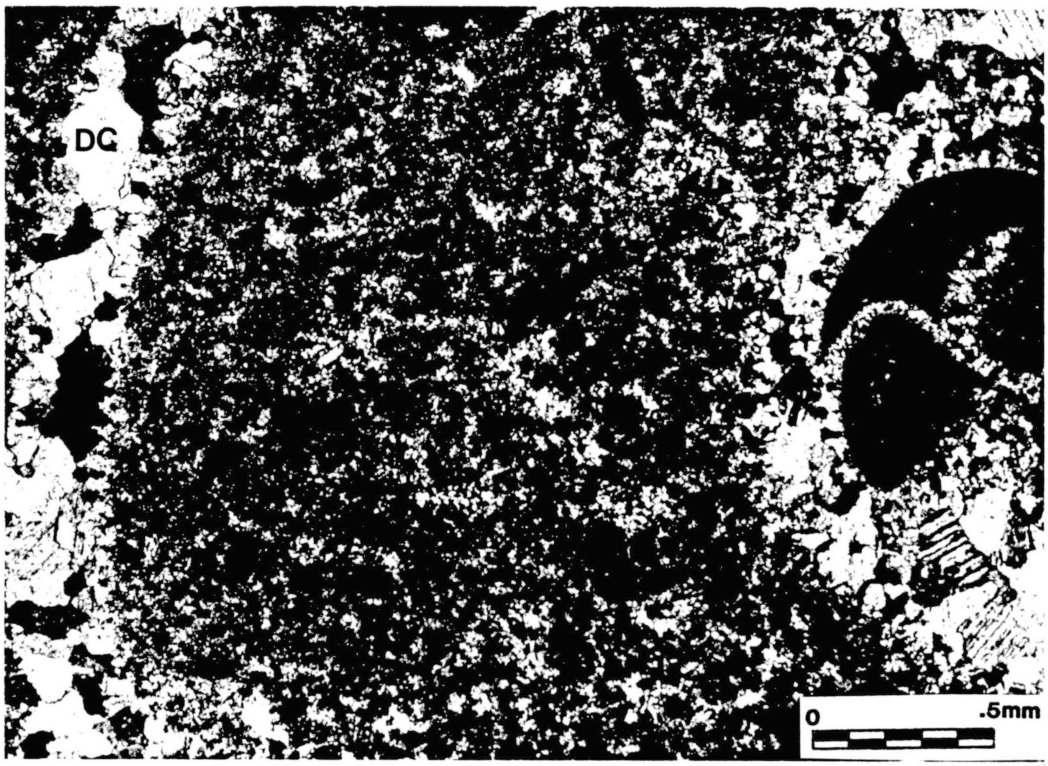

Figure 38. Drusy calcite gastropod shell. The photomicrograph of BM 24.5 (XN) illustrates that part of a gastropod shell was filled with isopachous (IC) (first stage) and drusy (DC) (second stage) calcite cements after dissolution of the original aragonite shell. Note that the internal cavity of the shell is filled with pellet-rich micrite.

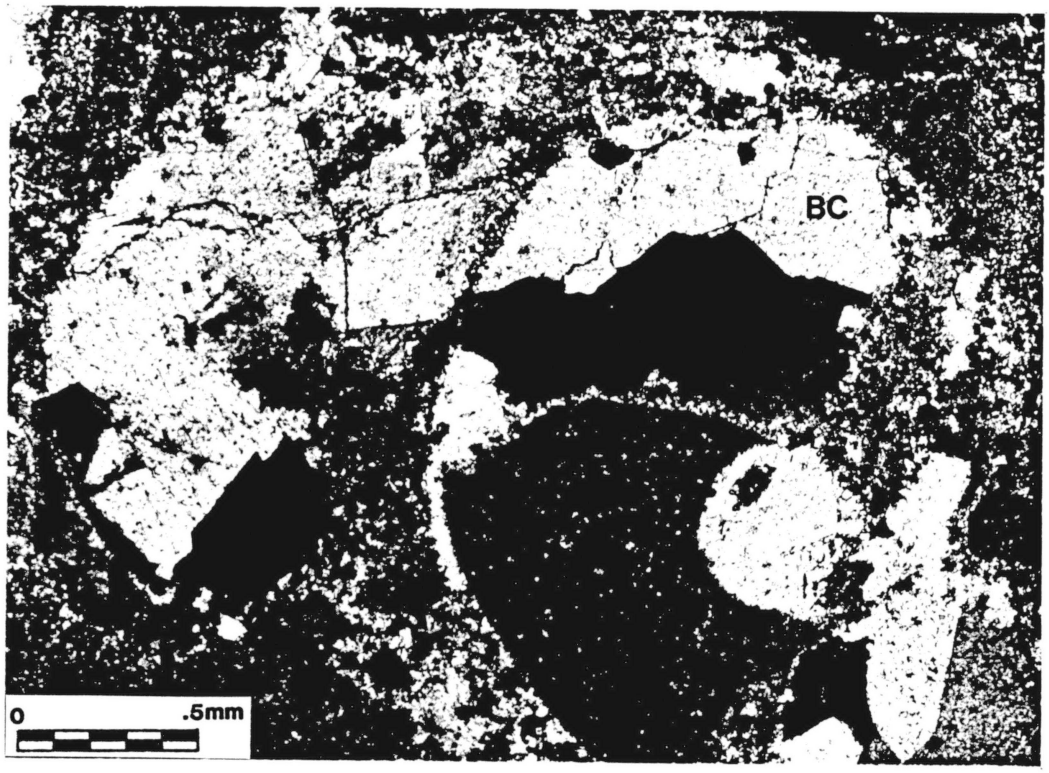

Figure 39. Sparry baroque ankerite and calcite gastropod shell. The photomicrograph of BM 627.8 (XN) illustrates that blocky calcite (BC) and baroque ankerite (A) spar have filled both the void created by the dissolution of the original aragonite shell and the top part of the internal cavity of the shell (creating a geopetal structure).

Figure 40. Quartz and feldspar (rare) in a pelleted gastropod wackestone. Siliciclastic grains are seen as white specks and compose up to 7% of the wackestone.

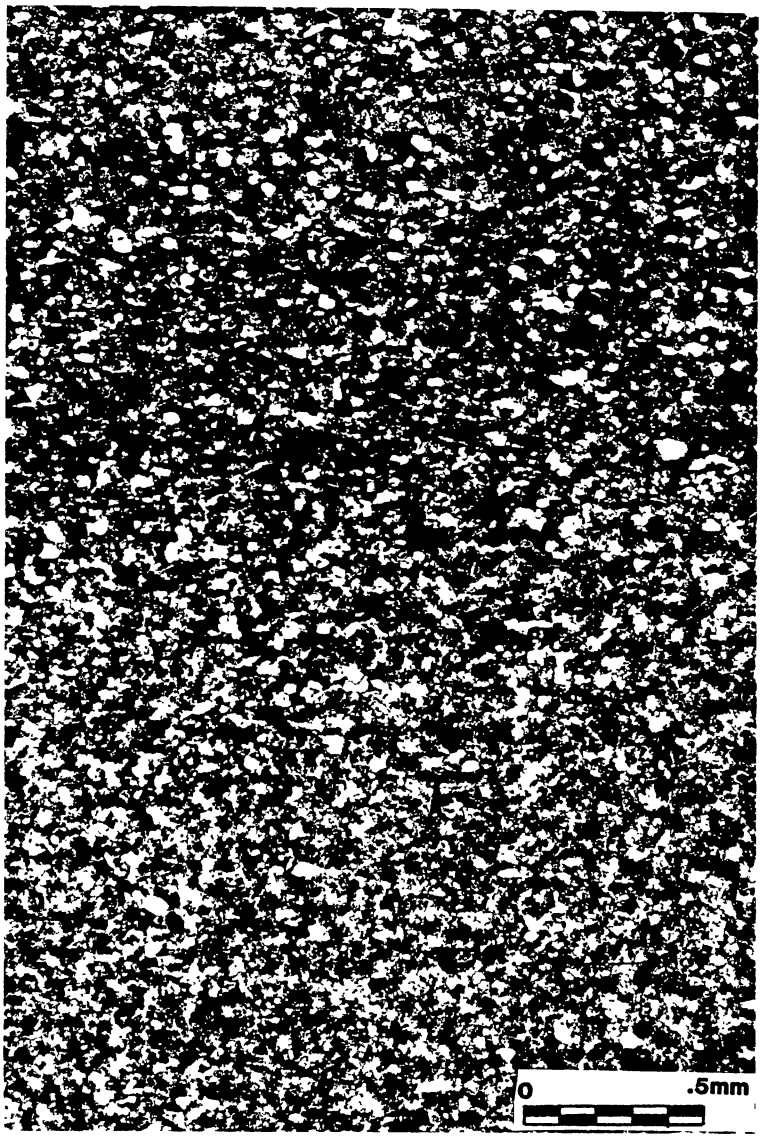

Figure 41. Siliciclastic rich peloidal grainstone grades upward into a calcareous siltstone. The photomicrograph of BM 406.0 (XN) illustrates siliciclastic silt composed of abundant quartz plus minor feldspar and muscovite. Calcite is stained pink. Quartz, feldspar, and muscovite silt are white to gray (partial extinction) to black (complete extinction).

Diagenetic Constituents

Calcite Spar

Calcite spar occurs as non-fibrous isopachous rims, pore-filling cement, and syntaxial overgrowths. Isopachous calcite is commonly the first stage in the cementation of voids and pores (Figures 42 and 43). Seldom can the isopachous rims be classified as ideally representative of fibrous calcite. Crystal size is generally less than 0.2 mm.

Pore filling calcite is drusy (Figure 44), blocky (Figure 45), and more rarely radiaxial fibrous (Figure 46). Crystal size ranges from 0.02 to 1.5 mm.

Syntaxial calcite overgrowths commonly form on pelmatazoan parts in grainstones (Figure 47) and constitute the major cementing agent of many pelmatozoan sand grainstones. The syntaxial overgrowths are typically euhedral and occasionally poikilotopic.

Fibrous calcite cement in voids associated with stylolites was also observed. This type of fibrous calcite is evidence for crystallization in some type of stress field.

Lime Mud

Microcrystalline calcite (micrite) is the most abundant constituent of the Signal Mountain Formation (Figure 48). Many of the lime muds have undergone partial neomorphism to microspar. Some of the mudstones contain minor amounts of skeletal debris and fine silt-sized quartz.

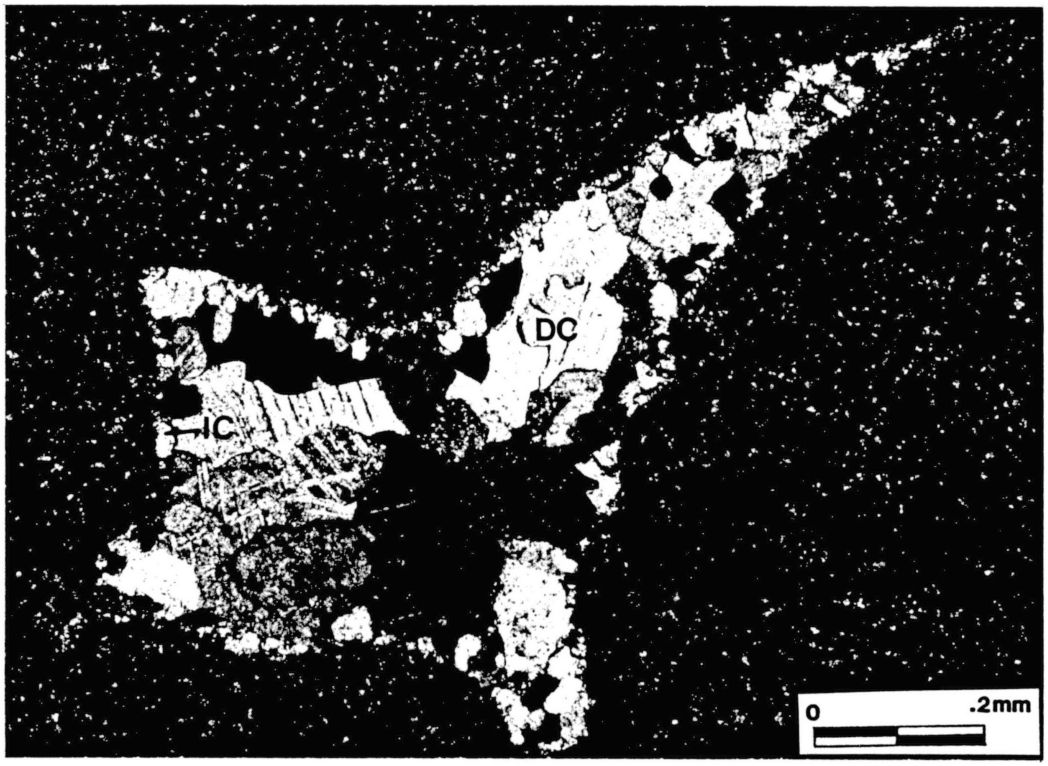

Figure 42. Isopachous calcite lining the walls of a Birdseye void. The photomicrograph of BM 502.0 (XN) illustrates a first stage isopachous calcite (IC) rim followed by a later stage of drusy calcite (DC) in the cementation of a fenestral texture in a mudstone. Note the clearly bimodal size distribution of the crystals.

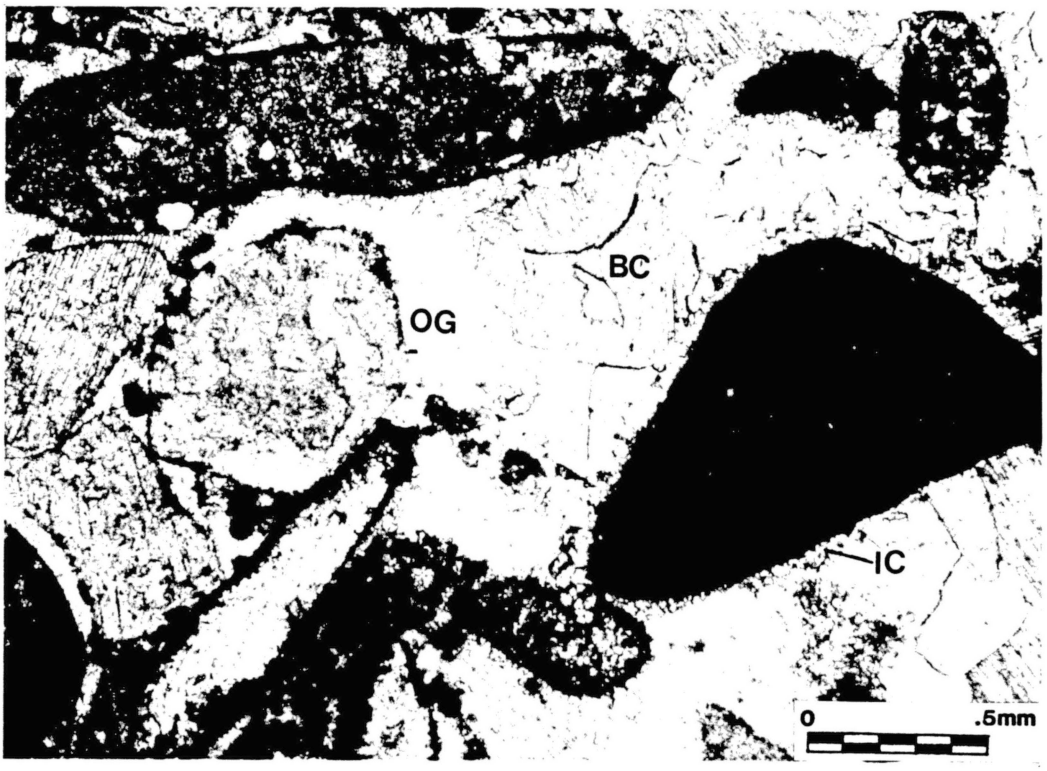

Figure 43. Isopachous calcite lining pore space. The photomicrograph of BM 310.0 (PPL) illustrates a first stage thin isopachous calcite (IC) rim around intraclasts and fossils in an intraclast pelmatozoan sand grainstone. Later cements, of syntaxial calcite overgrowths (OG) on pelmatozoan fragments and blocky calcite spar (BC), have completely filled the pore space. Note that many of the clasts exhibit micrite envelopes interpreted as being due to boring endolithic algae. Some pelmatozoans are partially silicified.

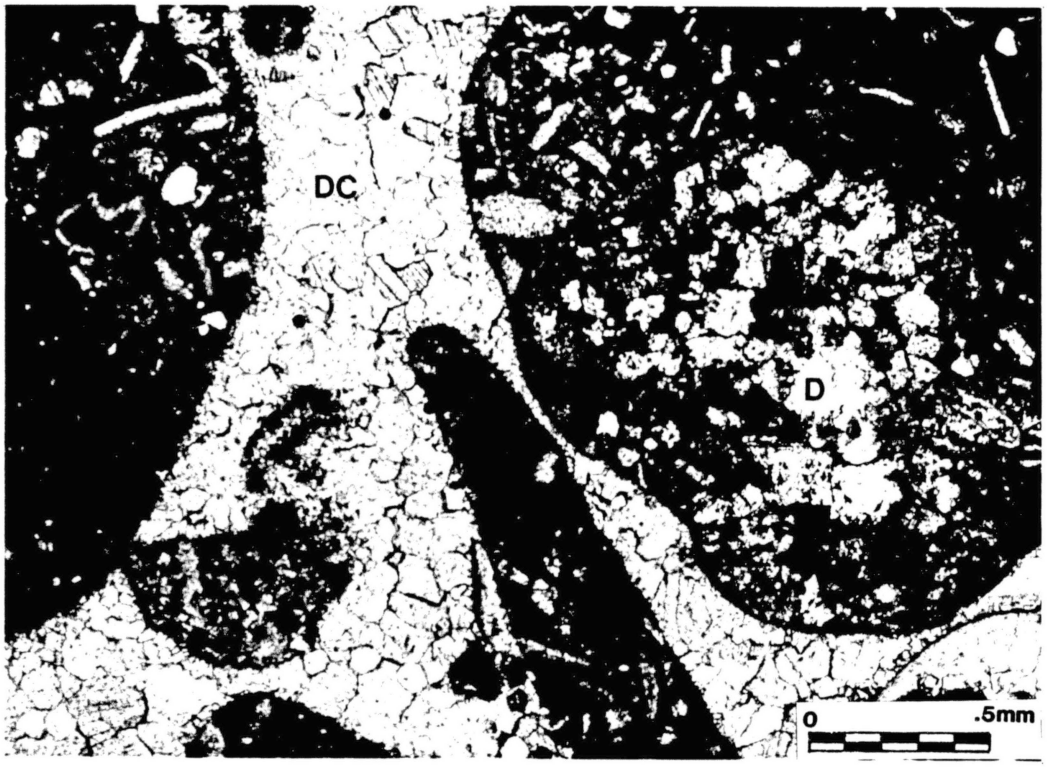

Figure 44. Drusy calcite cement. The photomicrograph of BM 424.5 (PPL) illustrates the single generation of drusy calcite (DC) that cemented a pebble IFC limestone. Ferroan dolomite (D) selectively replaced the lime mud portion of the clast seen on the right.

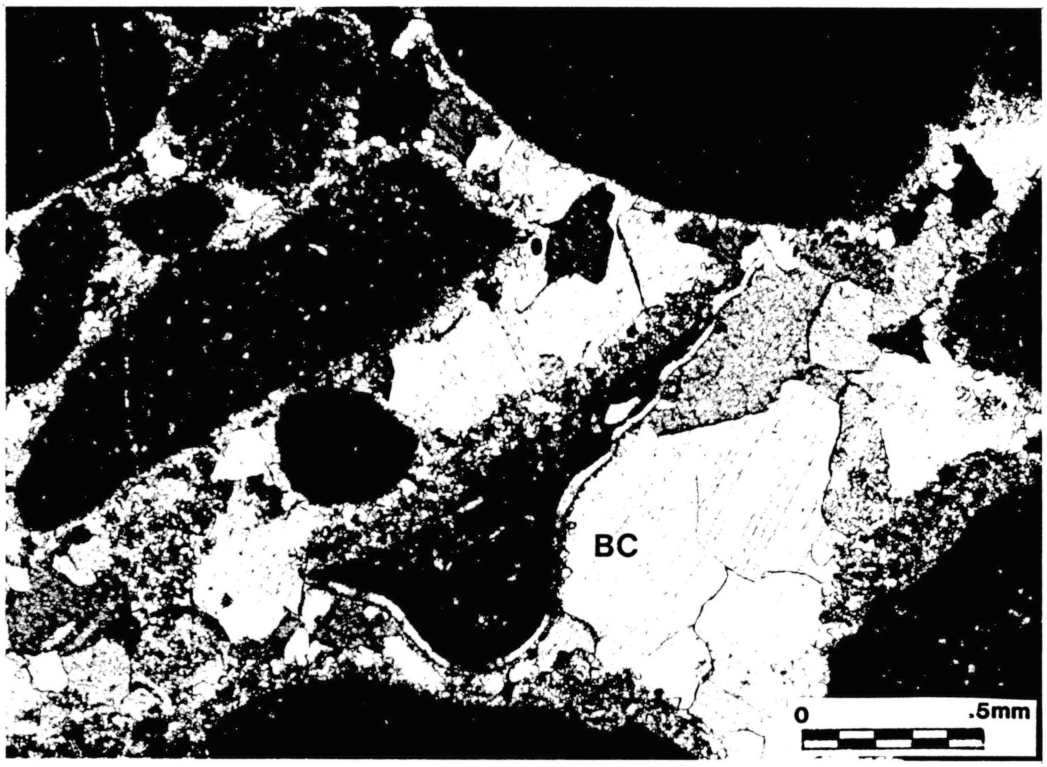

Figure 45. Blocky calcite cement. The photomicrograph of BM 521.1 (PPL) illustrates blocky calcite (BC) cementation of a pebble IFC limestone. Note that the edge of one clast is formed by a thin shelled trilobite. The less dense micrite which can be observed on this clast is interpreted as an "armoured-mud ball" effect due to the cohesion of micrite to the clasts following sedimentation. Two generations of cement are clearly visible (as in Figure 42).

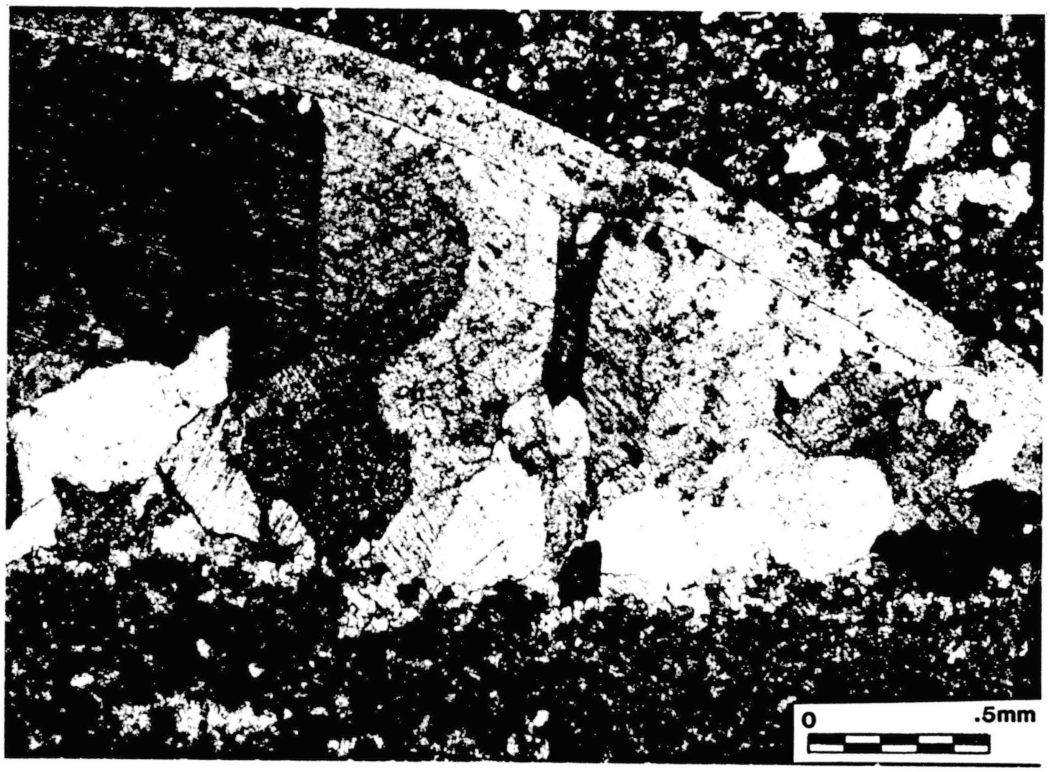

Figure 46. Possible radiaxial fibrous calcite cement developed in a geopetal structure. The photomicrograph of BM 357.7 (XN) illustrates a rare occurrence of radiaxial fibrous calcite forming part of the cement fill of a zone of shelter porosity developed beneath a trilobite shell. Ghosts of inclusions in the fibrous calcite crystals nucleated on the underside of the shell may record the former presence of aragonite. By contrast the lower drusy cement sprouting from the lime mud is inclusion free.

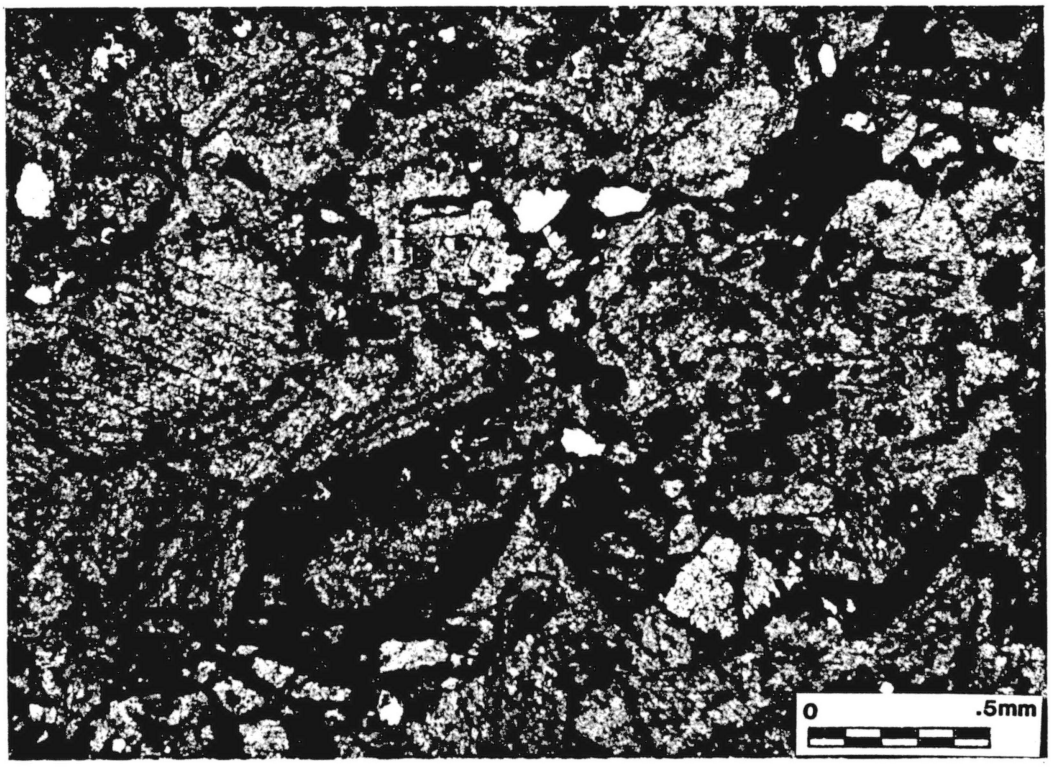

Figure 47. Syntaxial overgrowths on pelmatozoan parts. The photomicrograph of BM 510.0 (PPL) illustrates syntaxial calcite overgrowths (OG) cementation in a dolomitic pebble intraclast pelmatozoan (P) sand grainstone. Ferroan dolomite (D) was the final pore filling cement; it also replaces pelmatozoan parts and their overgrowths.

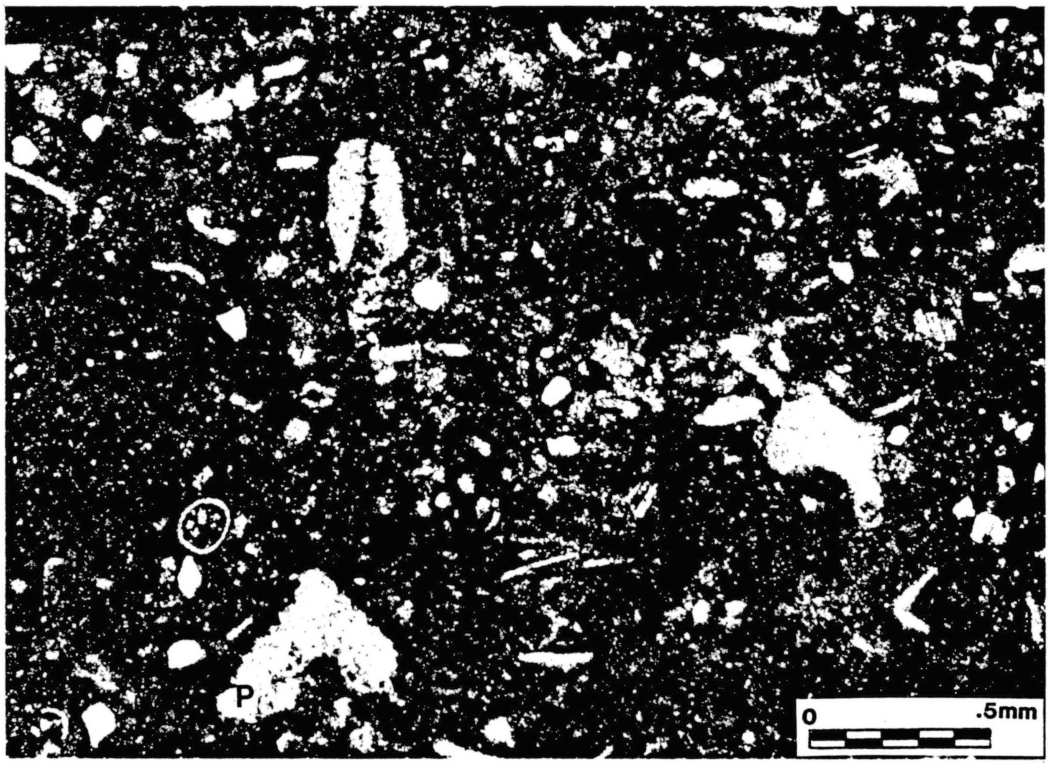

Figure 48. Lime mud cementation. The photomicrograph BM 357.6 (PPL) illustrates lime mud matrix and cementation of a pelmatozoan (P)-trilobite (T) sand wackestone. Some angular quartz silt is present.

Dolomite Spar

Dolomite is either disseminated in the limestone or selectively concentrated in distinct zones. Although only thin laminae are pure dolomite, many zones are partly dolomitized.

At outcrop, the dolomite is easily recognized by distinctive orange color. The orange weathering color is produced by the oxidation of iron in the dolomite lattice to produce limonite. Bedded zones of oxidized dolomite are seen as distinctive orange bands that stripe the Formation parallel to strike (Figure 49).

Thin section staining (in a solution of Alizarin red S and potassium ferricyanide) confirmed that the Signal Mountain dolomite is ferroan. X-ray diffraction of several thin sections specifically identified the dolomite as ankerite. Petrographic examination revealed that the ankerite is also baroque (Figure 50).

Signal Mountain dolomite is both pore filling and replacive. The pore filling dolomite typically forms rhombic crystals ranging in size from 0.05 to 0.5 mm (Figure 51).

Replacive dolomite is selective of the following textures: (i) lime mud and the lime mud of intraclasts, (ii) lime mud filled burrows and bioturbated zones, and (iii) pelmatazoan parts and their overgrowths (Figures 44, 52, 53, 54, and 55). Replacement is partial to complete.

Silica

Silica of diagenetic origin is a minor constituent that is seen at outcrop in the form of silicified body fossils (Figures 35, 36) and burrows, and as small chert nodules 4 to 5 cm long. In thin section,

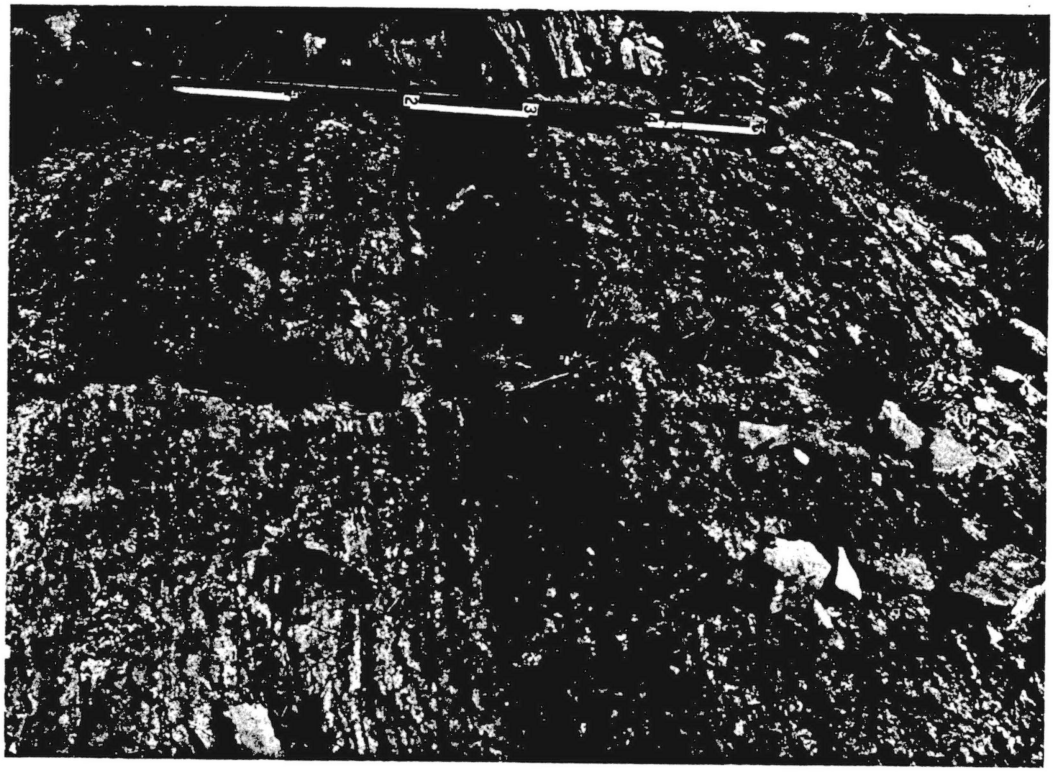

Figure 49. Orange weathered bands of ferroan dolomite. The 1 foot mark on the Jacob's staff is 385.0 feet above the base of the Bally Mountain measured section.

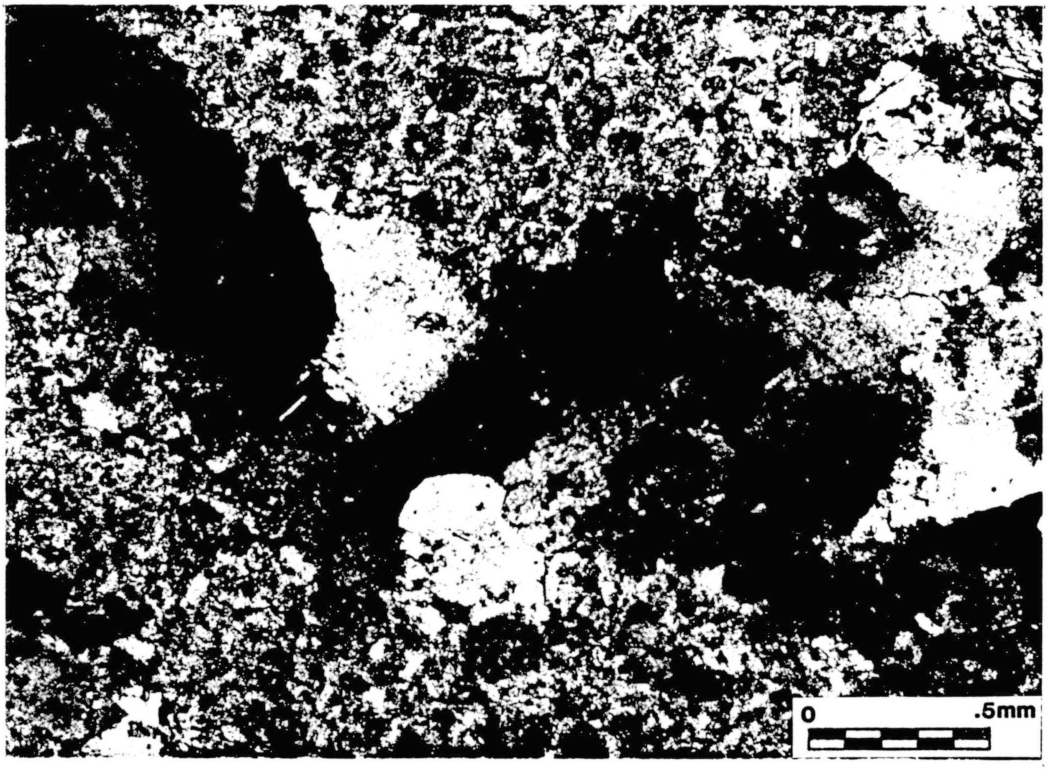

Figure 50. Baroque ankerite. The photomicrograph of BM 590.0 (XN) illustrates void-filling baroque ankerite cement in a dolomitic intraclast-peloidal sand grainstone. The undulose extinction is typical of baroque dolomites.

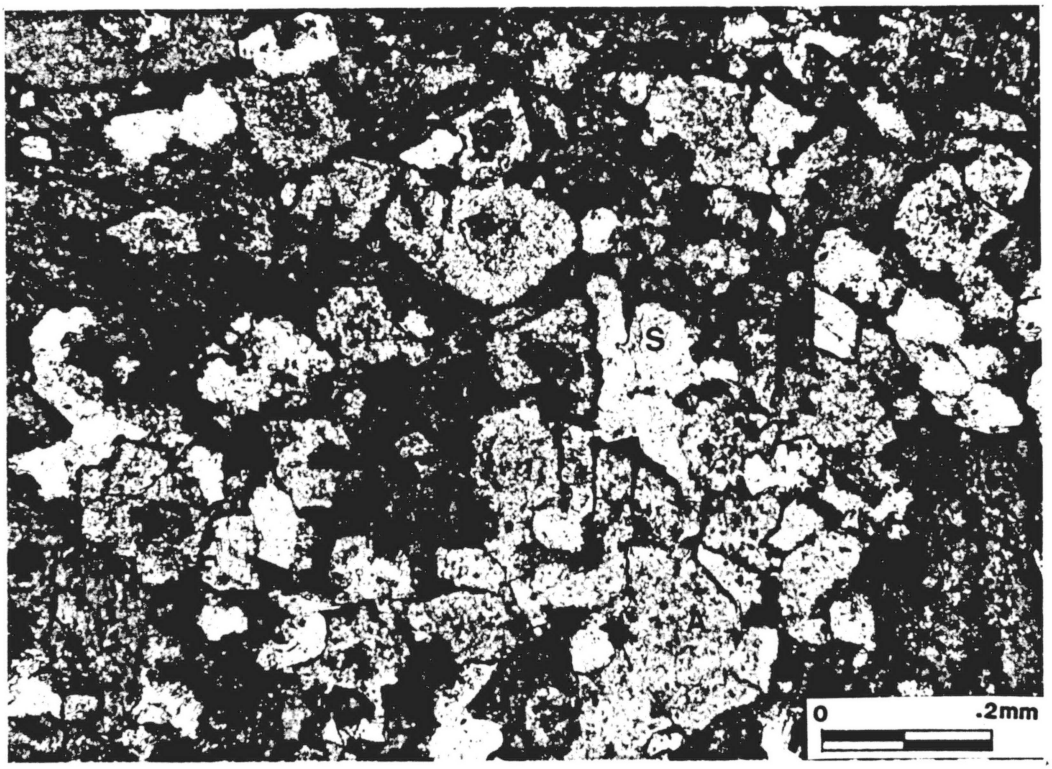

Figure 51. Pore-filling ankerite. The photomicrograph of BM 47.2 (PPL) illustrates ankerite (A), silica (S), and calcite (C) as cements in a dolomitic, silicic, pelmatozoan-trilobite sand grainstone. Cementation progress in the following order; calcite, ankerite, and finally silica. Dolomite rhombs with pink centers indicate that the dolomite crystal has partly dedolomitized.

Figure 52. Lime mud laminae selectively replaced by ferroan dolomite. The photomicrograph of BM 392.5 (PPL) illustrates a micrite laminae that has been partially replaced by dolomite. Enveloping the mudstone laminae are dolomitic pelmatozoan-trilobite sand wackestones.

Figure 53. Intraclasts and pelmatozoan parts selectively replaced by ferroan dolomite. The photomicrograph of BM 513.0 (PPL) illustrates that ferroan dolomite (D) selectively replaced only intraclasts and pelmatozoan parts of a dolomitic pelmatozoan sand grainstone. Glauconite (G) has also partially replaced some of the intraclasts. Intraclasts are mudstone and wackestone. Some superficial ooids are present. In some instances the ooids coat grains with micritic envelopes.

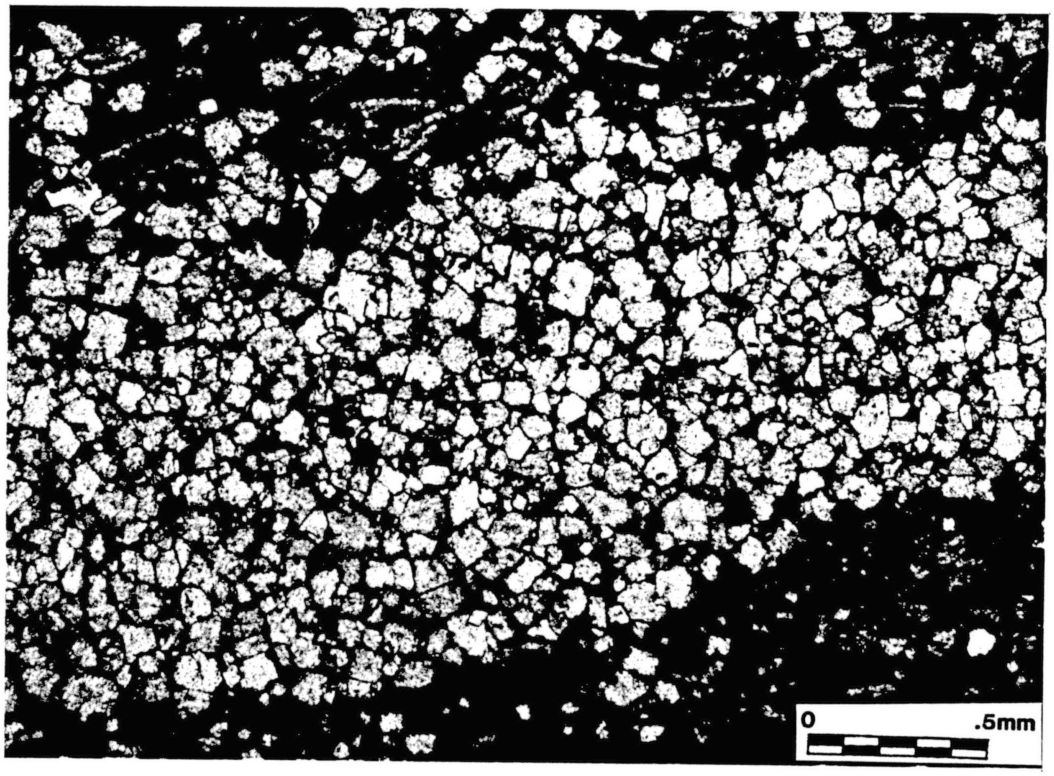

Figure 54. Horizontal burrow selectively replaced by ferroan dolomite. The photomicrograph of BM 541.0 (PPL) illustrates a horizontal worm burrow (center) that was selectively replaced by ferroan dolomite in a dolomite trilobite-pelmatozoan sand wackestone.

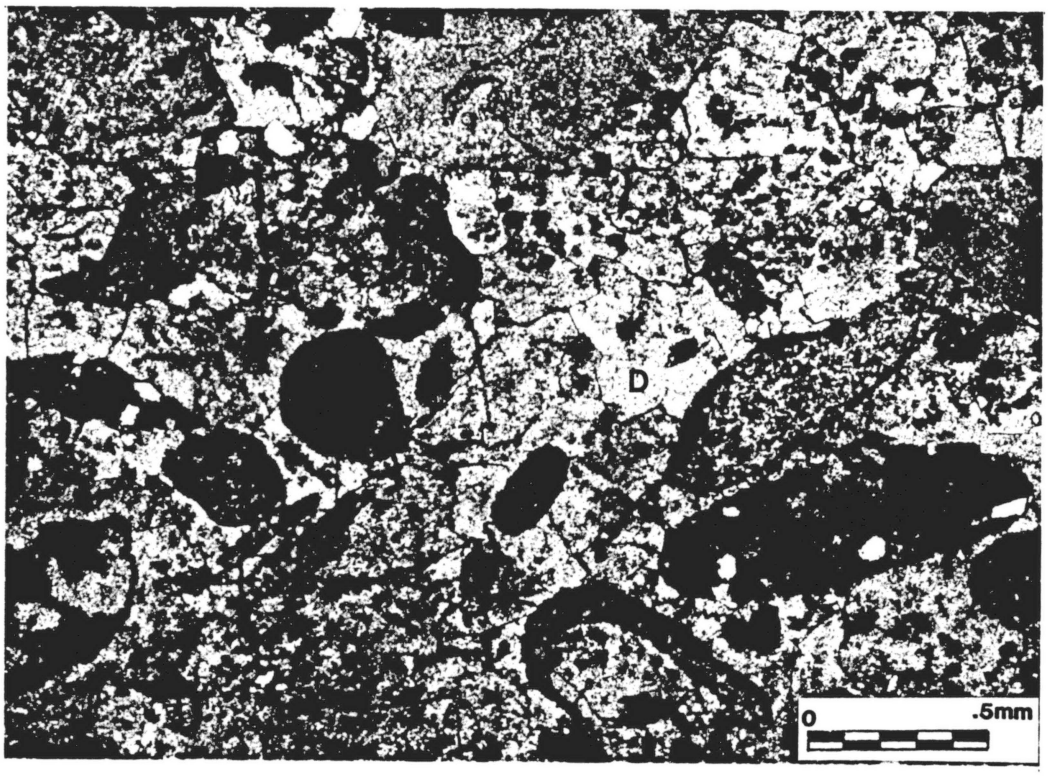

Figure 55. Pelmatozoan parts and their overgrowths selectively replaced by ferroan dolomite. The photomicrograph of BM 718.2 (PPL) illustrates that ferroan dolomite (D) has preferentially replaced pelmatozoans and their overgrowths in a dolomitic intraclast pelmatozoan sand grainstone.

silica occurs as (i) syntaxial overgrowths on detrital quartz grains, (ii) megaquartz, (iii) microquartz, and (iv) chalcedonic quartz. Syntaxial overgrowths are on most quartz grains. Feldspar grains may exhibit epitaxial quartz overgrowths (Figure 56).

Of the varieties of chert present, megaquartz is primarily pore filling and only slightly invasive (Figure 57). On the other hand, microquartz and chalcedony are replacive. The two forms constitute the bulk of the chert nodules seen at the outcrop (Figure 58). These cherts preserved the original textures of the limestone (Figure 59). Microquartz and chalcedony also commonly replace pelmatazoan fragments throughout the formation (Figures 33, 34, and 60). The chalcedony is length fast chalcedonite.

Pyrite

Pyrite is a minor constituent of the limestones. It may be disseminated or as nodules as large as small pebbles. Pyrite also is commonly in burrows.

Glauconite

Glauconite is typically a replacement of the lime mud of intraclasts, but also is found as distinct grains (Figure 53). Although rare at the Bally Mountain measured section glauconite, is more plentiful elsewhere in the Signal Mountain Formation in the Wichita Mountains. For example, at the Zodletone measured section, glauconite grains constitute up to approximately 15% of several discrete zones.

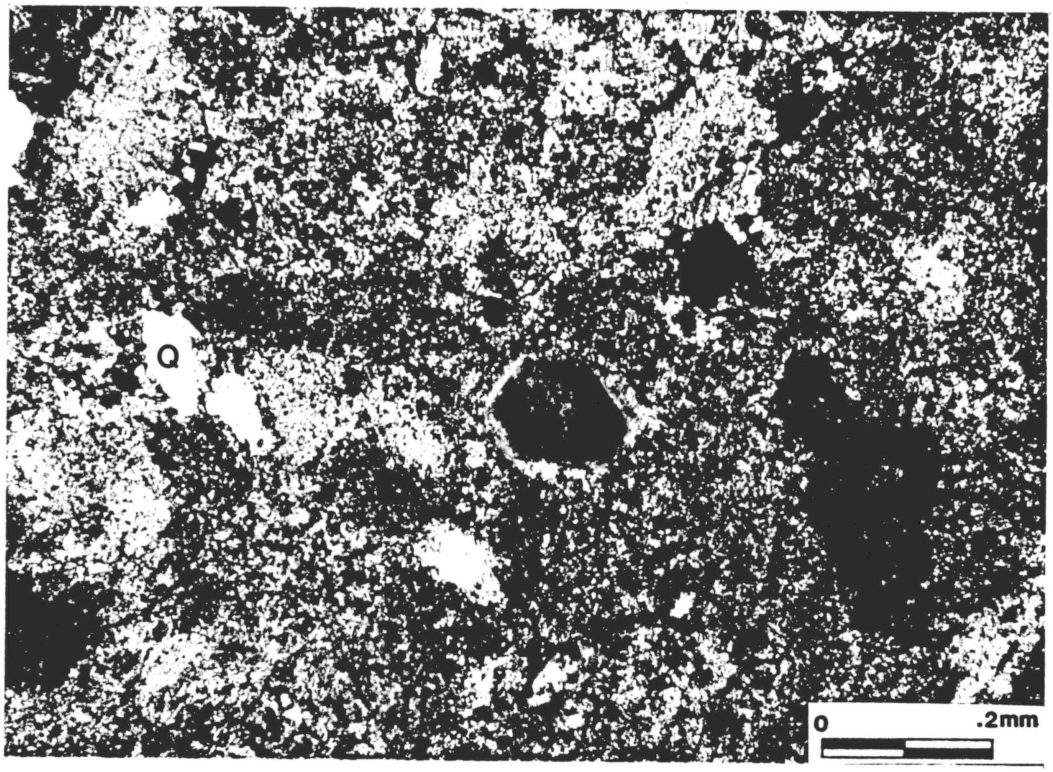

Figure 56. Syntaxial silica overgrowth on an orthoclase sand grain. The photomicrograph of BM 146.5 (XN) illustrates an epitaxial quartz overgrowth on an orthoclase (O) grain in a pelmatozoan sand wackestone. Several quartz (Q) grains have overgrowths that have been etched by micrite cement.

Figure 57. Megaquartz pore filling cement. The photomicrograph of BM 547.5 (XN) illustrates megaquartz (MQ) as a final pore filling cement after blocky calcite spar (BC) in a portion of a peloidal gastropod wackestone. Chalcedonic quartz (CQ) near the margin of the pore represents an earlier phase of precipitation from waters more saturated with silica than those from which the megaquartz precipitated. The chalcedony records a temporary pause in the precipitation of drusy calcite. Such a pause probably reflects minor variations in the pH of circulating groundwater.

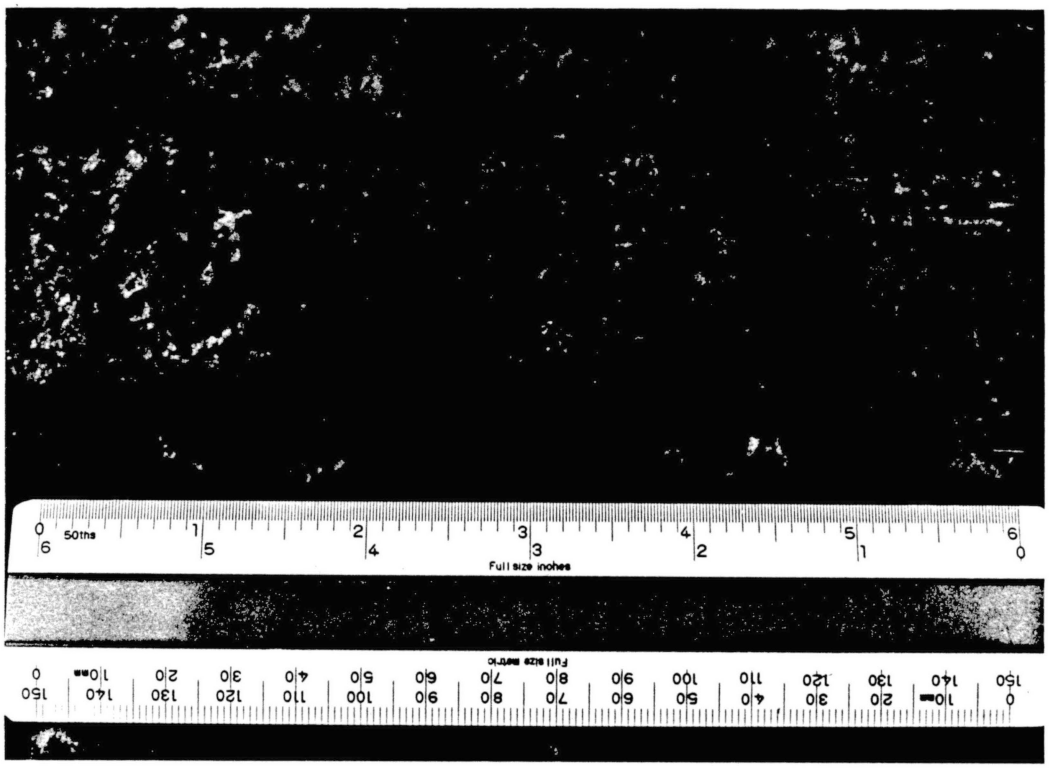

Figure 58. Chert nodule at outcrop. The photograph was taken 399 feet above the base of the Bally Mountain measured section. The chert nodule is now incorporated in a stylolite.

Figure 59. Chert nodule in thin section. The photomicrograph of BM 399.2 (XN) illustrates that microquartz (MQ) and chalcedonic quartz (CQ) (in this case length fast chalcedonite) have replaced a portion of trilobite-pelmatozoan sand wackestone. Silicification was incomplete, but does not appear to have been fabric selective. Note that there are ghosts of the original fossils (F), now chalcedony, in the large microquartz nodule.

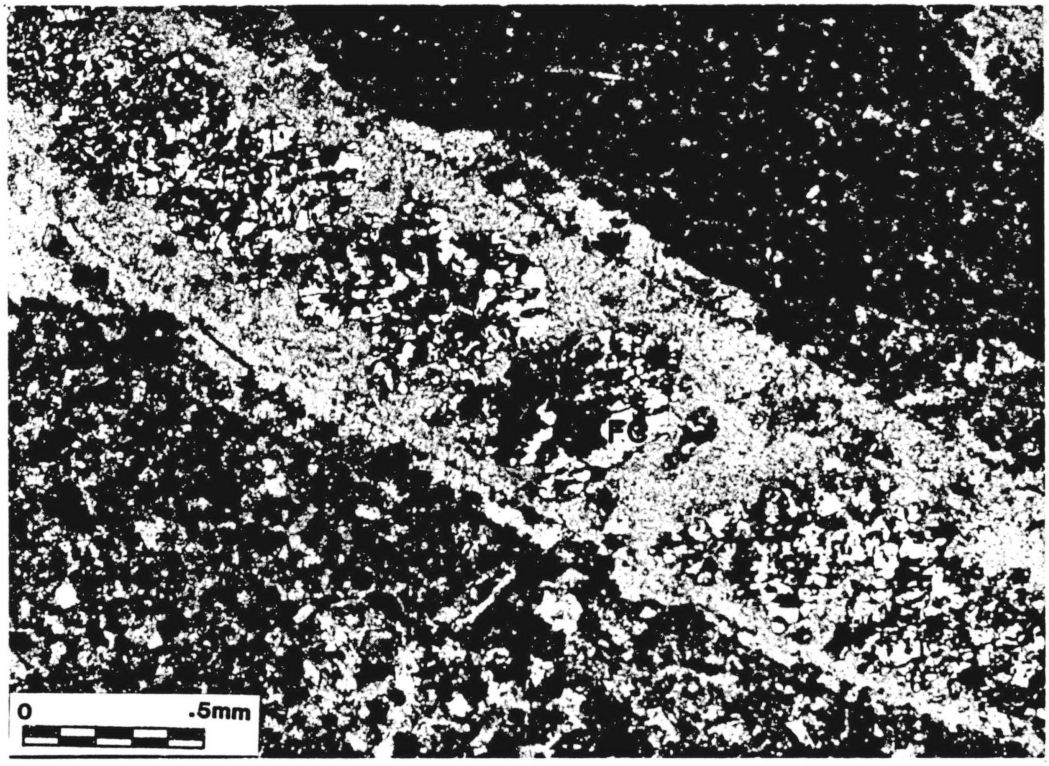

Figure 60. Fibrous chalcedony replaced pelmatozoan columnal. The photomicrograph of BM 24.5 B (XN) illustrates that fibrous chalcedony (FC) has replaced the center portion of a pelmatozoan columnal in a fossiliferous intraclast sand wackestone.

Miscellaneous Diagenetic Features

Hardgrounds

Abundant hardgrounds occur throughout the Signal Mountain Formation. Although often a subtle feature at the outcrop, hardgrounds are easily recognized in both hand-sample and thin section. Hardgrounds record syndepositional cemention by lime mud at or just below the sediment surface. Evidence of subsequent erosion down to the level of the hardground in seen in the form of truncated allochems and sedimentary structures (Figure 61). Some hardgrounds have a hematite crust on their top surfaces, perhaps recording syndepositional oxidation of disseminated pyrite.

Stylolites

Stylolites occur in two forms; (i) diagenetic and (ii) tectonic. Diagenetic stylolites result from the pressure solution in response to the tremendous overburden pressure produced by the sedimentary rock pile. These stylolites are typically; (i) low in amplitude (less than 1 cm), (ii) horizontal to inclined, (iii) simple wavelike or sutured, and (iv) they form interconnected networks (Figure 62). Stylolites of this type are abundant and commonly are spaced a centimeter or less apart. The abundance of stylolites suggests that a substantial volume of rock has been lost to this form of pressure solution.

Of lesser importance are the tectonic stylolites. These stylolites are typically vertical to inclined, of moderate amplitude (several centimeters), and wavelike or sutured in form (Figure 63). They presumably formed during Pennsylvanian tectonic activity.

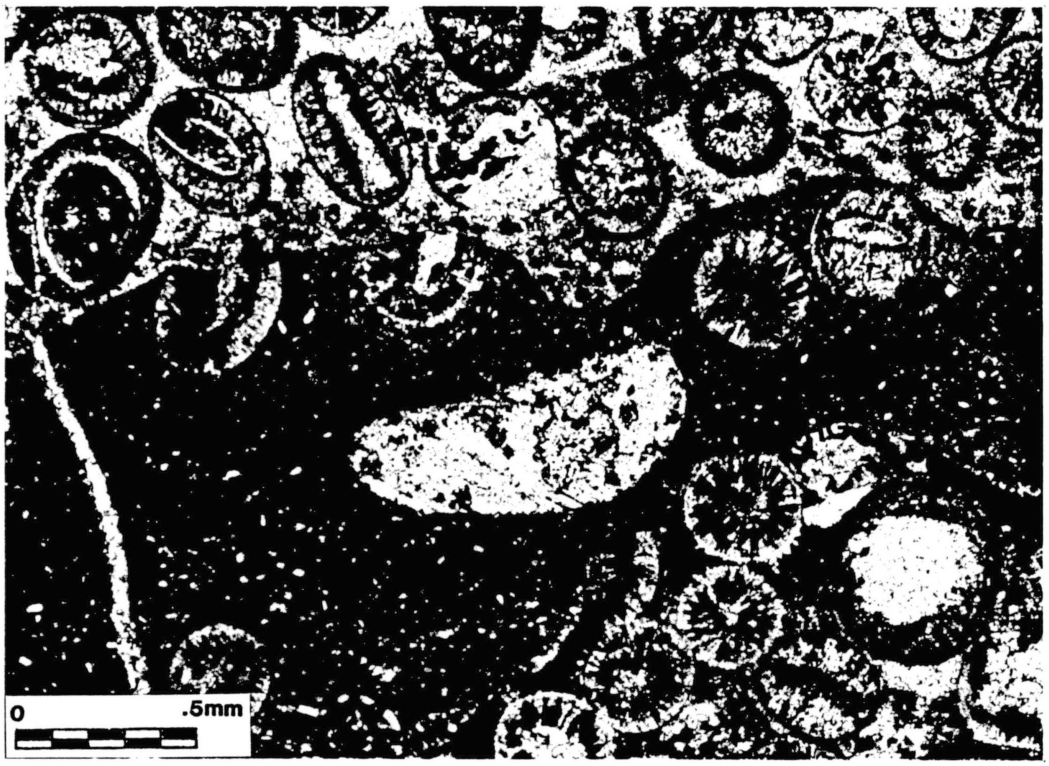

Figure 61. Hardgrounds. The photomicrograph of BM 532.8 (PPL) illustrates three distinct hardgrounds (H) that formed during the deposition of an interlaminated sequence of oolitic grainstones and oolitic mudstones and packstones. Several ooliths are truncated by the hardground surfaces.

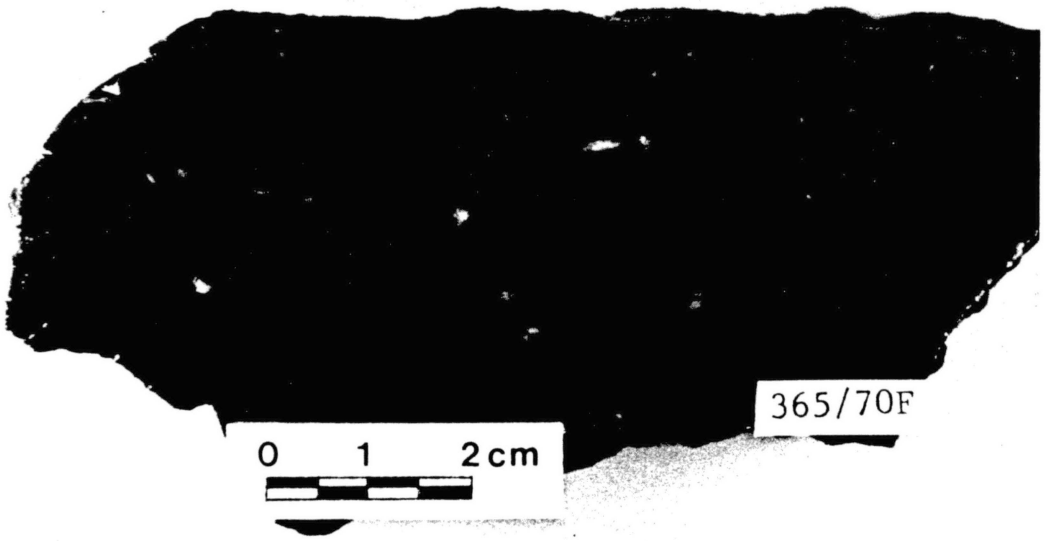

Figure 62. Interconnected network stylolites. Hand-sample BM 365/70F illustrates interconnected network stylolites in a mudstone. The sinuousity of the stylolites is a simple wavelike or sutured variety.

Figure 63. Vertical stylolites. The photomicrograph was taken 399 feet above the base of the Bally Mountain measured section. Wave amplitude is 2 to 3 cm and the shape is simple wavelike to sutured. Chert nodules are now incorporated in the stylolites.

CHAPTER V

LITHOTYPES AND SEDIMENTARY STRUCTURES OF THE SIGNAL MOUNTAIN FORMATION

Introduction

Lithotypes of the Signal Mountain Formation are difficult to recognize in the field, because a thin modern calcrete coats the limestone and obscures its textures. Detailed hand-sample collection, lab preparation, and microscope examination were required to properly identify specific lithotypes. A particular lithotype seldom occurs as discrete beds, but more often is very thinly interbedded (beds are 1/2 to 2 in.) to interlaminated (beds are 1/10 to 1/2 in.) with other lithotypes.

The principal lithotypes fall into two main categories: (i) clastic limestones; grainstones, packstone, wackestones, and intraformational-conglomerate (IFC) limestones and (ii) mudstones. The author defines these lithotypes, using Dunham's (1962) classification of carbonate rocks (somewhat modified) as follows:

1. Grainstone - a grain-supported limestone that is cemented principally by calcite spar, but that may contain significant amounts of lime mud.
2. Packstone - a grain-supported limestone that is cemented principally by lime mud, but that may contain significant amounts of calcite spar.

3. Wackestone - a limestone containing more than 10% grains, which are supported principally by lime mud, but the cement may contain significant amounts of calcite spar
4. IFC Limestone - a special classification of limestones containing principally intraclasts of pebble size (2 to 64 mm) or larger. Textures may be clast- or matrix-supported. The matrix may be any of the before mentioned lithotypes and may be cemented principally by calcite spar or lime mud or a combination of both (Donovan, 1983).
5. Mudstone - a limestone composed of lime mud and less than 10% grains.

Clastic Lithotypes

Grainstones

Although common throughout the Formation, grainstones rarely form discrete beds. More often they occur in zones interbedded with other lithotypes. At outcrop and in hand-samples (Plate I and Appendix C), grainstones are predominantly composed of intraclast sands interbedded with packstone and wackestone intraclast sands or mudstones. Except in the lower portion of the Formation, fossiliferous, oolitic, or peloidal grainstones were not apparent at outcrop.

On the other hand, thin-section studies reveal that fossiliferous grainstones are more common than suspected (Figure 64). The principal reason for the discrepancy is that the "matrix" of coarse intraclast grainstones is much more fossiliferous than is apparent in hand

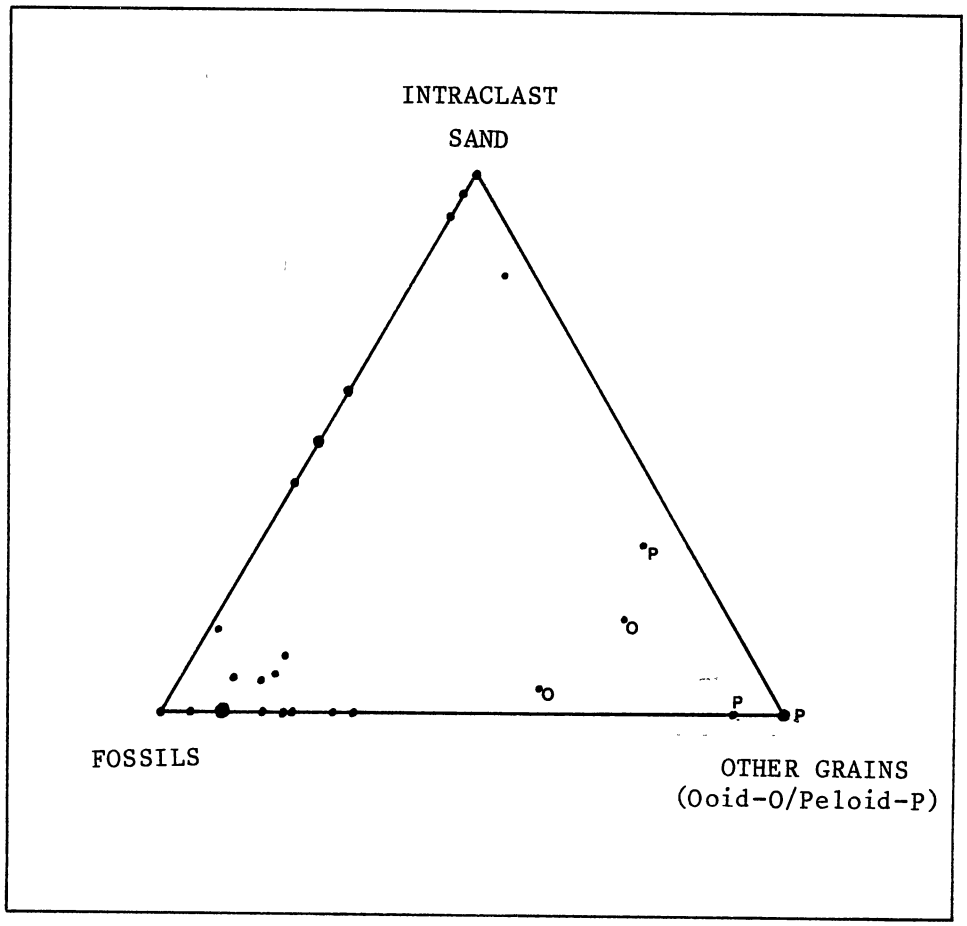

Figure 64. Total allochems of grainstones in thin section.

specimen. Some positive selection also exists in favor of oolitic and peloidal grainstones.

The triangular diagram of fossil allochems (Figure 65) illustrates that pelmatozoans and trilobites are the principal fossils in grainstones and commonly occur together in significant amounts.

Packstones

Packstones preferentially occur in zones interbedded with other lithotypes, rather than as discrete beds. They also are a common lithotype. At outcrop and in hand-sample, packstones can be more or less equally divided into intraclast sand and fossiliferous packstones. Peloidal and oolitic packstones are rare.

The triangular diagram of the allochems of packstones in thin section (Figure 66) illustrates that fossiliferous packstones are more abundant than intraclast sand and peloidal packstones (the discrepancy between hand specimen and thin section observation is explained in the same way as that existing in grainstones). No oolitic packstones were sectioned. As in the case of the grainstones, most of the fossils are either pelmatozoans or trilobites, the two types of fossils commonly occurring together (Figure 67).

Wackestones

Unlike the previously discussed clastic lithotypes, wackestones may occur as discrete beds. However, most wackestones are found interbedded with packstones and mudstones, and to a lesser extent with grainstones. At outcrop and in hand-sample wackestones have the greatest allochem diversity and constitute one of the most common lithotypes.

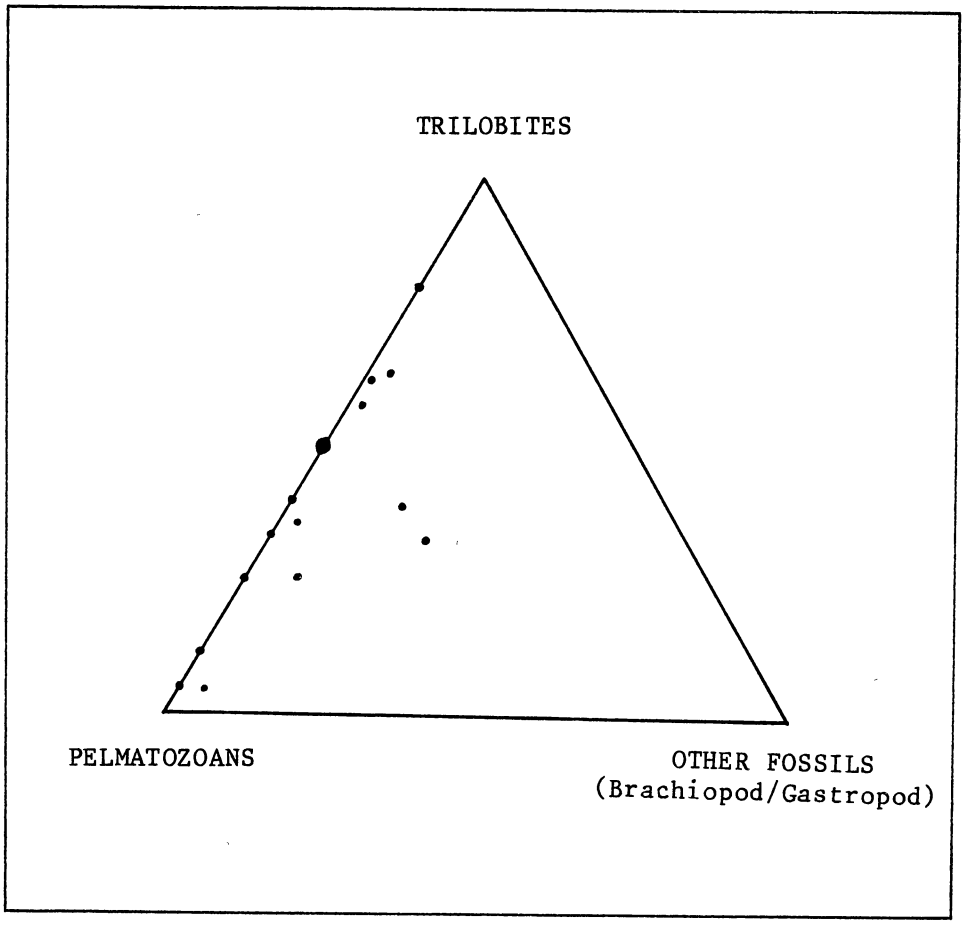

Figure 65. Types of fossils in fossiliferous grainstones in thin section.

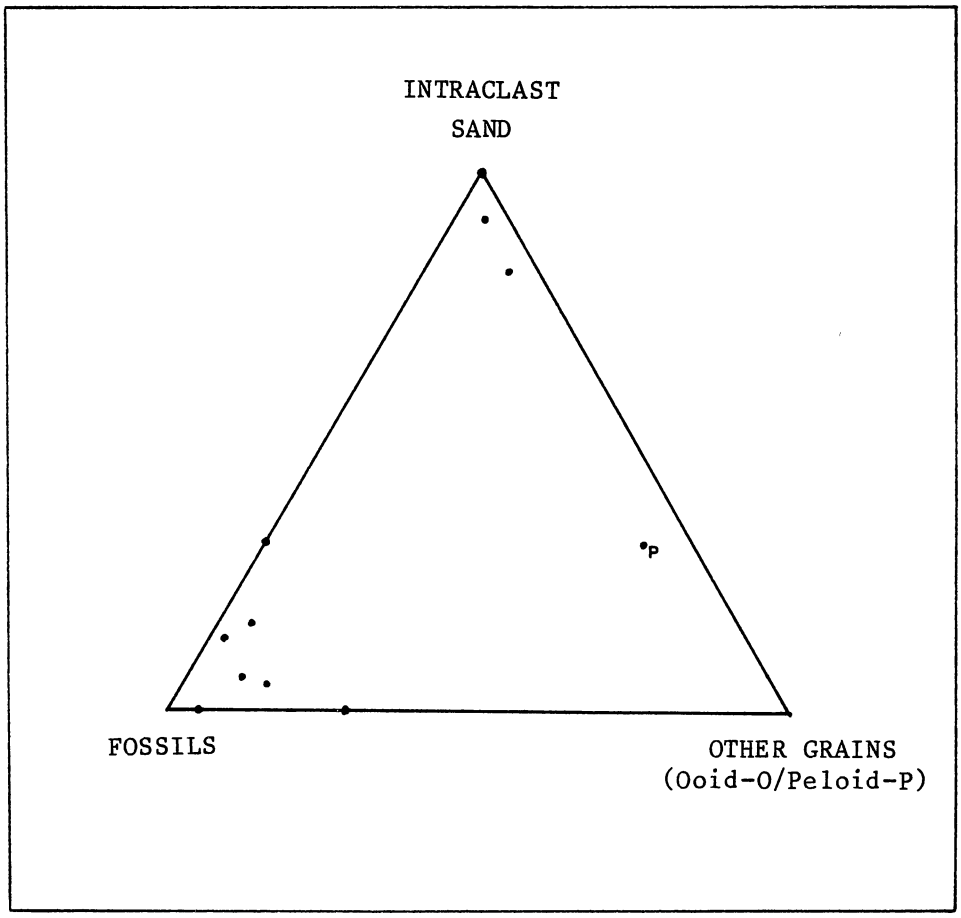

Figure 66. Total allochems in packstones in thin section.

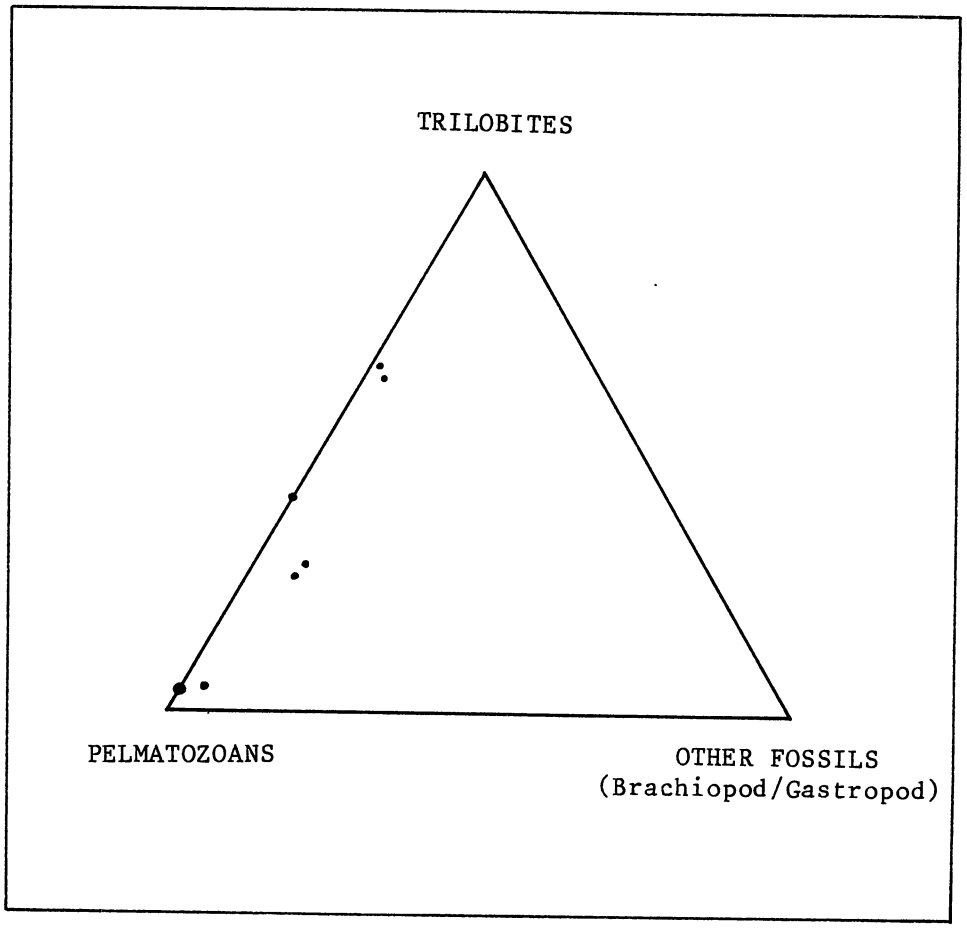

Figure 67. Types of fossils in fossiliferous packstones in thin section.

Fossiliferous and intraclast sand wackestones are the most abundant types.

The triangular diagram of the allochems of wackestones in thin section (Figure 68) illustrates that fossiliferous wackestones with variable amounts of intraclast sand, peloids and ooids are dominant. Intraclast sand and peloidal wackestones are rare and oolitic wackestones were not sectioned. Although trilobites and pelmatozoans are the most common fossils, the triangular diagram of the fossils of wackestones in thin section (Figure 69) illustrates the common occurrence of gastropods and brachiopods. Fossiliferous wackestones in thin section commonly consist of a diverse fauna of trilobites, pelmatozoans, and gastropods or brachiopods. Brachiopod valves and gastropods shells rarely occurred together in significant amounts.

IFC Limestones

IFC limestones are typical of the Signal Mountain Formation and, except for mudstones, they constitute the most abundant lithotype. Although more often found interbedded with wackestone and mudstone lithotypes, IFC limestones do form many distinct beds 1/2 to 1 foot thick. Fossiliferous and intraclast sands commonly constitute the matrixes of the IFC limestones. Pelmatozoan parts and trilobite carapace fragments are the most abundant matrix fossils.

Mudstones Lithotypes

Mudstones are the most abundant lithotype in the Formation and commonly constitute discrete beds up to 15 feet thick. Characteristically they are thinly laminated (less than 1/10 in. thick) or laminated (1/10

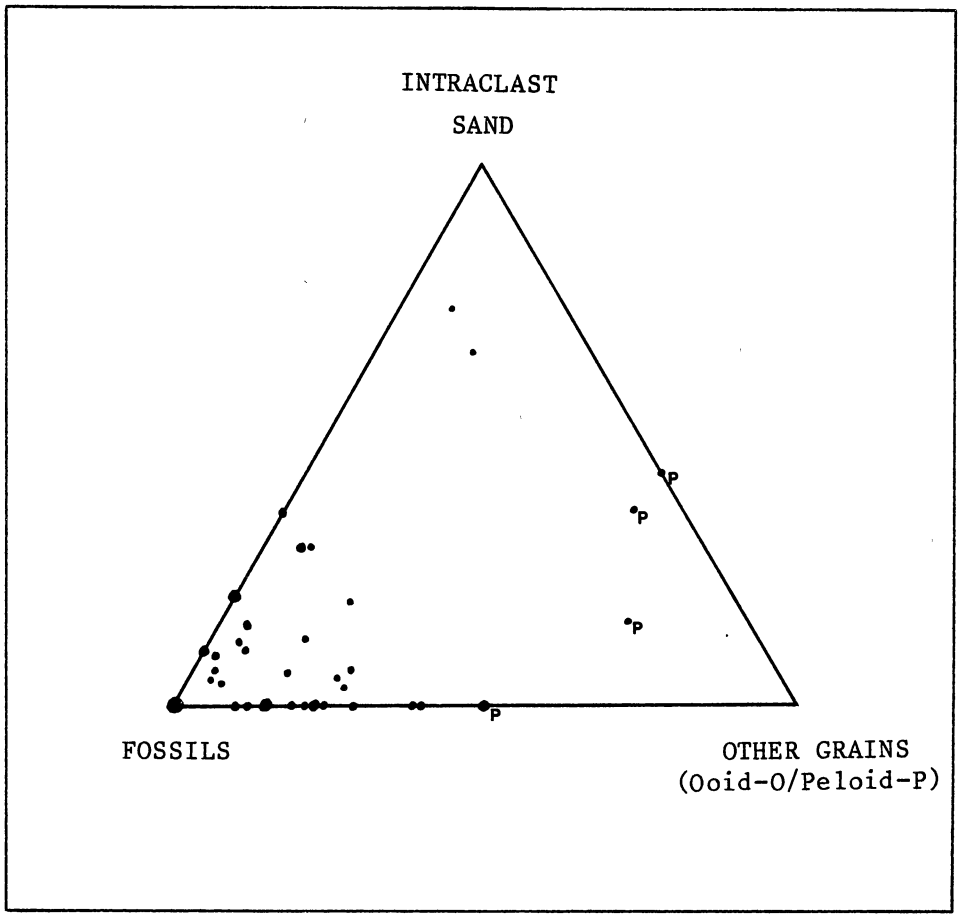

Figure 68. Total allochems in wackestones in thin section.

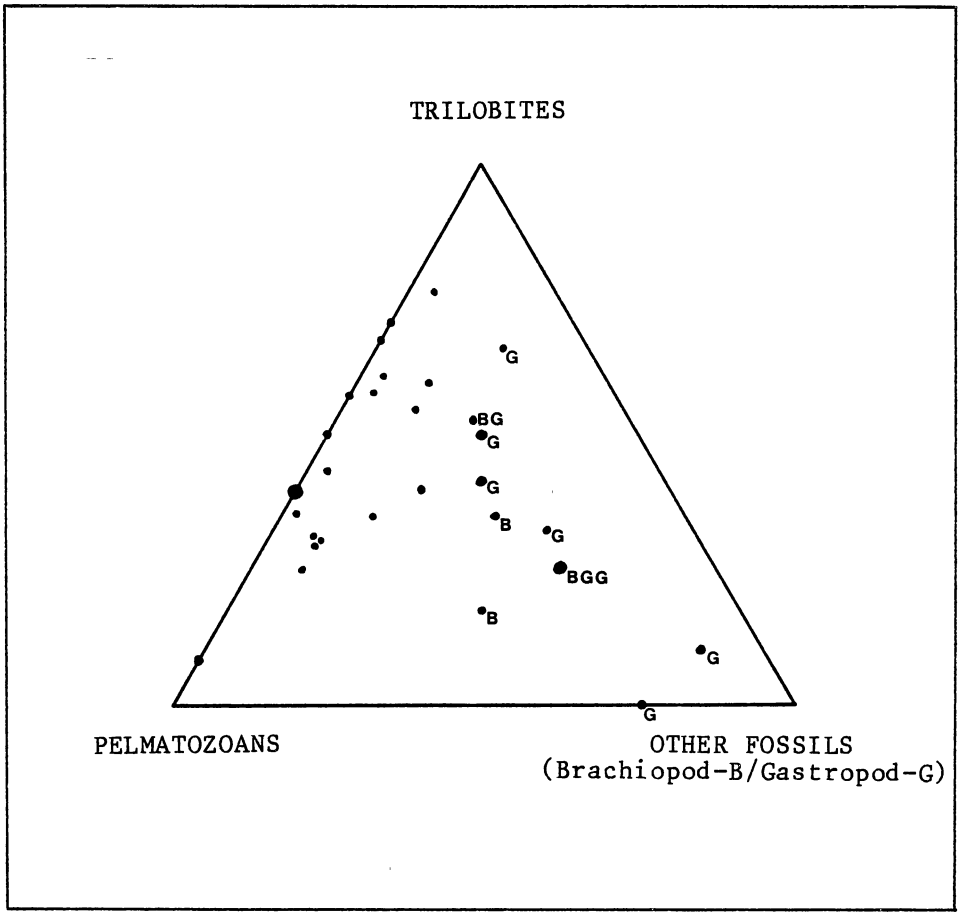

Figure 69. Varieties of fossils in wackestones (thin section data).

to 1/2 in. thick). Also mudstones are commonly interbedded with all other lithotypes and may contain distinct allochems, such as trilobites, in quantities less than 10 percent.

A triangular diagram, of the major constituents of all lithotypes observed in thin section (Figure 70), illustrates the overwhelming abundance of lithotypes composed of allochems and micrite.

Sedimentary Structures

Laminations

Thin to thick laminations are generally restricted to mudstones, although other lithotypes are laminated.

Interbedding

As previously noted, interbedding is a characteristic feature of the Signal Mountain Formation. A variety of lithotypes are commonly very thinly interbedded to interlaminated (Figure 71). The interbedding of lithotypes records the fluctuation of sediment types placed into the depositional system.

Ripples and Small Scale Cross-bedding

Ripple laminations appear restricted to the mudstones. Ripple geometry is more commonly asymmetrical and than symmetrical. Well preserved ripples are rare. However, ripple laminations may be more common, but they are masked by the immense number of bedded stylolites common to mudstone sequences. In fact, stylolites themselves imprint a

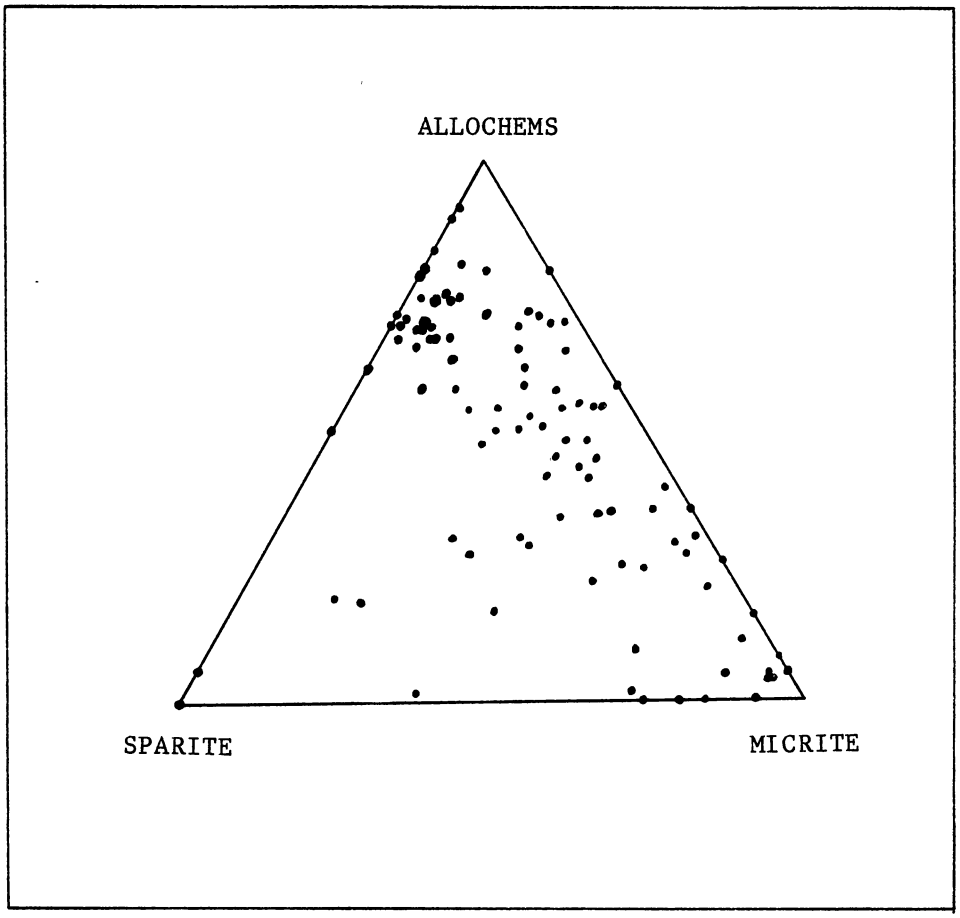

Figure 70. Total major constituents of the limestones in thin section.

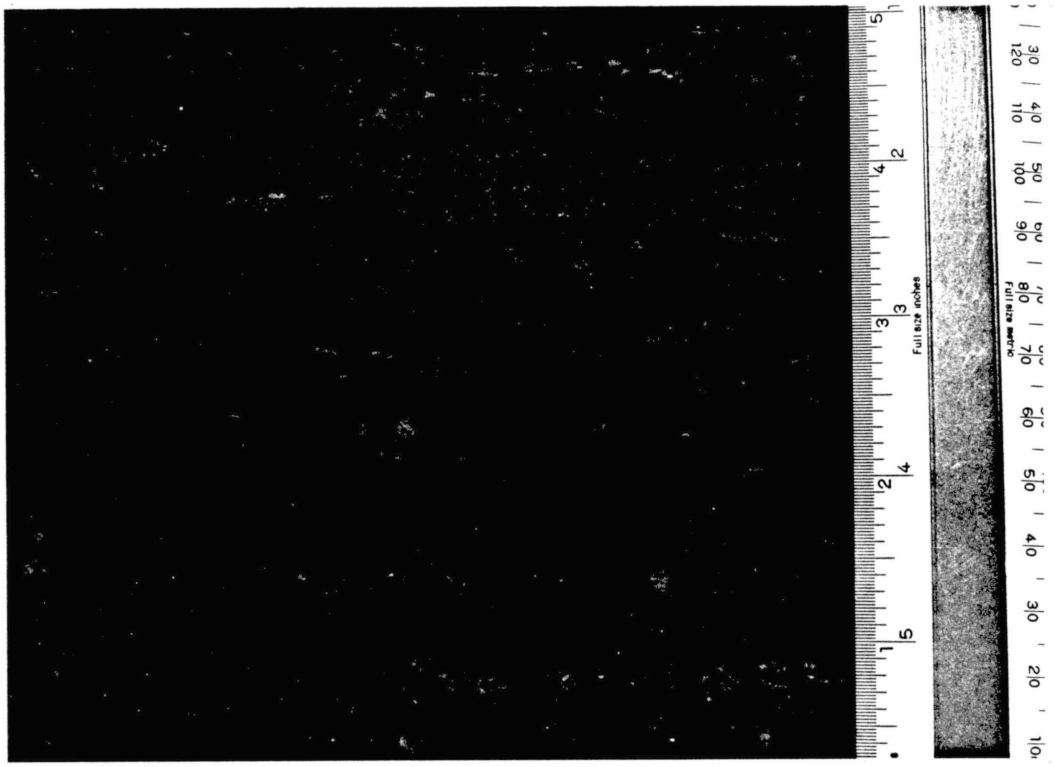

Figure 71. Interlaminated sequence at outcrop, 357 feet above the base, Bally Mountain measured section. The interlaminated sequence is primarily made up of intraclast sand packstones (P) and wackestones (W), and mudstones (M). Oolitic mudstone, brachiopod - trilobite sand wackestone, and trilobite sand wackestone laminae are also present, but not recognizable in the photograph.

wavy laminated texture often difficult to decipher from true ripple laminations.

Cross-bedding is a subtle texture rarely discovered or recognized at outcrop, except in a few discrete mudstone and intraclast sand grainstone sequences (Figure 72). The cross-beds are small scale and have a trough geometry.

Erosive and Scoured Bases

Erosive and scoured bases are characteristically associated with IFC limestones (Figures 24 and 26). Although less distinctive, grainstone and packstone intervals also commonly have erosive and scoured bases. Channeling with grainstone infill is a common sedimentary structure in many interbedded intervals (Figure 73).

Burrows, Bioturbation, and Borings

Burrowing typically occurs in most mudstone and wackestone beds. Packstones and IFC limestones (generally restricted to those with micrite matrix) are less commonly burrowed. Rarely were burrows discovered in grainstone laminae. Borings were recognized in individual intraclasts, but were never found in place.

Horizontal and vertical worm burrows, interpreted as Thalassinoides and Skolithos types respectively, are typical of the Signal Mountain Formation (Figure 74). "U" shaped worm burrows, Diplocraterion type, and possibly Zoophycos type burrows also occur (Tucker, 1981; Enos, 1983). Commonly distinct burrow forms are not present, but the sediments have been churned and mottled by moderate to intense bioturbation.

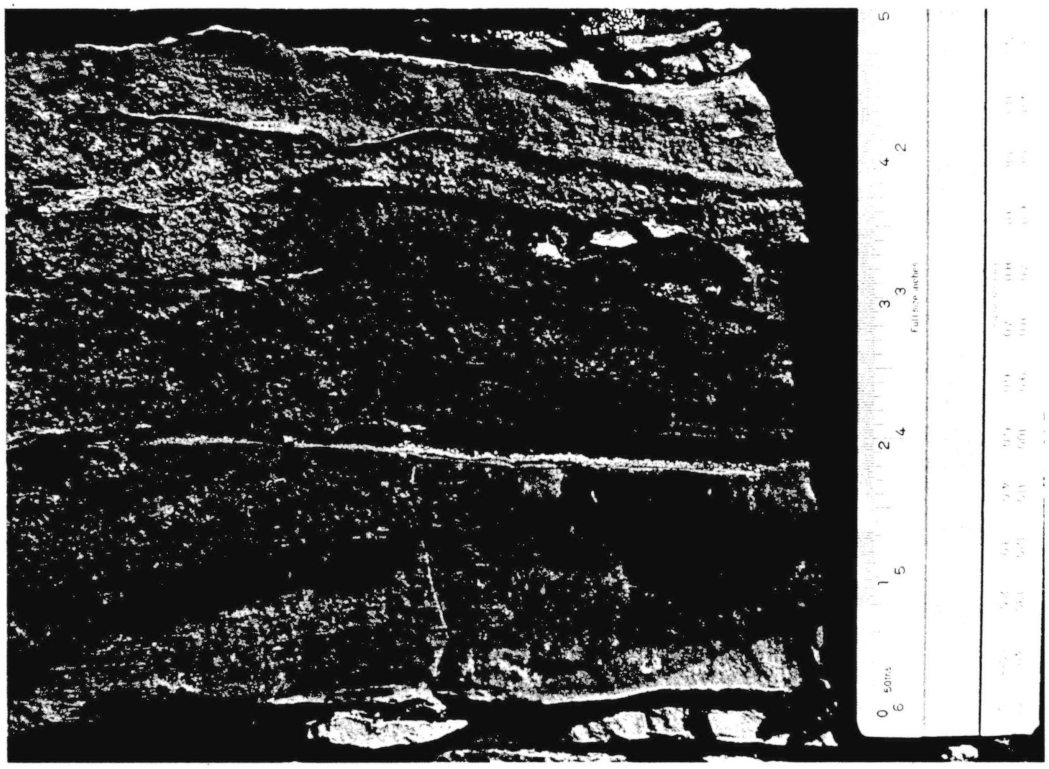

Figure 72. Subtle small scale trough cross-bedding in a mudstone bed. Delineation of the trough cross-bedding as enhanced by brown weathering ferroan dolomite along discrete laminae. Note that stylolites have obscured and distorted much of the cross-bedding.

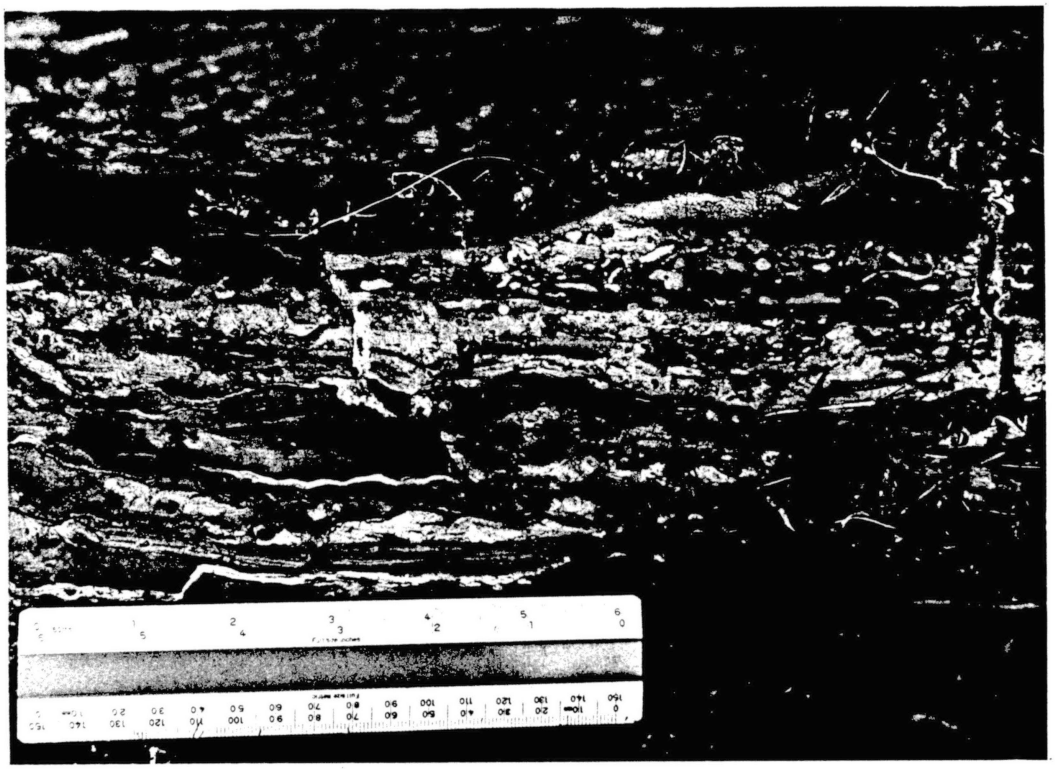

Figure 73. Small scale channels infilled with grainstones. Trilobite sand and pebble intraclast trilobite sand grainstones fill small channels (CH) in a very thinly interbedded sequence of mudstones, wackestones, and packstones. Photograph was taken 53 feet above the base of the Bally Mountain measured section. Incipient stylolites have distorted the sequence.

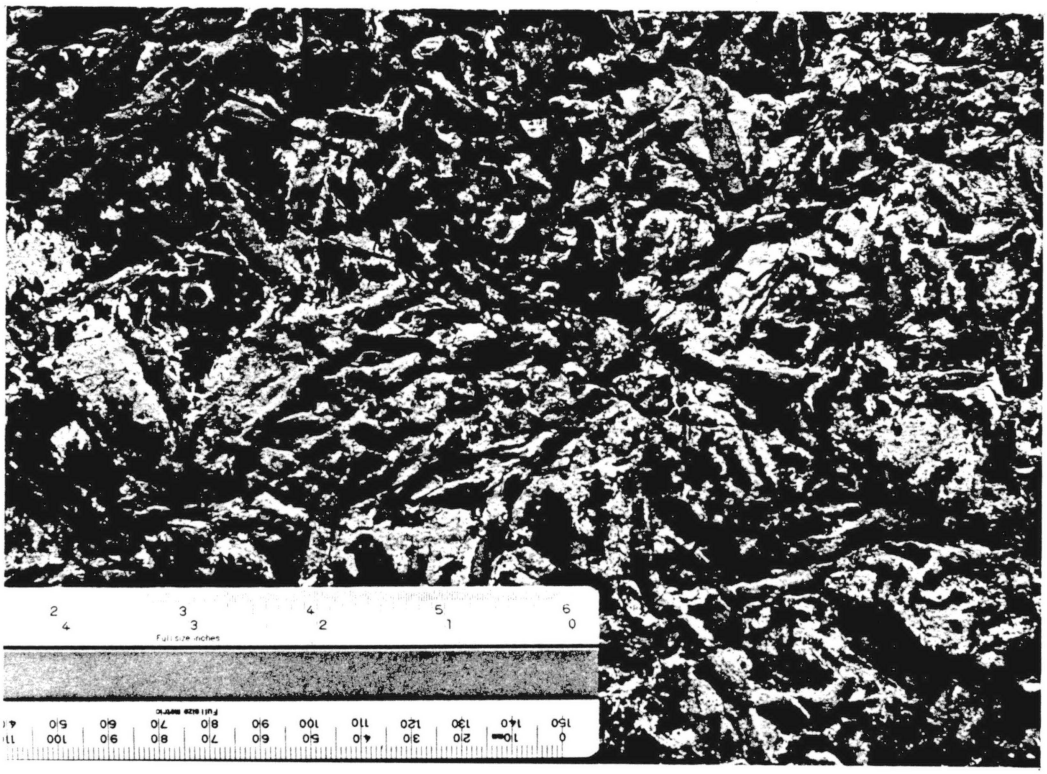

Figure 74. Horizontal and vertical burrows interpreted as Thalassinoides and Skolithos types respectively. The photograph shows Thalassinoides (T) and Skolithos (S) burrows on the base of a vertical dipping mudstone bed in the lower 350 feet of Signal Mountain Formation of an abandoned quarry at the Red Hill reference location.

Fenestral Textures

Fenestral textures are principally restricted to mudstone and wackestone (with high micrite content) lithotypes. Calcite spar has cemented most fenestrae. Tucker (1981) classified fenestrae as tubular (vertical to subvertical), laminar (generally parallel to bedding), and irregular (true birdseye). All of these forms are present in the Formation, but tubular fenestrae are most abundant.

Tubular fenestrae are interpreted as subaqueous shrinkage cracks formed by syneresis (Donovan and Foster, 1972). On the bedding plane surface the subaqueous shrinkage cracks characteristically appear as trilete and single elongate healed cracks. Rarely do tubular fenestrae appear related to burrowing organisms as suggested by Tucker (1981).

Laminar and irregular fenestrae (Figure 42) indicate the syndepositional accumulation of organic matter and its subsequent decay.

Miscellaneous Sedimentary Structures

Penecontemporaneous deformation commonly occurs in thinly laminated and laminated beds. However, soft sediment deformation is difficult to recognize due to the intense stylolitization throughout the formation.

Geopetal structures (spirit levels) are also common. They formed in burrows and in the (now occluded) shelter porosity beneath fossil fragments (Figure 46) or intraclasts.

CHAPTER VI

DEPOSITIONAL ENVIRONMENT OF THE SIGNAL MOUNTAIN FORMATION

Introduction

The stratigraphic logging of the Signal Mountain Formation did not reveal a consistant pattern of lithological relationships. The interbedded nature of the Formation is testimony, to the constant variability and poorly sorted stacking of lithotypes.

Overall, the Signal Mountain Formation may be considered as part of a major transgressive and minor regressive sedimentary sequence that began with deposition the Reagan Formation and ended with the deposition the Cool Creek Formation. This transgressive-regressive cycle was part of the major marine inundation of much of the North American Craton (Figure 75) that began in the Eocambrian and spanned nearly 300 million years (Dott and Batten, 1981).

In the Wichita Mountains, the marine transgression began with the onlap of Carlton Rhyolite paleotopographic highs by the Timbered Hills and basal portion of the Arbuckle Groups. Lower and upper siliciclastic sandstones of the Reagan Formation are interpreted as shallow marine shoreline deposits and as marine sand ridges, respectively. Upward passage of the siliciclastic Reagan sandstone into the Honey Creek Formation records a gradual change from marine siliciclastic sand-to a

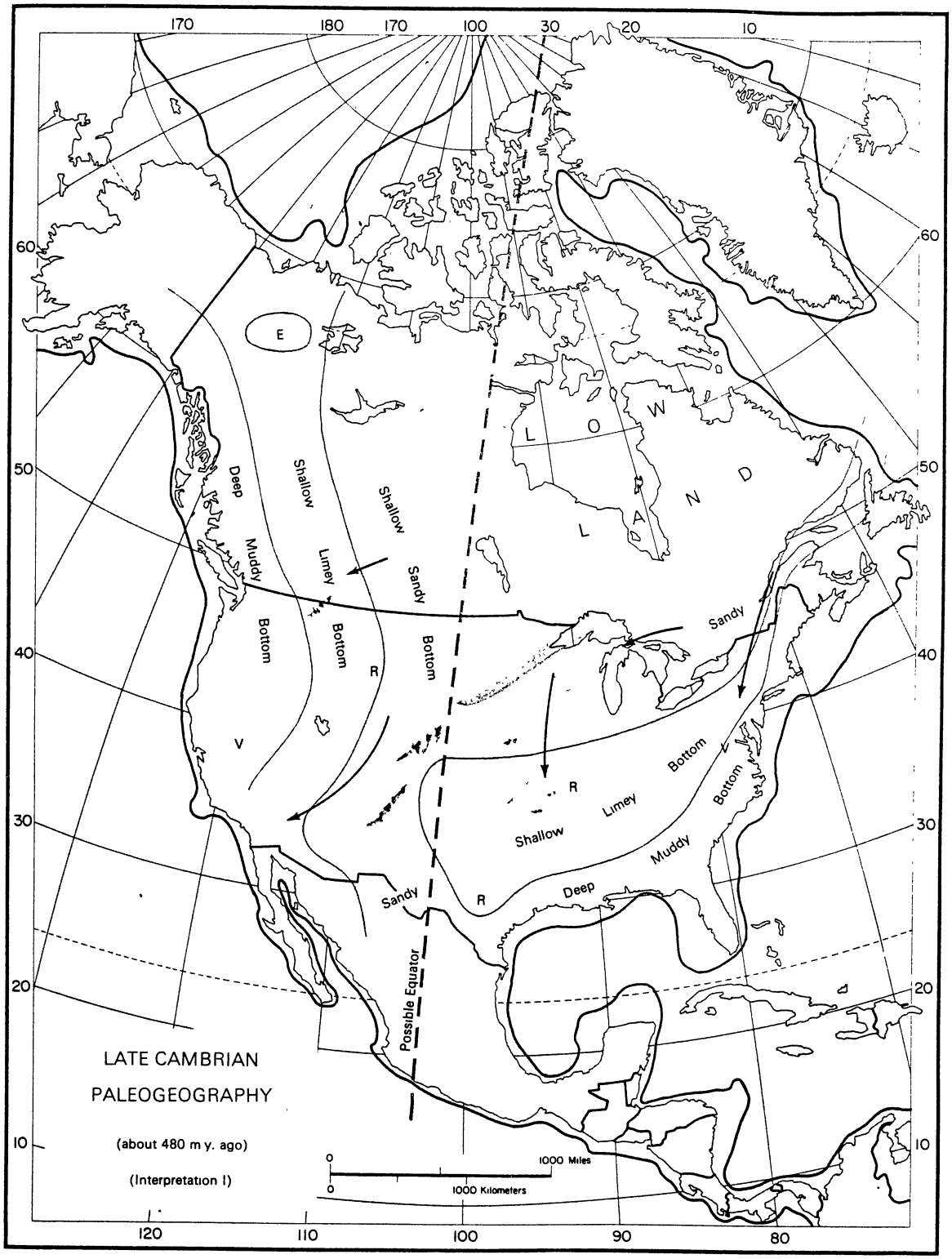

Figure 75. Late Cambrian Paleogeography of North America (Dott and Batten, 1981).

carbonate sand-dominated shoreline. Gradual passage of the Honey Creek carbonate sands upward into the micritic and generally unfossiliferous Fort Sill Formation records the continued transgression and subsequent shifting of the carbonate sand shoreline away from the area. Small scale (ripple) cross-bedding in the middle unit and algal boundstones of the upper unit of the Fort Sill Formation are interpreted to have been deposited in low energy, shallow waters with restricted circulation (Donovan, 1982). Algal mounds, stromatolites, and algal mats of the upper unit of the Fort Sill Formation are indicative of marine sedimentation in the upper subtidal, intertidal, and possibly the lower supratidal zones.

The Fort Sill algal boundstones cease abruptly at the contact with the overlying Signal Mountain Formation. The lack of stromatolites and the abundance of interbedded mudstones and clastic limestones suggest a deeper water environment during Signal Mountain deposition. This deeper water sedimentation seems to represent a middle shelf environment. The gradational upward passage of the Signal Mountain Formation into mudstones and occasional clastic limestone beds of the non-cherty, lower member of the McKenzie Hill Formation signifies the continuation of a shelf environment. However, the appearance of stromatolites, in the upper portion of the lower unit of the McKenzie Hill Formation, suggests a slight marine regression. The cherty, upper unit of the McKenzie Hill Formation records continued marine regression as evidenced by the increased occurrence of stromatolites and algal mounds. Abundant siliciclastic sand, abundant stromatolite, algal-mounds, and algal-mat boundstones, and several sabkha cycles in the Cool Creek Formation (Ragland,

1983) record sedimentation within the upper subtidal, intertidal, and supratidal zones.

Indicators of Environments

Algal Boundstones

The absence of algal boundstones, in the Signal Mountain Formation, may be a good indicator of water depth. Since Cambro-Ordovician algal boundstones most commonly formed in the upper subtidal, intertidal, and lower supratidal zones (Ragland, 1983), it is suggested that the Formation probably was deposited in the deeper waters of the subtidal zone.

IFC Limestones

IFC limestones are believed to represent layers produced by major storms, such as hurricanes and typhoons. Waves generated by these storms ripped up lithified to partially lithified sediments of the ocean floor. Packing orientations of individual clasts in the IFC's are indications of water turbulance and depositional setting as follows: (i) random packing - either not reworked and deposited within the subtidal and shelf zones or rapidly buried in nearshore zones; (ii) parallel to bedding (Figure 24) - little or no reworking and deposited within the subtidal to intertidal zones; (iii) imbricate to parallel to bedding (Figure 25) - reworked by tidal (especially if bimodally imbricate) or long-shore currents and deposited within the intertidal or subtidal zones; and (iv) vertical to imbricate (Figures 76 and 77) - reworked by waves (Sanderson and Donovan, 1974) and deposited within the intertidal zone. A matrix of lime mud and allochems suggests that these elements

Figure 76. Imbricate to vertical packing of cobble IFCs at outcrop. The photograph was taken 649 feet above the base of the Bally Mountain measured section. Pictured is a portion of a 1 foot thick bed of imbricate and vertical packed cobble IFCs. Orientation of the IFCs has recorded that the clasts were packed by waves during sedimentation in the intertidal zone.

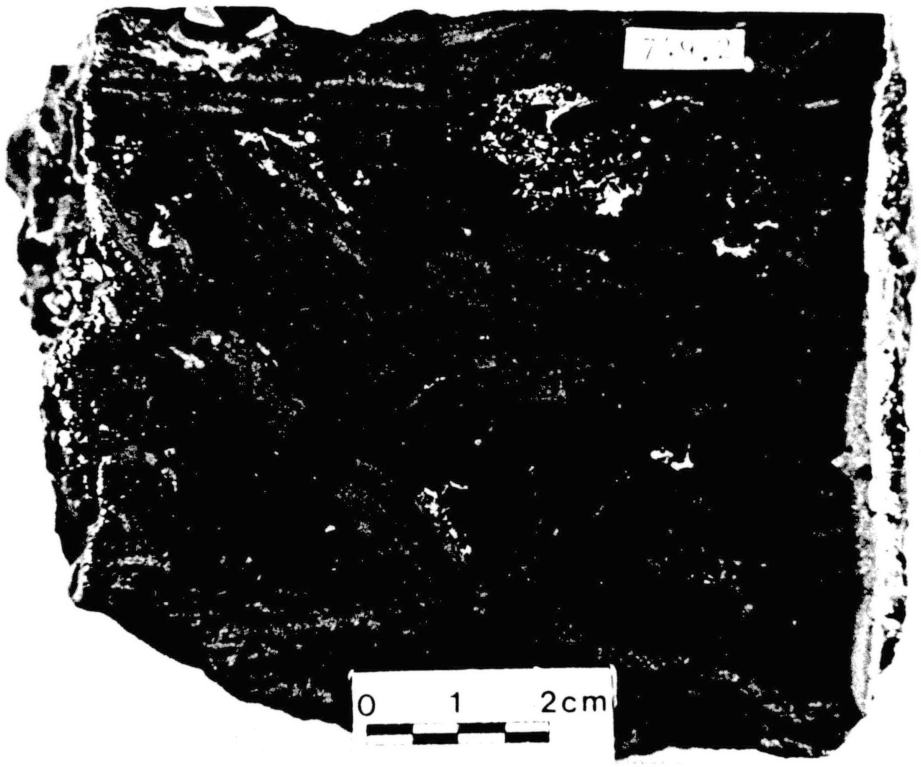

Figure 77. Imbricate to vertically packed cobble IFCs in hand-sample 649.2. The photograph is of a sample collected from the zone pictured in Figure 76. Sample face was cut parallel to strike and the view is opposite to the dip direction. This cobble IFC limestone has a matrix of trilobite fragments, pelmatozoan parts, and intraclast sand cemented by lime mud. The IFCs are composed of thinly laminated fossiliferous peloidal wackestones derived from the zone directly below (a portion of which is seen of the base of the sample). Many sand intraclasts are partially replaced by hamatite and appear reddish.

were washed in post-depositionally. Complete calcite spar cementation either represents, (i) current-laid IFCs, (ii) a winnowing of lime mud from between previously deposited IFC's by waves or tidal currents, or (iii) accumulation of IFC's too rapidly for mud to infiltrate.

Most IFC limestones suggest a deeper water environment with little reworking.

Grainstones

Since grainstones are principally cemented by calcite spar, certain conclusions (similar to those relative to the IFC limestones) can be inferred as to their origin. They may indicate any of the following four conditions; i) current laid and well washed, (ii) current (including wave) winnowing of lime mud from previously muddy sediment, (iii) bypassing of local areas by mud, and (iv) accumulation of grains so rapidly as to prevent mud infiltration (Dunham, 1962). Collectively grainstones suggest sedimentation either in the intertidal to subtidal zones or as shoaling sequences in the shelf zone.

Packstones

Packstones are peculiar because they possess two distinctly contrasting rock properties; grain support, which is indicative of deposition in agitated waters, and micrite matrix, which is suggestive of deposition in quiet waters (Dunham, 1962). Signal Mountain packstones are interpreted as representative of grains which were washed into deeper, quieter lime muddy environments by tides and storms. Additionally current-laid grains have been infiltrated with lime mud after deposition to

form packstones. Many packstones may represent compacted wackstones (a lithotype with which packstones are commonly associated).

Wackestones and Mudstones

Wackestone and mudstone lithotypes are interpreted as a record of either sedimentation in deeper water subtidal and shelf zones or in shallow intertidal zones of restricted circulation.

Fauna

As previously stated the most abundant fossil assemblages are pelmatozoans and trilobites. Gastropods and brachiopods also are common. According to Tucker (1981), trilobites, brachiopods, and especially gastropods commonly inhabited a variety of shallow marine environments. Pelmatozoans on the other hand, commonly dwell in deeper water environments such as the shelf zone. Some pelmatozoan species, such as crinoids, are strictly found in deeper water zones.

Sedimentary Structures

Shallow water sedimentary structures in the Signal Mountain Formation are ripple laminations and small scale trough cross bedding, erosive and scoured bases, channeling, and burrows, bioturbation, and borings. Skolithos burrows are generally restricted to the intertidal zone whereas Thalassinoides burrows are common to both intertidal and subtidal zones (Tucker, 1981).

Hardgrounds and subaqueous shrinkage cracks occur in micritic sediments deposited in calm waters (Leader, 1982). Thus they are suggestive

of either sedimentation in deeper water zones or in shallow water zones with restricted circulation.

Siliciclastics

Siliciclastic grains are generally silt to very fine sand size and rarely constitute more than 3 to 5% of the limestone. The general lack of siliciclastic grains, coupled with their small size, suggests that sedimentation of the Signal Mountain Formation was far removed from siliciclastic shorelines. Siliciclastic detritus in the Formation likely represents wind blown dust. Rare calcareous siltstone and siliciclastic mudstone laminae may record either dust storms that blanketed the area with siliciclastic silt or shoals in the shelf environment.

Evaporites

The absence of evaporites or their pseudomorphs rules out sedimentation in the supratidal (sabkha) zone.

Organic Matter

Organic mater content (O.M.) analysis of several Signal Mountain samples (Chapter VII) revealed an O.M. content of between 0.22 and 0.25%. These values are close to the mean average of 0.29% for limestones (Leader, 1982). The preservation of significant amounts of O.M. suggests that the burial environment was somewhat reducing and therefore at greater depths than the well oxygenated sediments of the intertidal zone. It is pertinent that O.M. analysis of the Cool Creek Formation (which does have a strong intertidal imprint) showed that practically no O.M. is present (Donovan, 1984).

Depositional Model

The Cambro-Ordovician paleolatitude of southwestern Oklahoma was approximately 25° south of the paleoequator (Figure 78) (Habicht, 1979). This interpretation is based on paleomagnetic data and supported by the fact that thick limestone and some evaporite sequences accumulated across the North American Craton during that time.

During Cambro-Ordovician time vast epeiric seas covered most of the North American Craton. Relatively shallow water depths covered thousands to hundreds of thousands of square miles of continental shelf (Figure 75). These epicontinental seas were generally less than 330 to 500 feet (100 to 150 m) deep (Dott and Batten, 1981). Today, there are no true scale uniformitarian examples of the Cambro-Ordovician epicontinental seas. However, certain analogies may be drawn from the depositional style of the modern carbonate depositional environments on the sea floor around the Qatar Peninsula.

The carbonate factory in the Persian Gulf, off the Qatar Peninsula, is probably the best present day model for the sedimentation of the Signal Mountain Formation (Figure 79). The Persian Gulf is 1,561 miles long (2,512 km), varies in width from 547 to 88 miles (880 to 142 km) (Bathurst, 1975), and roughly spans 496,000 square miles (1,284,640 km^2). Water depths across much of the carbonate platform are less than 97 feet (30 m). The central Persian Gulf, between the Qatar Peninsula and Iran, is 384 feet (117 m) deep. According to Bathurst (1975), the open Gulf floor, off Qatar, consists of predominantly calcarenites on near- and off-shore terraces and marls in the central Gulf (Figure 80). Near-shore terrace sediments are composed of rounded calcarenites.

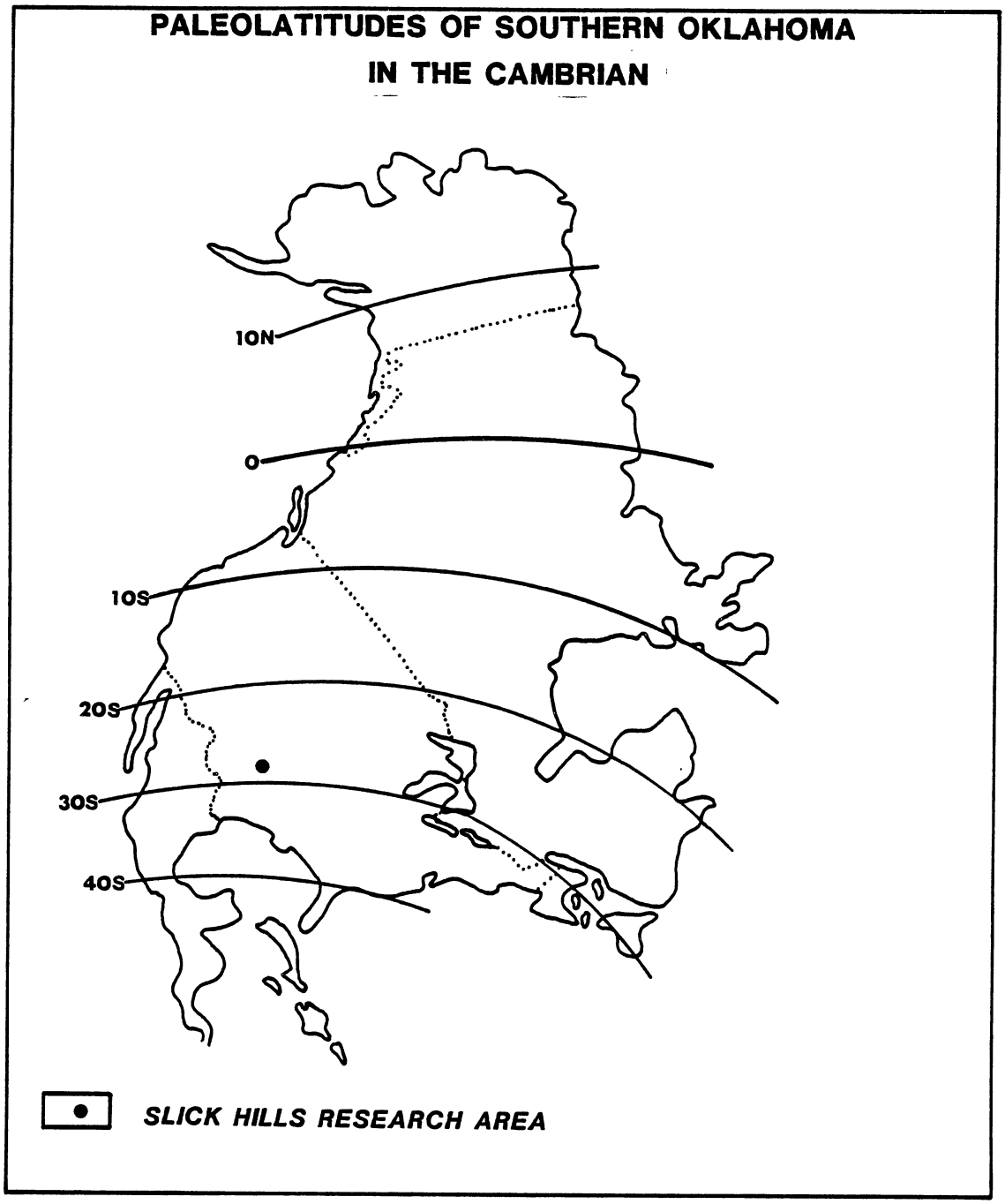

Figure 78. Paleolatitudes of southwestern Oklahoma in the Cambrian Period (adapted from Habicht, 1979 and drafted by D. Ragland, 1983).

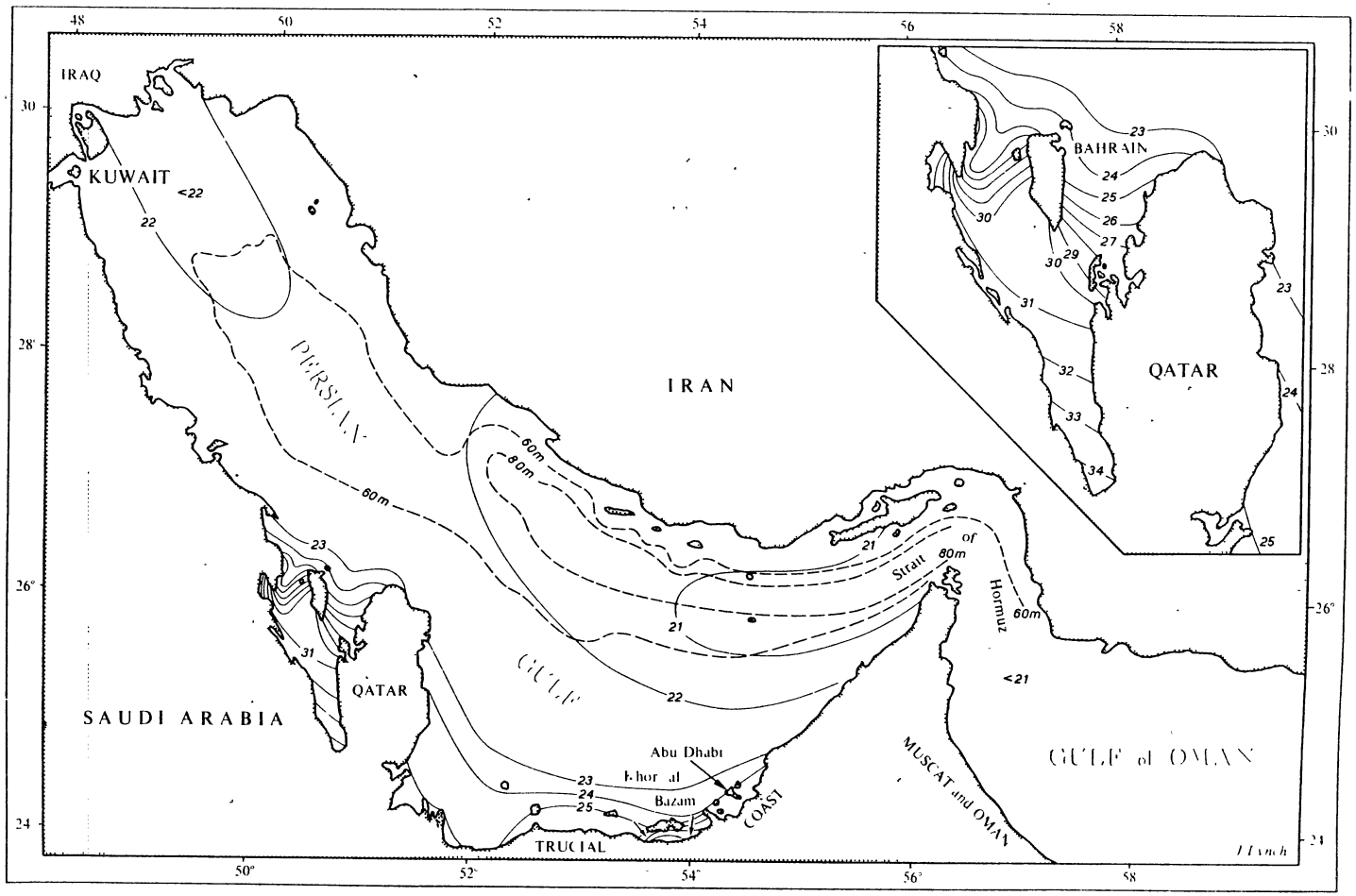

Figure 79. Qatar Peninsula location map, Persian Gulf. (Bathurst, 1975; adapted from Sugden, 1963).

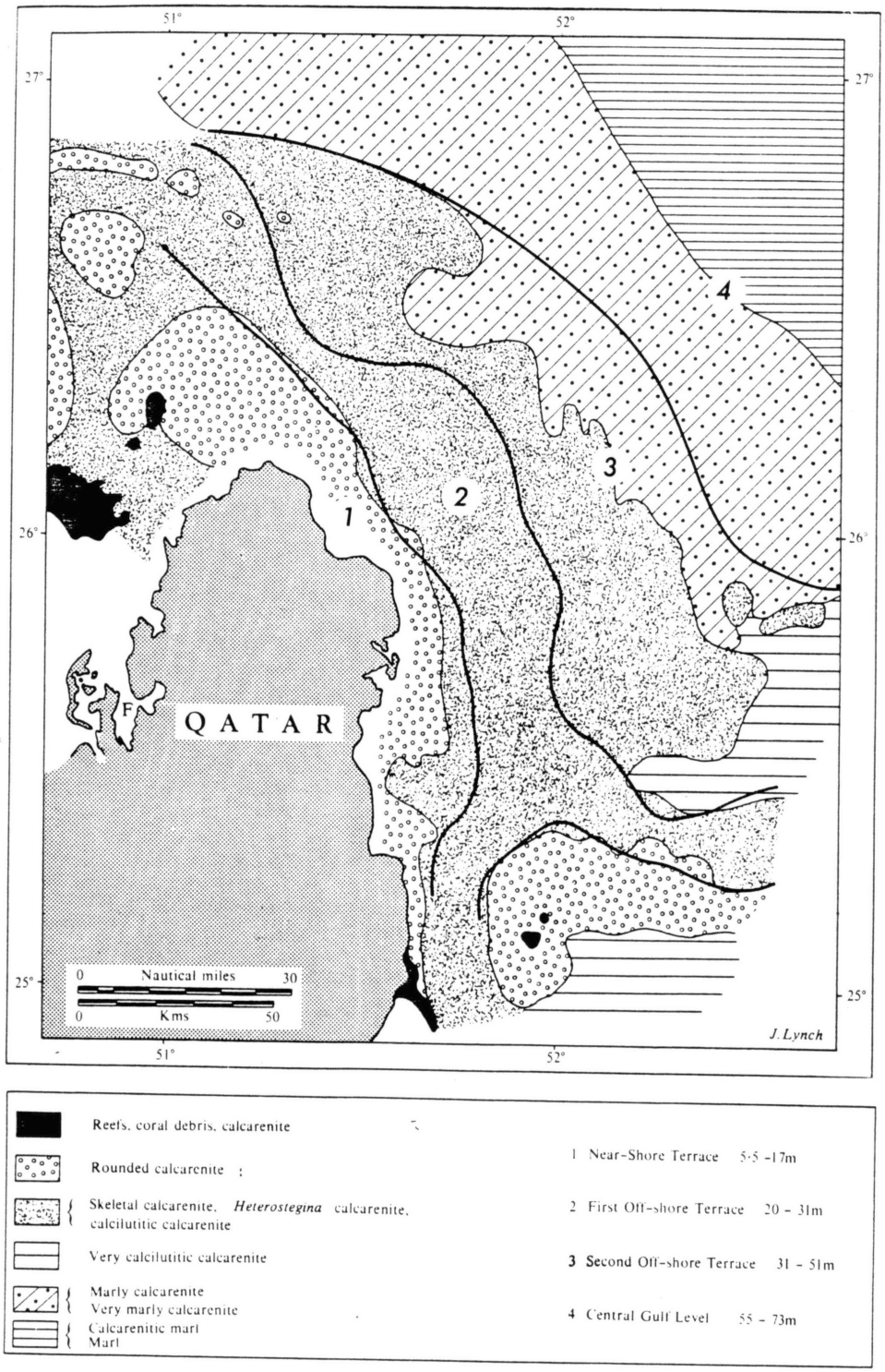

Figure 80. Lithofacies off the Qatar Peninsula, Persian Gulf. (Bathurst, 1975; adapted from Houbolt, 1957).

Water depth is 18 to 56 feet (5 to 17 m). These calcarenites are principally subrounded to rounded carbonate grains equivalent to mudstone, wackestone, and packstone clasts that are abundant lithotypes of the Signal Mountain Formation. Quartz sand grains and skeletal debris compose minor amounts of this facies. Water turbulence near the shore prevents the accumulation of micrite. Micrite-free rounded calcarenites will eventually be cemented to form intraclast sand grainstones similar to those in the Signal Mountain Formation. Wheredeposited in more restrictive zones micrite can accumulate to form packstone lithotypes.

Rounded calcarenites grade seaward into skeletal calcarenites and calcilutitic calcarenites (5 to 30% micrite) of the first off-shore terrace. The water depth is 65 to 102 feet (20 to 31 m). Shell fragments are the dominant grains in skeletal calcarenites and micrite content is generally not greater that 5%. Skeletal calcarenites will generally form limestones similar to the fossiliferous sand grainstones of the Signal Mountain Formation. Calcilutitic calcarenites are comparable to fossiliferous packstone and wackestone lithotypes.
Skeletal and calcilutitic calcarenites facies extend out onto the second off-shore terrace where the Gulf is 101 to 167 feet (31-51 m) deep. These facies pass seaward into marly (10 to 30% marl) to very marly (30 to 70% marl) and very calcilutitic (30 to 70% micrite) calcarenites. Although marl-poor, intraclast and fossiliferous sand wackestone lithotypes of the Signal Mountain Formation, are analogous to these lithofacies.

The central Gulf level is where facies of the second off-shore terrace grade into calcarenitic marl (70 to 95% marl) and marl (95 to 100% marl) of the central basin. These lithofacies are representative of

wackestone and mudstone lithotypes, respectively, found in the Signal Mountain Formation.

Lithotypes of the sea floor around Qatar exhibit distinct facies development from near shore to central basin. In contrast, the Signal Mountain Formation records the sedimentation of very poorly sorted lithotypes. The facies are subtle and only expressed by a relatively greater concentration of one or more lithotypes in crude zones. Mudstones, mudstones and wackestones, and the clastic limestones are considered the generalized facies of the Formation.

In Cambrian-Ordovician seas lithotypes were probably not sorted into distinct facies. During that time, the seas were so vast and shallow, and the slope of the continental shelf so very gentle that ocean currents were unable to segregate lithotypes quickly into the organized facies suggested by the Qatar analogy. Subsidence was rapid (Beauchamp et al., 1982); therefore, sediments were buried before the weak currents sorted them into facies. Erosion on the shelf was enormous, as recorded by the abundant IFC limestones, scours, and hardgrounds in the Formation. Storms, which produced the IFC limestones, redistributed sediments throughout the shelf into indistinct facies as is evident on the stratigraphic log of the formation.

CHAPTER VII

PARAGENESIS AND ORGANIC MATTER CONTENT OF THE SIGNAL MOUNTAIN FORMATION

Paragenesis

Signal Mountain lithotypes accumulated on the ocean bottom in the subtidal zone of the Cambro-Ordovician shelf across present southwestern Oklahoma. Syndepositional marine cementation of lime mud-rich limestone, at or just below the sediment-water interface, produced abundant hardgrounds. As sediments passed into the phreatic zone, micrite cementation began. At time, pore water pH apparently fluctuated. Acidic pore waters dissolved originally aragonitic gastropod shells leaving voids in the lime mud. These acidic waters contained low concentrations of silica, which precipitated as syntaxial overgrowths on quartz and feldspar siliciclastic grains.

Most grainstones and micrite-poor IFC limestones, in the phreatic zone, subsequently were partially cemented by pore filling drusy calcite, syntaxial calcite overgrowths on pelmatozoan parts, and blocky calcite. Some drusy calcite either crystallized in a single generation or in stages as the pH and calcite concentration of pore waters fluctuated. In the latter case, drusy calcite initially crystallized as isopachous rims on allochems. Shell voids, fenestrate, and shelter porosity in lime mud rich limestones were also partially to completely

filled by the same cements. As sediments compacted, shells voids, that had escaped cementation, collapsed. Pelmatozoan parts converted from high to low magnesium calcite to release magnesium ions into solution. Micro-dolomite rhombs formed in the pelmatozoan parts during the conversion. As pH fluctuated, silica, in the form of chalcedony, replaced the centers of most pelmatozoan parts. Brachiopod shells also commonly were silicified. Before deep burial, primary porosity was probably reduced to less than 10%.

Deeper burial placed the limestones in the zone of formation water diagenesis. Where formation waters were locally saturated in silica, rare chert nodules formed by the non-selective replacement of limestone fabrics by microquartz and fibrous chalcedony. Late pore filling silica initially crystallized fibrous chalcedony along intercrystalline boundaries between blocky calcite crystals as the silica concentration in pore waters was high. As silica was depleted, minor amounts of megaquartz crystallized in the remaining pore space.

Formation waters were rich in Mg^{2+} and Fe^{2+} ions. Ferroan dolomite rhombs along naturally permeable and bioturbated zones. Open pores, especially in grainstones and IFC limestones, were filled by sparry ferroan dolomite rhombs of baroque ankerite. Lime mud intraclasts, pelmatozoan parts, and syntaxial calcite overgrowths on pelmatozoan parts were subject to replacement by ferroan dolomite. Discontinuous crystallization variation in ionic concentration produced zoned dolomite rhombs. Ferroan dolomite was the final pore filling cement of many grainstones.

Deep burial pressure solution produced abundant stylolites. Stylolites formed in mudstone and lime mud rich limestone intervals.

The Signal Mountain Formation was tightly cemented during deep burial. Eventual uplift to surface to near surface conditions has resulted in the minor generation of secondary porosity. Secondary porosity occurs as the result of dissolution of calcite along partings and fractures. The paragenesis of the Signal Mountain Formation is summarized in Figure 81.

Organic Matter

BM 93.6, BM 382.5, and BM 595.0 were selected for total organic carbon analysis. Enough of each sample was crushed to accommodate two analyses. Each sample and a duplicate were treated to dissolve all calcium carbonate and prepare the samples for analysis (Metson and others, 1979). Using Metson's technique, Wante (a graduate hydrology student at Oklahoma State University) performed the analysis and computer processing of the generated data.

The organic matter (O.M) of each sample and duplicate was determined as follows:

Sample	O.M. (%)
BM 93.6	0.242
Duplicate	0.242
BM 382.6	0.226
Duplicate	0.231
BM 595.0	0.248
Duplicate	0.254

According to Leeder (1982), the average organic matter content of carbonates is 0.29%. The 0.22 to 0.25% range of values for the Signal Mountain samples falls just below this average. Given that the organic matter of limestones is usually sapropel, the organic content and the

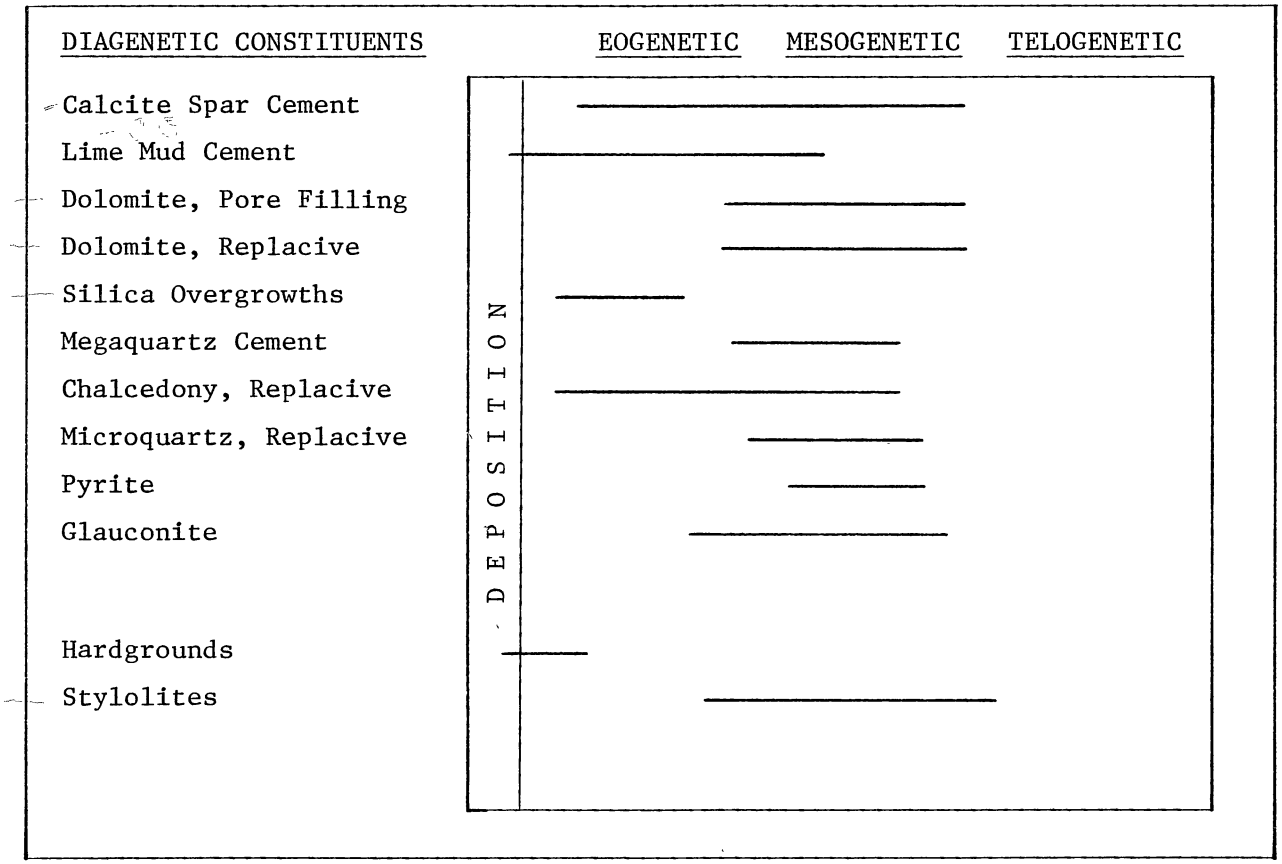

Figure 81. Paragenesis of diagenetic events in the Signal Mountain Formation.

thickness (approximately 800 feet) suggest that the Signal Mountain Formation may have been a source for hydrocarbons.

The analysis of the Formation for organic matter was a preliminary investigation and in itself was not conclusive. Further study is required to properly evaluate the source rock potential of the Signal Mountain Formation.

CHAPTER VIII

SUMMARY AND CONCLUSIONS

Deposition of the Signal Mountain Formation occurred in the middle shelf zone of the Cambro-Ordovician sea that once covered southwestern Oklahoma. The depositional environment was somewhat similar to that in the Persian Gulf off the Qatar Peninsula today. However, there was insufficient energy in the Cambro-Ordovician sea to sort lithotypes into distinct facies (as is the case in the Qatar analogy). Instead, the Signal Mountain lithotypes are very thinly interbedded and poorly sorted throughout the section.

A high percentage of the lime mud, numerous subaqueous shrinkage cracks and diagenetic hardgrounds, plus the lack of stromatolites and evaporites indicate that the Formation was deposited in the relatively deep and calm waters of the subtidal zone. Ripples, crossbedding, erosive and scoured bases, and imbricate to vertical packing of clasts indicate that much deposition occurred in the intertidal zone or on shoals developed on the shelf environment.

Lithotypes of the Formation are mudstones and clastic limestones. Siliciclastic content is minor. Clastic limestones include intraformation conglomerate (IFC) limestones, grainstones, packstones, and wackestones. IFC limestones constitute the most characteristic and one of the most abundant lithotypes. Intraclast sand and fossiliferous grainstones, packstones, and wackestones are well represented. Trilobite

carpaces and pelmatozoan parts are the most abundant fossils of fossiliferous limestones. Brachiopod and gastropod fossils are also common. Only a few oolitic limestones were discovered. Peloids tend to be mixed with other limestone constituents, but also may form discrete laminae.

Principal cements in the Formation are lime mud and calcite spar. Lime mud is the most common cementing agent, owing to the high percentage of mudstones and limestones with lime mud matrixes. Lime mud cements have commonly undergone neomorphism to microspar. Isopachous calcite often preceded the drusy and block calcite spar cementation of open pore space.

The Formation contains moderate amounts of dolomite throughout. At outcrop bedded zones of oxidized dolomite are seen as distinctive orange bands that stripe the limestone beds. The orange coloration suggested that the dolomite was highly ferroan. X-ray diffraction and staining techniques identified the dolomite as ankerite. High iron content and baroque crystalline form indicate that most of dolomitization occurred as a result of deep burial formation water diagenesis. Signal Mountain dolomites are more commonly replacive than pore filling. Replacive dolomite crystallizes in rhombic forms that are commonly zoned and it is selective of the following textures: lime mud and the lime mud of interclasts; lime mud filled burrows and bioturbated zones; and pelmatozoan parts and their syntaxial calcite overgrowths. Pore filling dolomite forms coarse rhombic and distinctly baroque crystals.

Diagenetic silica is a minor constituent. At outcrop the presence of silica is recognized by the silicification of body fossils and burrows, and the formation of small chert nodules. Microquartz and chalcedonic quartz record the silification of brachiopod shells and

pelmatozoan parts, and formed the chert nodules. Rare megaquartz was a late diagenetic pore filling cement.

Pyrite and glauconite are minor diagenetic constituents. Pyrite is disseminated in the limestone or has formed small pebble size nodules. Glauconite is typically a replacement of the lime mud of intraclasts. Although distinct grains of glauconite were rare at the Bally Mountain measured section, they were more plentiful elsewhere in the study area.

Overburden pressures, exerted by the sedimentary pile on the deeply buried limestone, produced a high degree of stylolitization. These diagenetic stylolites are of the low amplitude, horizontal to inclined, simple wavelike or sutured, and interconnected network variety. Vertical to inclined tectonic stylolites of low to moderate amplitude are also present. Tectonic stylolites presumably formed during the Pennsylvanian tectonic activity.

The principal source of information was derived from the section at Bally Mountain, in Kiowa County, Oklahoma; where the Signal Mountain Formation measured 753 feet in thickness. A section of Ring Top Mountain, in Caddo County, Oklahoma, measured 829 feet in thickness. Other partial sections were also examined.

The Signal Mountain Formation is part of the lower Arbuckle Group and disconformably overlies the Fort Sill Formation and conformably underlies the McKenzie Hill Formation. The Signal Mountain-McKenzie Hill Formational contact is difficult to determine because there is no lithologic break that corresponds to the break in trilobite fauna (which defines the contact). In fact, the two Formations interfinger through approximately 100 feet of section. Refined paleontologic skills and excavation of trilobite carpaces are required to located the exact

boundary. For field mapping, the base of the first continuous blocky to massive parting limestone is chosen as the approximate contact. Flaggy to slabby, "tombstone," parings of the Signal Mountain Formation contrast well with the blocky to massive partings of the McKenzie Hill Formation.

The Signal Mountain-Fort Sill Formational contact is easily recognized by an abrupt lithologic and color change. Upper Fort Sill white to light gray algal mound boundstones abruptly end as the Signal Mountain orange mottled dolomitic mudstones begin. This contact is regionally diachronous, for within the first 12 feet of Signal Mountain Formation a 3 feet thick white to light gray algal boundstone unit, similar to the upper Fort Sill Formation, is present.

The Signal Mountain Formation contains the Cambrian-Ordovician boundary. At the Bally Mountain measured section the boundary is approximately 339 feet above the base of the Signal Mountain Formation. This boundary is solely picked according to a break in trilobite fauna because there is a lithologic continuity across the boundary.

Regionally the study area is located in the northwest to southeast trending Frontal fault zone between the Wichita Mountain Uplift (to the southwest) and the Anadarko Basin (to the northeast) of southwestern Oklahoma. The principal tectonic elements of the Frontal fault zone are a series of northwest to southeast-trending folds and faults. Specifically, the study area is located on the northeast limb of the Blue Creek Canyon anticline on the Blue Creek Canyon horst. Uplift of the Horst occurred along the Mountain View and Blue Creek Canyon faults to the northwest and southwest respectively.

REFERENCES CITED

Bain, H. Foster, 1900, Geology of the Wichita Mountains: Bull. Geol. Soc. of Amer., vol. 7, p. 127-44.

Bathurst, Robin G. C., 1975, Carbonate Sediments and Their Diagenesis: Elsevier, New York.

Beauchamp, Weldon, 1983, The Structure of the Southern Slick Hills in Southwestern Oklahoma: Unpub. M.S. Thesis, Oklahoma State University, Stillwater, Oklahoma.

Brookby, H. E., 1969, Upper Arbuckle (Ordovician), Outcrops in Richards Spar-Kindblade Ranch Area, Northeastern Wichita Mountains, Oklahoma: Unpub. M.S. Thesis, University of Oklahoma, Norman, Oklahoma.

Decker, Charles E., 1939, Progress Report on the Classification of the Timbered Hills and Arbuckle Groups of Rocks: Arbuckle and Wichita Mountains, Oklahoma: Okla. Geol. Surv., Circular No. 22, p. 1-61.

Donovan, R. Nowell, 1982, Geology of Blue Creek Canyon Wichita Mountains Area: in Gilbert, M. C. and Donovan, R. N. eds., Geology of the Eastern Wichita Mountains Southwestern Oklahoma: Okla. Geol. Surv., Guidebook 21, Norman, Oklahoma, p. 65-77.

Donovan, R. Nowell, 1983, Sedimentology Class Notes: Oklahoma State University, Stillwater, Oklahoma.

Donovan, R. Nowell, 1984, Personal Communication: Stillwater, Oklahoma.

Donovan, R. Nowell and Cloyd, Kelly, 1983, Map of Bally Mountain, Kiowa County: Unpub., Oklahoma State University, Stillwater, Oklahoma.

Donovan, R. Nowell, et al., 1982, Subsidence Rates in Oklahoma During the Paleozoic: in Donovan, R. N., ed., The Selenite Blade: Department of Geology, Oklahoma State University, Stillwater, Oklahoma.

Donovan, R. Nowell and Foster, R. J., 1972, Subaqueous Shrinkage Cracks from the Caithness Flagstone Series (Middle Devonian(of Northeast Scotland: Jour. of Sed. Pet., Vol. 43, p. 309-317.

Donovan, R. Nowell and Ragland, Deborah A., 1983, General Stratigraphic Log for the Slick Hills of Southwestern Oklahoma: Unpub. M. S. Thesis, Oklahoma State University, Stillwater, Oklahoma.

Dott, Robert H. Jr. and Batten, Roger L., 1981, Evolution of the Earth: McGraw-Hill, New York.

Dunham, R. J., 1962, Classification of Carbonate Rocks: in Ham, W. E. ed., Classification of Carbonate Rocks-a Symposium: Amer. Assoc. of Petroleum Geol., Memoir 1, Tulsa, Oklahoma, p. 108-21.

Enos, Paul, 1983, Shelf Environment: in Scholle, Robert A., Bebout, Don. G., and Moore, Clyde H. eds., Carbonate Depositional Environments: Amer. Assoc. of Petroleum Geol., Memoir 33, Tulsa, Oklahoma.

Folk, R. L., 1962, Spectral Subdivision of Limestone Types: in Ham, W. E. ed., Classification of Carbonate Rocks-a Symposium: Amer. Assoc. of Petroleum Geol., Memoir 1, Tulsa, Oklahoma, p. 108-121.

Frederickson, E. A., Chase, Gerald W. and Ham, William E., 1965, Resume of the Geology of the Wichita Mountains, Oklahoma: in The Petroleum Geology of Southern Oklahoma: Amer. Assoc. of Petroleum Geol., Tulsa, Oklahoma, p. 36-55.

Gilbert, M. Charles, 1982, Geologic Setting of the Eastern Wichita Mountains with a Brief Discussion of Unresolved Problems: in Gilbert M. C. and Donovan R. N. eds., Geology of the Eastern Wichita Mountains Southwestern Oklahoma, Okla. Geol. Surv., Guidebook 21, Norman, Oklahoma, p. 1-30.

Habicht, J. K. A., 1979, Paleoclimate, Paleomagnetism, and Continental Drift: Amer. Assoc. of Petroleum Geol., Studies in Geology, No. 9, Amer. Assoc. of Petroleum Geol., Tulsa, Oklahoma.

Harlton, Bruce H., 1963, Frontal Wichita Fault System of Southwestern Oklahoma: Amer. Assoc. of Petroleum Geol. Bull., vol. 47, no. 8, pp. 1552-1580.

Haves, John S., 1977, The Reconnaissance of the Water Resources of the Lawton Quadrangle, Southwestern Oklahoma: U.S. Geol. Surv.

Houbolt, J. J. H. C., 1957, Surface Sediments of the Persian Gulf near the Qatar Peninsula: Doctoral Thesis, University of Utrecht, Utrecht.

Johnson, Kenneth S., et al., 1979, The Mississippian and Pennsylvanian (Carboniferous) Systems in the United States Oklahoma: U. S. Geol. Surv. Prof. Paper 1110-R, Washington D. C.

Katz, Amitai and Friedman, Gerald M., 1965, The Preparation of Stained Acetate Peels for the Study of Carbonate Rocks: Jour. of Sed. Pet., Vol. 35, No. 1, p. 248-249.

Leeder, M. R., 1982, Sedimentary: Process and Product: George Allen and Unwin, London.

Leutloff, Alan H. and Meyers, William J., 1984, Regional Distribution of Microdolomite Inclusions in Mississippian Echinoderms from Southwestern New Mexico: Jour. Sed. Pet., Vol. 54, p. 442-446.

McConnell, David, 1983, The Structure of the Northern Slick Hills in Southwestern Oklahoma: Unpub. M.S. Thesis, Oklahoma State University, Stillwater, Oklahoma.

Myers, J. D., Gilbert, M. C., and Loiselle, M. C., 1981, Geochemistry of the Cambrian Wichita Granite Group and Revisions of its Lithostratigraphy: Oklahoma Geology Notes, Vol. 41, p. 172-195.

Rafalowski, Mary, 1984, Personal Communication: Stillwater, Oklahoma.

Ragland, Deborah Ann, 1983, Sedimentary Geology of the Ordovician Cool Creek Formation as it is Exposed in the Wichita Mountains of Southwestern Oklahoma: Unpub. M.S. Thesis, Oklahoma State University, Stillwater, Oklahoma.

Reading, H. G., 1982, Facies: in Reading, H. G. ed., Sedimentary Environments and Facies: Elsevier, New York.

Rupke, N. A., 1982, Deep Clastic Seas: in Reading H. G. ed., Sedimentary Environments and Facies: Elsevier, New York.

Sanderson, David J., and Donovan, R. Nowell, 1974, The Vertical Packing of Shells and Stones on Some Recent Beaches: Jour. of Sed. Pet., Vol. 44, p. 680-688.

Scholle, Peter A., 1979, A Color Illustrated Guide to Carbonate Rock Constituents, Textures, Cements, and Porosities: Amer. Assoc. of Petroleum Geol., Memoir 27, Tulsa, Oklahoma.

Sellwood, B. W., 1982, Shallow-water Carbonate Environments: in Reading, H. G. ed., Sedimentary Environments and Facies: Elsevier, New York.

Shinn, Eugene A., 1983, Tidal Flat: in Scholle, Peter A., Bebout, Don G., and Moore, Clyde H. ed., Carbonate Depositional Environments: Amer. Assoc. of Petroleum Geol., Memoir 33, Tulsa, Oklahoma.

Stitt, J. H., 1968, Late Cambrian and Earliest Ordovician Trilobite Faunas, Western Arbuckle Mountains: Murray County, Oklahoma: in Regional Geology of the Arbuckle Mountains: Amer. Assoc. of Petroleum Geol., Field Trip Guidebook, Tulsa, Oklahoma, p. 31-34.

Stitt, James H., 1971, Late Cambrian and Earliest Ordovician Trilobites, Timbered Hills and Lower Arbuckle Groups, Western Arbuckle Mountains, Murray County, Oklahoma: Okla. Geol. Surv., Bull. 110, University of Oklahoma, Norman, Oklahoma.

Stitt, J. H., 1978, Biostratigraphy and Depositional History of the Timbered Hills and Lower Arbuckle Groups, Western Arbuckle Mountains, Oklahoma: in Ham, W. E. ed., Regional Geology of the Arbuckle Mountains, Oklahoma: Okla. Geol. Surv. Guidebook for Amer. Assoc. of Petroleum Geol. and Society of Economic Paleontologists and Mineralogists Annual Meeting, Oklahoma City, Field Trip 1, p. 19-23.

Stitt, James H., 1983, Trilobites, Biostratigraphy, and Lithostratigraphy of the McKenzie Hill Limestone (Lower Ordovician), Wichita and Arbuckle Mountains, Oklahoma: Okla. Geol. Surv., Bull. 134, University of Oklahoma, Norman, Oklahoma.

Stubbs, Milton, 1983, The Geology of the Ketch Creek Fault: Unpub. Map, Oklahoma State University, Stillwater, Oklahoma.

Sugden, W., 1963, The Hydrology of the Persian Gulf and its significance in respect to evaporate deposition: Amer. Jour. of Science, Vol. 261, p. 741-55.

Swanson, R. G., 1981, Sample Examination Manual: Tulsa, Amer. Assoc. of Petroleum Geol. Tulsa, Oklahoma.

Taff, J. A., 1928, Geology of the Arbuckle and Wichita Mountains: U. S. Geol. Surv., Prof. Paper 31.

Till, R., 1982, And Shorelines and Evaporites: in Reading, H. G. ed., Sedimentary Environments and Facies: Elsevier, New York.

Tsegay, Tekleab, 1983, The Reagan Sandstone as it is Exposed in the Wichita MOuntains of Southwestern Oklahoma: Unpub. M. S. Thesis, Oklahoma State University, Stillwater, Oklahoma.

Tucker, M. E., 1981, Sedimentary Petrology An Introduction: John Wiley and Sons, New York.

Wilson, James, E. and Jordan, Clif, 1983, Middle Shelf: in Scholle, Peter A., Bebout, Don G., and Moore, Clyde H. eds., Carbonate Depositional Environments: Amer. Assoc. of Petroleum Geol., Memoir 33, Tulsa, Oklahoma.

Ulrich, E. O., 1932, Preliminary Description of the Honey Creek, Fort Sill, Royer, and Signal Mountain Formations of Oklahoma: Bull. Geol. Soc. of Amer., Vol. 43, p. 742-47.

APPENDIX A

PETROGRAPHIC LOG OF THE CONSTITUENTS IN THE THIN SECTIONS FROM THE SIGNAL MOUNTAIN FORMATION, BALLY MOUNTAIN MEASURED SECTION

APPENDIX A

Thin Section (feet above datum) Position on Slide U = Upper M = Middle L = Lower	Composition %																			
	Intraclasts	Ooliths	Peloids	Trilobites	Pelmatazoans	Gastropods	Brachiopods	Micrite cement	Sparite cement	Dolomite cement	Chert	Chalcedony	Siliciclastic Grains (Quartz & Feldspar)	Muscovite	Pyrite	Hematite	Organics	Porosity	Glauconite	Illite (Smectite)
753.5-U								5	24	70			1							
753.5-L	10	T	15		T	2		42	30	T			1							
750.7	2		5	5	60	T		22	5				1			T				
740.5-U				3	2			92					3							
740.5-M	70		2	10	10				8				T							
740.5-L	5		10	T	10	30	T	41	3				1							
729.0	1		15	10	10	20		25	7	7			5							
723.0	1		7	7	6	T	7	32	20	10			10							
718.2	30			10	30		1		18	10			1							
708.0	1			1	2			84	5	7			T							
706.5	5		3	30	15	1	T	20	26	T			T							
701.0	45			10	20		T	3	19	3			T							
677.0	60		3	4	5	T	1	15	9	1			2							

Thin Section (feet above datum) Position on Slide U = Upper M = Middle L = Lower	Composition %																			
	Intraclasts	Ooliths	Peloids	Trilobites	Pelmatozoans	Gastropods	Brachiopods	Micrite cement	Sparite cement	Dolomite cement	Chert	Chalcedony	Siliciclastic Grains (Quartz & Feldspar)	Muscovite	Pyrite	Hematite	Organics	Porosity	Glauconite	Illite (Smectite)
676.0				T	T		T		79	5			3			3		10		
659.8	5		5	2	3	10	1	62	5	T			7							
651.3			40		7		T	24	24				5			T				
649.2	25			10	15			26	15	2			3			2	2			
645.4	10		3	15	7	T	1	52	5	T			7							
641.0-U				2	3			95					T							
641.0-M				15	10	20		45	10				T							
641.0-L			20	3	3	T		74					T							
634.2			5	7	5	5		56	20				2							
627.8-U			1	5	5	40		29	15	5			T							
627.8-L				5	1	1		68	20				5							
622.0-U	T		20	10	2	3	T	50	15				T							
622.0-M	T		10	2	T	1		85	3				T							
622.0-L				5				85	10				T							
612.0-U	3	T	7	20	15		T	38	10	5			2							

Thin Section (feet above datum)	Composition %																			
Position on Slide U = Upper M = Middle L = Lower	Intraclasts	Ooliths	Peloids	Trilobites	Pelmatazoans	Gastropods	Brachiopods	Micrite cement	Sparite cement	Dolomite cement	Chert	Chalcedony	Siliciclastic Grains (Quartz & Feldspar)	Muscovite	Pyrite	Hematite	Organics	Porosity	Glauconite	Illite (Smectite)
612.0-M	T		5	20	10	5	3	43	10	2			2							
612.0-L				10	20	3		44	13	7			3							
590.0	20	T	40		5			5	26	3			1					1		
585.8	T		20	2	43	10		7	16				2							
583.7	35		37	1	7				20				T		T	T				
576.0-U	80				1	T		10	4	1	4									
576.0-L		T	70			T		4	24				2							
556.0-U				1	1			92	4				2							
556.0-L	25			2	53			19			1		T			T				
547.5	4	T	15	10	10	20		26	12	T	2		1							
541.0	T		7	15	15			29	3	30			1		T					
537.0-U	4		10	15	40		5	3	20				3							
537.0-L	49		2	10	25		3		10				1							
532.8	15	55			13				17		T									

Thin Section (feet above datum) Position on Slide U = Upper M = Middle L = Lower	Composition %																				
	Intraclasts	Ooliths	Peloids	Trilobites	Pelmatozoans	Gastropods	Brachiopods	Micrite cement	Sparite cement	Dolomite cement	Chert	Chalcedony	Siliciclastic Grains (Quartz & Feldspar)	Muscovite	Pyrite	Hematite	Organics	Porosity	Glauconite	Illite (Smectite)
521.1	65			1			T	7	27											
516F								74	25				1							
513.0	10	5		2	50	T		5	18	10	T		T							
510.0	30		2	7	30	2		2	15	10	1		1							
506.8	3		2	20	25	1	1	30	10	7			1	T						
502.0								80	20											
500.5-U			15	30	30		T	7	15	T			3							
500.5-L				25	10			64					1							
489.7			7	20	25	15	1	5	17	7			2			1				
482.4			7	20	10	10		37	3	10			3			T				
443.1-U	T		3	15	35	5		15	21	5			1							
443.1-L			25	5	10	1		38	17	3			1			T				
424.5-U	45			12	5	5	3	20	9	1			1							
424.5-L	60			10	4	2	3		21				T							

Thin Section (feet above datum) Position on Slide U = Upper M = Middle L = Lower	Composition %																				
	Intraclasts	Ooliths	Peloids	Trilobites	Pelmatozoans	Gastropods	Brachiopods	Micrite cement	Sparite cement	Dolomite cement	Chert	Chalcedony	Siliciclastic Grains (Quartz & Feldspar)	Muscovite	Pyrite	Hematite	Organics	Porosity	Glauconite	Illite (Smectite)
417.2	1	T		10	3	3		20	1	61			1							
413.6	T	7	10	15	7	3	T	45	7	T			3			3			T	
406.0-U							T		12				75	T	3					10
406.0-L			60	3	2				24				10		1	T				T
399.2	5		2	20	30		T	31	2	2	3		5							
395.0	15			25	25	T	T	22	T	10			3							
392.5-U	65			3	2			2	28											
392.5-L	40		3	4	1			42	10				T							
385.4	70		3	2	T			7	16				1		T	1				
378.1-U			15	35	20	1	T	5	14				10							
378.1-M	3			10	5			15		66			1							
378.1-L				1	2			91	2	3			1							
375.2	50		3	2				34	10				1					T		
373.6	50			1				33	15				1							

Thin Section (feet above datum) Position on Slide U = Upper M = Middle L = Lower	Composition %																				
	Intraclasts	Ooliths	Peloids	Trilobites	Pelmatozoans	Gastropods	Brachiopods	Micrite cement	Sparite cement	Dolomite cement	Chert	Chalcedony	Siliciclastic Grains (Quartz & Feldspar	Muscovite	Pyrite	Hematite	Organics	Porosity	Glauconite	Illite (Smectite)
370.2				40	10			8	25	15			T			2				
365F				T				92	5				T			3				
357.8-U	38	1		15	10			5	10				20		1					
357.8-L				5	5	5		83	T				1	1						
357.7-U	T			1	1	1		95					2							
357.7-L	3	T		20	5	1		65	3				2			1				
357.6-U			7	20	40	T		10	20		T		3							
357.6-L			3	15	10	1		64	1	T			3			3				
357.5	3		1	10	10			58	2	15			1							
326.5	40			12	12			30	3				2			1				
310.0-U	10	1		3	55	2		5	23	T									1	
310.0-M	20			20	12	2	2	40	3				T			1				
310.0-L			20	20	30			27	2		T					1				
251.6-U	70			T	T				30									T		

Thin Section (feet above datum)	Composition %																				
Position on Slide U = Upper M = Middle L = Lower	Intraclasts	Ooliths	Peloids	Trilobites	Pelmatozoans	Gastropods	Brachiopods	Micrite cement	Sparite cement	Dolomite cement	Chert	Chalcedony	Siliciclastic Grains (Quartz & Feldspar)	Muscovite	Pyrite	Hematite	Organics	Porosity	Glauconite	Illite (Smectite)
251.6-L	70			T	T			25	5											
219.5	5			7	10	2	1	62	5	1	1		3			3				
199.0				T	T	T		92	6				2							
175F-U	3	40		5	15		5	T	30				T			2				
175F-L		2	7	10	10		5	57	5				2			2				
146.5	3		10	7	15		2	54	3		T		5			1				
133.0	60			1	1				38		T							T	T	
119.2	50		3	3	10	2	1	5	22	1	1		2			T		T	T	
57.0B-U				3	7		7	60	3	1			18		1					
57.0B-UM			20	5	5		10	29					30	T	1					
57.0B-LM	10		7	20	30			3	20	T	T		10	T				T		
57.0B-L									5				69	7	3	1			T	15
57.0A-U								95	2				3							
57.0A-L			20	5	40		T	1	17	7	T		10	T						

Thin Section (feet above datum)	Composition %																			
Position on Slide U = Upper M = Middle L = Lower	Intraclasts	Ooliths	Peloids	Trilobites	Pelmatozoans	Gastropods	Brachiopods	Micrite cement	Sparite cement	Dolomite cement	Chert	Chalcedony	Siliciclastic Grains (Quartz & Feldspar)	Muscovite	Pyrite	Hematite	Organics	Porosity	Glauconite	Illite (Smectite)
47.2-U			10	30	21		1	2	12	8	1		15							
47.2-L			3	20	35		1	10	28	2			1							
24.5B	58		7	6	8	T		14	5	T	T		1			1				
24.5A	40		10	7	2	3		25	8	T	T		5	T		T				
17.0	T		7	15	25	1		33	7				11						1	
9.8			30	T				40	29				T		T	1				
5.5				1				37	17	45			T		T	T				
+0.1	10			3				37	20	15			15	T						
-0.1	35		15	T			T		35	15										

APPENDIX B

CLASSIFICATION OF THIN SECTIONS FROM THE SIGNAL MOUNTAIN FORMATION, BALLY MOUNTAIN MEASURED SECTION

Thin Section Number (Feet above datum)	Classification
753.5-U	Dolosparite
753.5-L	Intraclast-peloidal sparitic wackestone
750.7	Pelmatazoan sand wackestone-packstone interlaminated with mudstone
740.5-U	Mudstone
740.5-M	Fossiliferous pebble IFC limestone cemented by calcite spar
740.5-L	Gastropod wackestone
729.0	Peloidal dolomite-gastropod wackestone
723.0	Dolomitic fossiliferous microsparitic wackestone
718.2	Dolomitic pebble intraclast pelmatazoan sand grainstone
708.0	Fenestrate mudstone
706.5	Pelmatazoan-trilobite sand grainstone interbedded with packstone and mudstone
701.0	Pebble IFC limestone with a trilobite-pelmatazoan sand matrix cemented by calcite spar
677.0	Pebble IFC limestone with an intraclast sand matrix cemented by lime mud and locally by calcite spar
676.0	Crystalline limestone
659.8	Fossiliferous wackestone, interlaminated with mudstone
651.3	Peloidal microsparitic wackestone
649.2	Fossiliferous intraclast sand grainstone interbedded with trilobite-pelmatazoan sand wackestone and mudstone

Thin Section Number (Feet above datum)	Classification
645.4	Intraclast-trilobite sand wackestone
641.0-U	Mudstone
641.0-M	Trilobite-pelmatazoan-gastropod wackestone
641.0-L	Peloidal wackestone
634.2	Fossiliferous wackestone
627.8-U	Gastropod wackestone
627.8-L	Microsparitic mudstone
622.0-U	Trilobite sand peloidal wackestone
622.0-M	Peloidal mudstone-wackestone
622.0-L	Mudstone
612.0-U	Pelmatazoan-trilobite sand wackestone
612.0-L	Trilobite-pelmatazoan sand wackestone
590.0	Intraclast sand peloidal grainstone-packstone
585.8	Peloidal gastropod pelmatazoan sand grainstone
583.7	Pebble IFC limestone with a fossiliferous peloidal matrix cemented by calcite spar
576.0-U	Pebble IFC limestone interbedded with peloidal grainstone
576.0-L	Peloidal grainstone
556.0-U	Mudstone
556.0-L	Intraclast-pelmatazoan sand packstone
547.5	Peloidal fossil sand gastropod wackestone
541.0	Dolomitic trilobite-pelmatazoan sand
537.0-U	Pelmatazoan sand grainstone interlaminated with packstone and wackestone of the same
537.0-L	Pebble IFC limestone with a trilobite-pelmatazoan sand matrix cemented by calcite spar
532.8	Dolo-oolitic grainstone

Thin Section Number (Feet above datum)	Classification
521.1	Pebble IFC limestones cemented by lime mud and calcite spar
516F	Birdseye mudstone
513	Dolomitic pelmatazoan sand grainstone graded upward to packstone
510.0	Dolomitic pebble IFC limestone with a matrix of pelmatazoan sand cemented by calcite spar
506.8	Trilobite-pelmatazoan sand wackestone
502.0	Fenestrate mudstone
500.5-U	Trilobite-pelmatazoan sand grainstone
500.5-L	Pelmatazoan-trilobite sand wackestone
489.7	Gastropod-trilobite-pelmatazoan sand grainstone
482.4	Dolomitic gastropod-pelmatazoan-trilobite sand wackestone
443.1-U	Trilobite-pelmatazoan sand packstone
443.10L	Pelmatazoan sand peloidal sparitic wackestone
424.5-U	Pebble IFC limestone with a fossil sand matrix cemented by lime mud
424.5-L	Pebble IFC limestone with a fossil sand matrix with a cement of calcite spar that grades upward into lime mud
417.2	Calcareous fossil sand dolosparite
413.6	Trilobite sand wackestone
406.0-U	Calcareous siltsone
406.0-L	Siliclastic peloidal grainstone
399.2	Trilobite-pelmatazoan sand wackestone
395.0	Dolomitic pelmatazoan-trilobite sand wackestone
392.5-U	Intraclast sand grainstone
392.50L	Intraclast sand wackestone

Thin Section Number (Feet above datum)	Classification
385.4	Pebble IFC limestone cemented by calcite spar and partly by lime mud
378.1-U	Siliciclastic peloidal pelmatazoan-trilobite sand grainstone
378.1-M	Trilobite dolosparite
378.1-L	Mudstone
375.2	Pebbly intraclast sand wackestone-packstone
373.6	Pebble IFC limestone with an interclast sand matrix cemented by lime mud and partly by calcite spar
370.2	Dolomitic pelmatazoan-trilobite hash grainstone
365F	Mudstone
357.8-U	Pebble IFC limestone with a siliclastic intraclast pelmatazoan-trilobite sand matrix cemented by calcite spar
357.8-L	Fossiliferous wackestone-mudstone
357.7-U	Mudstone, thinly laminated
357.7-L	Trilobite sand wackestone
357.6-U	Trilobite-pelmatazoan sand grainstone
357.6-L	Pelmatazoan-trilobite sand wackestone
357.5	Trilobite-pelmatazoan sand wackestone
326.5	Pebble IFC limestone with a matrix of trilobite-pelmatazoan sand cemented by lime mud
310.0-U	Intraclast-pelmatazoan sand grainstone-packstone
310.0-M	Pebble intraclast-pelmatazoan-trilobite hash wackestone
310.0-L	Peloidal trilobite-pelmatazoan sand wackestone-packstone
251.6-U	Intraclast sand grainstone
251.6-L	Intraclast sand packstone

Thin Section Number (Feet above datum)	Classification
219.5	Fossil sand wackestone
199.0	Mudstone
175F-U	Fossiliferous oolitic grainstone
175F-L	Trilobite-pelmatazoan sand wackestone
146.5	Peloidal pelmatazoan sand wackestone
133.0	Intraclast sand grainstone
119.2	Pebble IFC limestone with a fossil sand matrix cemented by calcite spar
57.0B-U	Siliciclastic fossil sand wackestone
57.0B-UM	Siliciclastic fossil sand peloidal wackestone
57.0B-LM	Siliciclastic trilobite-pelmatazoan sand grainstone
57.0B-L	Siltstone, laminated
57.0A-U	Mudstone
57.0B-L	Peloidal pelmatazoan sand grainstone
47.2-U	Siliciclastic pelmatazoan-trilobite sand grainstone
47.2-L	Trilobite-pelmatazoan hash grainstone
24.5B	Fossiliferous intraclast sand wackestone
17.0	Siliciclastic trilobite-pelmatazoan sand wackestone
9.8	Fenestrate peloidal wackestone
5.5	Dolomitic microsparitic mudstone
+0.1	Dolomitic siliciclastic microsparitic mudstone
-0.1	Dolomitic pebble IFC limestone with peloidal sand matrix cemented with calcite spar.

APPENDIX C

CLASSIFICATION OF HAND-SAMPLES FROM THE SIGNAL MOUNTAIN FORMATION, BALLY MOUNTAIN MEASURED SECTION

Sample Number (Feet above datum)	Classification
769.8	Mudstone; thinly laminated
769.0	Mudstone; thinly laminated
768.6	Mudstone and intraclast sand grainstone; thinly interbedded
768.1	Gastropod wackestone and mudstone; thinly interbedded
766.2	Oolitic mudstone, mudstone, and peloidal wackestone thinly interbedded
762.0	Oolitic wackestone
761.6	Trilobite sand wackestone and mudstone; very thinly interbedded
757.8	Pebble IFC limestones and mudstone; thinly interbedded, IFC's cemented by calcite spar or lime mud
755.1	Pebble IFC limestone with a matrix of trilobite, pelmatazoan, and gastropod fragments cemented by lime mud
753.7	Mudstone with several gastropod shells at base
753.2	Peloidal wackestone
752.8	Mudstone
750.7	Pelmatazoan sand wackestone
750.0	Mudstone with basal intraclast sand packstone
745.4	Mudstones, pelmatazoan-trilobite intraclast sand grainstones, and pelmatazoan-trilobite sand wackestones; very thinly interbedded
745.1	Pebble IFC limestone with a pelmatazoan-trilobite sand
740.5	Mudstones, intraclast sand wackestones, and a gastropod wackestone; very thinly interbedded

Sample Number (Feet above datum)	Classification
740.4	Flat pebble IFC limestone and peloidal mudstone; dolomitic; interbedded; IFC matrix is a trilobite sand cemented by lime mud
735.7	Flat pebble IFC limestones with a trilobite-pelmatazoan sand matrix cemented by lime mud
729.0	Trilobite sand dolomite gastropod wackestones and peloidal mudstones; very thinly interbedded
727.7	Pelmatazoan-trilobite sand wackestone
723.0	Mudstones and trilobite hash wackestones; dolomitic; very thinly interbedded
718.2	Pebble IFC limestone, very thinly bedded; with a pelmatazoan sand matrix cemented by calcite spar or lime mud
708.0	Mudstone; thinly bedded
706.5	Brachiopod-trilobite sand wackestone with basal mudstone
701.0	Pebble IFC limestone; thinly bedded; with an intraclast sand matrix cemented by calcite spar or lime mud
698.4	Intraclast sand grainstone, mudstone, and brachiopod-trilobite mudstone; interlaminated
698.0	Mudstones and pebble IFC limestone; very thinly interbedded; IFC matrix is an intraclast sand cemented by lime mud
695.0	Mudstone; thinly laminated
693.9	Brachiopod sand wackestones and mudstones; very thinly interbedded
685.6	Pebble IFC limestone capped by a peloidal mudstone; IFC matrix is a trilobite-pelmatazoan sand cemented by lime mud
677.0	Pebble IFC limestone and intraclast sand grainstone; interbedded; IFC matrix is an intraclast sand cemented by lime mud
676.0	Dolomitic crystalline limestone; thinly bedded, recrystallized mudstone-wackestone

Sample Number (Feet above datum)	Classification
667.9	Mudstone
659.8	Mudstones, intraclast sand wackestones-packstones, and fossiliferous wackestones; interlaminated
654.5	Fossiliferous peloidal wackestones and peloidal trilobite sand wackestones; very thinly interbedded
651.3	Mudstone; thinly laminated
649.2	Flat pebble IFC limestone with basal mudstone; matrix is an intraclast pelmatazoan-trilobite sand cemented by lime mud
645.4	Trilobite hash wackestone
642.0	Mudstone; thinly laminated
641.0	Flat pebble IFC limestone and mudstone; thinly interbedded; IFC matrix is an intraclast pelmatazoan sand cemented by lime mud
638.7	Cobble IFC limestone with a basal mudstone (thinly laminated); IFC matrix is a pelmatazoan sand cemented by calcite spar
634.2	Intraclast sand grainstone, fossiliferous peloidal wackestones, and peloidal mudstones; very thinly interbedded.
630.0	Fossilferous intraclast sand wackestone and peloidal wackestone; dolomitic, interlaminated.
627.8	Gastropod wackestones and packstones; very thinly interbedded
622.0	Mudstone, gastropod wackestone, trilobite sand wackestones, and pelmatazoan sand wackestones; very thinly interbedded
612.0	Flat pebble IFC limestone, trilobite mudstone, and trilobite sand wackestone; interlaminated; IFC matrix is a trilobite sand cemented by lime mud
605.0	Gastropod wackestones, mudstone, and fossiliferous intraclast sand wackestones and grainstones; very thinly interbedded

Sample Num (Feet above d	r um)	Classification
600.0		Peloidal wackestone
595.0		Mudstone; laminated
590		Peloidal mudstone-wackestone and pebble IFC limestone with a peloidal matrix cemented by lime mud.
590		Peloidal mudstone-wackestone and pebble IFC limestone with a peloid matrix cemented by lime mud
585.8		Pelmatazoan sand wackestone and mudstone; very thinly interbedded
583.7		Intraclast sand grainstone, pelmatazoan sand wackestone, and a basal mudstone; very thinly interbedded
576.8		Pebble IFC limestone with an intraclast sand matrix cemented by lime mud
576.0		Pebble IFC limestones and peloidal wackestones-packstones; cherty; thinly interbedded; IFC is cemented by lime mud
575.0		Pebble IFC limestones and peloidal packstones-wackestones; cherty; thinly interbedded; IFC is cemented by lime mud.
570.5		Pelmatazoan-trilobites sand wackestone and fossiliferous mudstone; very thinly interbedded
565.2		Flat pebble IFC limestone with an oolitic pelmatazoan-trilobite sand matrix cemented by lime mud
562.0		Mudstone; thinly laminated
561.0		Trilobite mudstone; thinly laminated
560.0		Mudstone; thinly laminated
558.5		Mudstone and silicified pelmatazoan sand wackestone; very thinly interbedded
556.0		Mudstone, intraclast pelmatazoan sand packstone-grainstone; interlaminated
553.5		Intraclast sand grainstone and peloidal wackestone; very thinly interbedded

Sample Number (Feet above datum)	Classification
547.5	Gastropod wackestone and peloidal mudstone, very thinly interbedded
541.0	Fossiliferous peloidal wackestone and fossiliferous intraclast sand wackestone; very thinly interbedded
537.0	Trilobite sand wackestones and packstone, and a pebble IFC limestone with trilobite sand matrix cemented by lime mud; very thinly interbedded
535.8	Mudstone; thinly laminated
532.8	Dolo-oolitic grainstone; very thinly bedded
531.0	Fossiliferous mudstone
524.8	Mudstone, thinly laminated
521.1	Flat pebble IFC limestones with an intraclast sand matrix cemented by lime mud or calcite spar
516.0	Fenestrate mudstone
513.0	Intraclast-silicified pelmatazoan oolitic sand packstone-grainstone; very thinly bedded
510.0	Dolomitic fossiliferous peloidal wackestone
508.8	Pelmatazoan-brachiopod-trilobite sand wackestone-packstone and fossiliferous intraclast sand wackestones; dolomitic; very thinly interbedded
506.8	Mudstone and trilobite-brachiopod-pelmatazoan sand wackestones
504F	Mudstone, brachiopod-trilobite sand wackestone, and a pebble IFC limestone cemented by lime mud; very thinly interbedded
503.0	Mudstone
502.1	Fenestrate mudstone; thinly laminated
502.0	Fenestrate mudstone; thinly laminated
500.5	Mudstone, trilobite-pelmatazoan sand grainstone, and pelmatazoan-trilobite sand wackestone; interlaminated

Sample Number (Feet above datum)	Classification
494.5	Fossiliferous Mudstone-wackestone
489.7	Pebble intraclast-brachiopod-trilobite sand wackestone and a trilobite-brachiopod sand packstone
482.4	Brachiopod-trilobite sand wackestones, gastropod wackestone, and mudstone; interlaminated
477.2	Mudstones and a pelmatazoan-trilobite-brachiopod sand grainstone-packstone; very thinly interbedded
476.4	Fenestrate mudstone; thinly laminated
470.1	Fossiliferous wackestone and mudstones; thinly interbedded
469.5	Mudstones and pelmatazoan intraclast sand packstone; thinly interbedded
465.0	Brachiopod-trilobite-pelmatazoan sand wackestones and mudstone, interlaminated
464.9	Brachiopod-trilobite-pelmatazoan sand wackestones and mudstones; interlaminated
463.8	Mudstone; thinly laminated
460F	Mudstone; thinly laminated
457.0	Brachiopod-trilobite sand wackestones and mudstones; interlaminated
450.0	Mudstone; laminated
445.0	Mudstone; thinly laminated
443.1	Brachiopod-trilobite-pelmatazoan wackestone and mudstone; dolomitic; interlaminated
437.2	Dolomitic trilobite-brachiopod sand sparitic packstone
433.1	Peloidal wackestone and intraclast sand packstone
429.5	Mudstone; laminated

Sample Number (Feet above datum)	Classification
427.3	Fossiliferous mudstones; oolitic wackestone, and trilobite sand gastropod wackestone; very thinly interbedded
424.5	Pebble IFC limestone and a brachiopod-trilobite wackestone; very thinly interbedded; IFC matrix is an intraclast sand cemented by lime mud
417.2	Mudstones and trilobite-brachiopod sand wackestone
416.1	Mudstones, peloidal intraclast sand wackestone-packstone, and peloidal wackestones; interlaminated
413.6	Dolo-oolitic mudstone, oolitic wackestones, oolitic brachiopod-trilobite sand wackestones,a and mudstone; interlaminated
406.0	Siliciclastic peloidal grainstone that grades upward into a calcareous siltstone; laminated
404.8	Siliciclastic mudstones and calcareous siltstones, mudstones, and siliciclastic peloidal grainstones; interlaminated
399.2	Cherty brachiopod-trilobite sand wackestone; thinly bedded
396.0	Dolomitic brachiopod-trilobite sand wackestone; very thinly bedded
395.0	Dolomitic brachiopod-trilobite sand wackestone; very thinly bedded
394.0	Dolomitic brachiopod-trilobite sand wackestone; very thinly bedded
392.5	Intraclast sand grainstone and an intraclast sand packstone that grades upward into a mudstone; very thinly interbedded
389.0	Dolomitic gastropod trilobite sand wackestone-mudstone; very thinly bedded
385.4B	Flat pebble IFC limestone with an intraclast sand matrix cemented by lime mud; thinly bedded
385.4A	Mudstone; thinly laminated

Sample Number (Feet above datum)	Classification
382.5	Mudstone, thinly laminated, with basal oolitic wackestone; thinly interbedded
379.3	Dolomitic mudstone; thinly laminated
378.1	Pebble IFC limestones and a trilobite sand wackestone; thinly interbedded; IFC matrix is a brachiopod-trilobite sand cemented by lime mud
375.2	Intraclast sand sparitic packstone; thinly bedded
373.6	Flat pebble IFC limestone with an intraclast sand matrix cemented by lime mud
370.2	Dolomitic intraclast-trilobite sand grainstone
365/70F	Mudstone; indistinctly bedded
357.8/357.7	Mudstones, brachipod-trilobite oolitic intraclast sand packstones wackestones, oolitic mudstone, and brachiopod-trilobite wackestone; interlaminated
357.6	Trilobite mudstone and a trilobite sand wackestone; very thinly interbedded
375.5	Dolomitic trilobite-brachiopod sand wackestone; very thinly bedded
357.0	Mudstone; thinly laminated
350/55F	Mudstone; thinly laminated
345.0	Siliciclastic peloidal wackestone; very thinly bedded
340.0	Intraclast trilobite-pelmatazoan sand grainstones, mudstone, and trilobite sand wackestone; interlaminated
335.4	Pebble IFC limestone, trilobite wackestone, and mudstone; interlaminated; IFC matrix is a pelmatazoan-trilobite sand cemented by calcite spar
334.5	Pebble IFC limestone with a pelmatazoan (silicified)-trilobite sand matrix cemented by calcite spar; thinly bedded

Sample Number (Feet above datum)	Classification
326.5	Pebble IFC limestones and mudstone; very thinly interbedded; IFC matrix is intraclast sand cemented by lime mud
325.0	Mudstone with a laminae of burrow filling intraclast sand packstone; thinly laminated
320.1	Intraclast trilobite-pelmatazoan (silicified) sand grainstone and mudstone very thinly interbedded
314.5	Mudstone and pelmatazoan sand wackestone; interlaminated
310.0	Oolitic intraclast sand grainstone, oolitic intraclast trilobite sand wackestone, and a brachiopod-trilobite mudstone; very thinly interbedded
302.5F	Mudstone, siliciclastic mudstone, and calcareous siltstone; interlaminated
300.0	Mudstone; thinly laminated
296.5	Trilobite sand wackestone; very thinly bedded
286.2	Pelmatazoan sand wackestone, fossiliferous mudstone, and a trilobite sand wackestone; very thinly interbedded
281.5	Pebble intraclast-trilobite-pelmatazoan sand wackestone; thinly bedded
274.5	Pebble intraclast-trilobite-pelmatazoan sand packstone and siliciclastic fossiliferous sand wackestone; dolomitic; very thinly interbedded
269.5F	Pebble IFC limestone with a brachiopod (silicified)-pelmatazoan sand matrix cemented by calcite spar
267.0	Pebble intraclast pelmatazoan-trilobite wackestone; burrow mottled
263.6	Intraclast trilobite-pelmatazoan (silicified-dolomitized) sand grainstone; thinly bedded
253.0	Intraclast sand grainstone-packstone-wackestone and mudstone; interlaminated

Sample Number (Feet above datum)	Classification
251.6	Intraclast sand grainstones and mudstones; very thinly interbedded
245.0	Pebble IFC limestone and pelmatazoan-trilobite sand wackestone; very thinly interbedded; IFC matrix is an oolitic trilobite-pelmatazoan sand cemented by lime mud
231.0	Dolomitic trilobite-pelmatozoan sand wackestone; very thinly bedded
224.0	Pebble IFC limestone and mudstone; very thinly interbedded; IFC matrix is a trilobite-pelmatozoan sand cemented by calcite spar
219.5	Mudstones and intraclast sand packstones; very thinly interbedded
213.2	Intraclast-trilobite-pelmatozoan sand wackestone and mudstone; dolomitic; interlaminated
204.5	Pebble intraclast-trilobite-pelmatozoan sand wackestone; thinly bedded
202.0	Intraclast trilobite-pelmatozoan sand wackestone; thinly bedded
199.0	Dolomitic mudstone; thinly laminated
195.2	Intraclast-peloidal-fossiliferous sand wackestone and trilobite-brachiopod peloidal wackestone; very thinly interbedded
190.5	Pebble IFC limestones with a peloidal oolitic intraclast sand cemented by lime mud; very thinly bedded
182.5	Pebble IFC limestone with a trilobite-pelmatozoan sand matrix cemented by lime mud; very thinly bedded
176.0	Oolitic wackestones and oolitic mudstones; very thinly interbedded
175/76F	Oolitic grainstone and peloidal wackestone; very thinly interbedded
174.0B	Intraclast oolitic pelmatozoan sand packstone; very thinly bedded

Sample Number (Feet above datum)	Classification
174.0A	Pebble IFC limestone and trilobite-pelmatozoan sand wackestone; very thinly interbedded; IFC matrix is a pelmatozoan sand cemented by lime mud
167.5	Pebble IFC limestone with a trilobite-pelmatozoan sand matrix cemented by lime mud; thinly bedded
164.5	Pebble IFC limestone cemented by lime mud and calcite spar; very thinly bedded
154.7	Pebble IFC limestone and trilobite sand wackestone; very thinly interbedded; IFC matrix is trilobite-pelmatozoan sand cemented by lime mud
146.5	Fossilferous peloidal wackestone; very thinly bedded
138.0	Oolitic pelmatozoan sand packstone and grainstone, and trilobite-pelmatozoan sand wackestone; very thinly interbedded
133.0	Intraclast sand grainstone; very thinly bedded
125.3	Brachiopod-trilobite sand wackestone; very thinly bedded
120.5	Trilobite-brachiopod sand peloidal wackestone
119.2	Pebble IFC limestone cementd by lime mud; thinly bedded
110.4	Dolomitic trilobite sand wackestone; very thinly bedded
101.2	Mudstone, intraclast sand packstones and wackestones; very thinly interbedded
95.5	Mudstone; thinly laminated
93.6	Mudstone; thinly laminated
70.0	Intraclast trilobite pelmatozoan sand grainstone and trilobite sand wackestone; very thinly interbedded
60.0	Fossiliferous mudstone; thinly bedded

Sample Number (Feet above datum)	Classification
57.0	Mudstones with burrow filling intraclast trilobite-pelmatozoan sand packstone-grainstone; very thinly bedded
47.2	Trilobite-pelmatozoan sand wackestone that grades upward into a packstone-grainstone
41.5	Pelmatozoan-trilobite sand wackestones and trilobite intraclast sand wackestone; very thinly interbedded
29.8	Pebble IFC limestone, mudstones, and pebble intraclast trilobite sand wackestone; very thinly interbedded into a packstone-grainstone; very thinly bedded
24.5	Pebble IFC limestones and a mudstone; very thinly interbedded; IFC's have matrixes of trilobite-brachiopod-gastropod-oolitic sand cemented by lime mud of calcite spar
17.0	Peloidal trilobite-pelmatozoan sand wackestone
9.8	Algal mat boundstone; laminated
5.5	Dolomitic microsparitic mudstone; thinly bedded
+0.1	Microspartic mudstone and crystalline dolostone; thinly interlaminated
-0.1	Algal intraclast sand grainstone; laminated
-4.0	Crystalline dolomite; laminated
-4.8	Algal mat boundstone; thinly laminated
-9.8	Dolomitic algal intraclast sand grainstone

VITA 2

Curtis Leon Ditzell

Candidate for the Degree of

Master of Science

Thesis: SEDIMENTARY GEOLOGY OF THE CAMBRO-ORDOVICIAN SIGNAL MOUNTAIN FORMATION AS EXPOSED IN THE WICHITA MOUNTAINS OF SOUTHWESTERN OKLAHOMA.

Major Field: Geology

Biographical:

Personal Data: Born in Midland, Texas, August 17, 1952, the son of Mr. and Mrs. Leon S. Ditzell, Jr.

Education: Graduated from Putnam City West High School, Oklahoma City, Oklahoma, June, 1971; Bachelor of Science in Criminal Justice Studies at the University of Tulsa, Tulsa, Oklahoma, May, 1975; Bachelor of Science in Geosciences at the University of Tulsa, Tulsa, Oklahoma, December, 1982; completed requirements for the Master of Science degree in Geology at Oklahoma State University, Stillwater, Oklahoma, December, 1984.

Professional Experience: Geologic Field Contractor for MAPCO Minerals Company, Tulsa, Oklahoma, June 1979 to April, 1980; Junior Geologist for John R. Wilson and Associates, Tulsa, Oklahoma, February, 1981 to April, 1982; Junior Geologist for Challenger Minerals Incorporated, Tulsa, Oklahoma, April, 1982 to February, 1983; Geological Teaching Assistant at Oklahoma State University, Stillwater, Oklahoma, September, 1983 to June, 1984; currently an Associate Geologist for Conoco Incorporated, Oklahoma City Division, Oklahoma.